Physiological response of *Pichia pastoris* to recombinant protein production under methanol induction

Von der Naturwissenschaftlichen Fakultät

der Gottfried Wilhelm Leibniz Universität Hannover

zur Erlangung des Grades

Doktorin der Naturwissenschaften

Dr. rer. nat.

genehmigte Dissertation

von

Ana Letícia de Souza Vanz

Mestre em Biologia Celular e Molecular

geboren am 19.05.1981, in Erechim, Brasilien

2013

Referent Prof. Dr. Thomas Scheper

Korreferentin Prof. Dr. Ursula Rinas

Tag der Promotion: 15. April 2013

Erklärung

Hierdurch erkläre ich, dass ich meine Dissertation mit dem Titel „Physiological response of *Pichia pastoris* to recombinant protein production under methanol induction“ selbständig verfasst und die benutzten Hilfsmittel und Quellen sowie gegebenenfalls die zu Hilfeleistungen herangezogenen Institutionen vollständig angegeben habe. Die Dissertation wurde nicht schon als Masterarbeit, Diplomarbeit oder andere Prüfungsarbeit verwendet.

Hannover, Januar 2013

Ana Letícia de Souza Vanz

Declaration

The work described in this thesis was carried out in the period from March 2009 to January 2013 at the Leibniz University of Hannover, Germany, under the supervision of Prof. Dr. Thomas Scheper and Prof. Dr. Ursula Rinas at the Institute of Technical Chemistry, Hannover. I hereby declare that this submission is my own work and that, to the best of my knowledge and belief, it contains no material previously published or written by another person nor material which has been accepted for the award of any other degree or diploma of the university or other institute of higher learning, except where due acknowledgment has been made in the text.

Hannover, January 2013

Ana Letícia de Souza Vanz

Acknowledgements

I would like to thank my supervisor Prof. Dr. Ursula Rinas for accepting me as her student and providing this privilege to carry out my PhD project in Germany. I also thank her for the support during my thesis and great efforts to explain things clearly and always stimulating me to see great discoveries where I could not see anything.

I would like to express my heartfelt gratitude to Prof. Dr. Thomas Scheper for accepting and providing me the opportunity to develop my PhD thesis at the Institute for Technical Chemistry, University of Hannover.

I want to thank all the people who had a part in this work, especially Dr. Adnan Ahmad (GCU, Pakistan), Dr. Chandrasekhar Gurramkonda (ICGEB, India) who started with this project. I am also very grateful to the people at HZI Braunschweig specially Dr. Heinrich Lünsdorf, Dr. Manfred Nimtz, Wolfgang Kessler not only for the valuable technical support but also for their friendly reception to make me feel comfortable working in their labs.

The colleges of the TCI Hannover have contributed immensely to my personal and professional life. My sincere thanks goes to Martina Weiss and Martin Pähler for their valuable technical assistance. I am also grateful to Dr. Frank Stahl for the helpful support and discussions concerning primer design and PCR analysis. I am especially grateful to my dear colleagues Dr. Maria Zahid, Dr. Zhaopeng Li, Dr. Öznur Kökpinar, Satish Nemani and Gesa Nöhren for fruitful discussions, good advice and for providing a stimulating and fun environment in which to learn and grow.

I would like to thanks CAPES, the Brazilian founding agency, for the financial support during these years.

Lastly, I would like to thank my family for all their love and encouragement during these almost five years so far away from home.

I would like to add a thought which gave me power and courage to keep on during this unforgettable and amazing period in a place so far from my home.

"*A man needs to travel. By his own means, not by stories, images, books or TV. By his own, with his eyes and feet, to understand what he is. To some day plant his own trees and give them some value. To know the cold to enjoy the heat. To feel the distance and lack of shelter to be well under his own ceiling. A man needs to travel to places he doesn't know to break this arrogance that makes us see the world as we imagine it, and not simply as it is or may be. That makes us teachers and doctors of what we have never seen, when we should just be learners, and simply go see it*."

Amyr Klink (Brazilian sailor and writer)

Table of contents

Abstract

The methylotrophic yeast *Pichia pastoris* has emerged as a powerful tool to produce heterologous proteins during the last years. The protein production in these cells is commonly controlled by the methanol-inducible *aox1* promoter. However, the current knowledge of the changes in physiology of this yeast during the shift from growth on glycerol to methanol-induced protein production under industrial relevant conditions is still scarce. To further understand the physiological changes in *P. pastoris* during production of recombinant proteins such as human insulin precursor (IP) and hepatitis B virus surface antigen (HBsAg), a comprehensive analysis of the intracellular proteome during the cultivation combined with electron microscopy analysis of *P. pastoris* cells was performed. Proteome analysis from different cultivation time points was done by two-dimensional gel electrophoresis combined with MALDI-TOF.

The most notable change in the proteome profile of *P. pastoris* cells after shift from glycerol to methanol was detected in the enzymes of the carbon metabolism. In particular, enzymes from the methanol dissimilation pathway started to dominate the proteome, suggesting here a potential to increase methanol incorporation into biomass/product through metabolic enhancement of the methanol assimilation pathway. In addition, the presence of alcohol dehydrogenases (ADHs) in the methanol-fed batch phase indicates that ADHs may play an important role in formaldehyde detoxification in *P. pastoris.*

Two stress responses were specially investigated, the oxidative stress provoked by methanol oxidation in peroxisomes and the stress related to the recombinant protein overproduction. Up-regulation of anti-oxidant enzymes as well as the autophagy of the peroxisomes was observed as a response to cope with the damage caused by the reactive oxygen species (ROS) generated during methanol metabolism. These results support for the first time that peroxisome degradation in *P. pastoris* during growth on methanol is a housekeeping mechanism.

The unfolded protein response (UPR) and endoplasmic reticulum associated degradation (ERAD) pathway were stimulated during the production of the hydrophobic HBsAg. On the other hand, the production of the small IP did not provoke any relevant stress to the cells. Thus, the individual physical properties of the heterologous protein have a significant effect on an efficient final production. Hence, the cell full capacity to produce a recombinant protein should be regulated according to the properties of the product of interest.

A profound understanding of the nature of whole-protein networks is fundamental to improve the performance of *P. pastoris* strains in various biotechnological processes. Therefore, the herein presented results are a valuable contribution for future rational strain engineering.

Keywords: *Pichia pastoris*, Recombinant protein production, Proteomics

Zusammenfassung

Die methylotrophe Hefe *Pichia pastoris* wird immer häufiger erfolgreich als Werkzeug zur Produktion heterologer Proteine in der Bioprozesstechnik eingesetzt. Dabei wird meist der methanol-induzierbare Promoter *aox1* zur regulierten Produktion der Fremdproteine genutzt. Trotz der weiten Anwendung ist bisher nur wenig über die metabolischen und physiologischen Abläufe und Veränderungen innerhalb der Hefezellen unter bioprozess-relevanten Umständen bekannt. Mit dieser Arbeit wird ein umfassender Einblick in die Physiologie zweier rekombinanter *P. pastoris* Stämme während des Kultivierungsprozesses gewährt. Der zweistufige Prozess setzt sich aus einer Glycerin-Batch Phase, zur Generierung hoher Biomasse, gefolgt von einer Methanol-Fed-Batch Phase zur Induktion des rekombinanten Proteins zusammen. Bevor und während der Produktion rekombinanter Proteine wie einem humanen Insulinvorläufer (insulin precursor, IP) und einem Oberflächenantigen des Hepatitis B Viruses (hepatitis B virus surface antigen, HBsAg) wurde das Proteom sowie die Morphologie der Zellen analysiert. Die Proteomanalysen der Zellen von verschiedenen Zeitpunkten der Kultivierung wurden mittels zwei-dimensionaler Gelelektrophorese in Kombination mit MALDI-TOF durchgeführt. Zur ultrastrukturellen Untersuchung der Zellen wurde ein Transmissionselektronenmikroskop verwendet.

Die Proteomanalysen zeigen, dass ein Wechsel der Kohlenstoffquelle von Glycerin zu Methanol unter den gewählten Prozessbedingungen starke Veränderungen innerhalb der Enzyme des Kohlenstoffmetabolismus zur Folge hat. Dabei wird vor allem die Synthese von Enzymen des dissimilatorischen Methanolabbaus induziert. Eine gentechnische Unterstützung des assimilatorischen Abbaus könnte zur Steigerung der Produktivität durch den Einbau von Methanol in Biomasse/Produkt genutzt werden. Des Weiteren wurde die Anwesenheit von Alkoholdehydrogenasen (ADHs) während der Methanolphase festgestellt, was auf eine Rolle dieser Enzyme bei der Formaldehyd Detoxifikation in *P. pastoris* hindeutet.

Ein besonderer Fokus wurde auf die zelluläre Stressregulation während der Kultivierung gelegt. Die Zellen sind zwei Arten von Stress ausgesetzt. Zum einen oxidativem Stress, der durch die Oxidation des Methanols in den Peroxisomen generiert wird und zum anderen Stress, der aus der Überexpression des rekombinanten Proteins resultiert. Als Antwort auf eine erhöhte Konzentration an reaktiven Sauerstoffspezies (reactive oxygen species, ROS), wurde die Hochregulation anti-oxidativer Enzyme sowie die Autophagy von Peroxisomen (Pexophagy) festgestellt. Der Abbau von Peroxisomen während des Wachstums auf Methanol, welcher vermutlich homeostatischen Nutzen bringt und somit als „Housekeeping Mechanismus“ bezeichnet werden kann, wird hier erstmalig für *P. pastoris* beschrieben.

Die Überproduktion des hydrophoben HBsAg stimuliert sowohl die "unfolded protein response" (UPR) als auch den "endoplasmatic reticulum associated degradation pathway" (ERAD). Während der Produktion des kleinen IP-Proteins scheinen hingegen keine dieser Stressreaktionen ausgelöst zu werden. Hierdurch wird der Einfluss der physikalischen Eigenschaften des Produkts auf die Zellphysiologie und damit auf die Produktivität deutlich. Um die volle Produktionskapazität der Zellen zu erzielen, sollte der Prozess somit den Produkteigenschaften angepasst werden.

Für die zukünftige Generierung leistungsfähiger und produktionsstarker *P. pastoris* Stämme ist ein grundlegendes Verständnis des gesamten Proteinnetzwerks von fundamentaler Bedeutung. Die vorgestellten Ergebnisse liefern hierzu einen wertvollen Beitrag und bieten eine gute Grundlage zum Design zukünftiger *P. pastoris* Stämme hinsichtlich einer gesteigerten Produktionsleistung.

Stichwörter: *Pichia pastoris*, Rekombinante Proteinproduktion, Proteomik

1. Theoretical background

Recombinant protein production in the last decades has paved a new way towards improvement in human health. The acquisition of profound knowledge and entire genome sequences of a number of expression platforms has lead to considerable success in production of many recombinant proteins of pharmaceutical importance. The biotechnology industry has grown considerably, and currently about 25% of commercial pharmaceuticals are biopharmaceuticals [1]. Initially, their industrial production has been performed in *Escherichia coli*, benefiting from the high amount of information accumulated on the genetics and biochemistry of this well-studied organism [2]. Nevertheless, as the demand for producing more complex proteins developed, novel yeast strains, among them *Pichia pastoris*, have been progressively invading the field of bio-pharmaceutical protein production dominated by *E. coli* and mammalian cell expression systems. This is best illustrated by the recent approval of KALBITOR® (ecallantide, a peptide used for the treatment of hereditary angioedema), the first *P. pastoris*-produced protein therapeutic approved by the Food and Drug Administration (FDA) [3].

Despite of being explored over the decades for protein production, *P. pastoris* is still not adequately characterized at the physiological and proteomic level, especially regarding the physiological responses to alleviate the stress generated during cultivation in bioreactor.

1.1. *Pichia pastoris* as expression system

After its first transformation reported in 1985 [4], *P. pastoris* became a well developed expression platform which has been utilized successfully to express a multitude of proteins for both basic research and industrial use [5-9]. *P. pastoris* includes characteristics of both prokaryotes and eukaryotes. As an unicellular organism, it includes ease of genetic manipulation and rapid growth on relatively inexpensive media similar to *E. coli* [10]. *P. pastoris* also combines unique characteristics of eukaryotes such as post-translational modifications, for instance glycosylation and disulfide bridges formation [11]. It possesses highly inducible and tightly regulated alcohol oxidase (*aox1*) promoter [12]. The *aox1* promoter is strongly repressed in cells grown on most carbon sources; such as glycerol, but it is

induced over 1000-fold when cells are shifted to a medium containing methanol as a sole carbon source, which is an advantage if the protein is toxic to the cell [10]. In addition, it shows a stable integration of expression plasmids into the genome and the ability to grow to high cell densities (> 100 g L^{-1} dry cell mass) in bioreactor cultures [8]. Another important characteristic that makes this expression system an attractive choice is the efficient secretion of heterologous protein and the relative low levels of endogenous proteins that are secreted to the medium, which facilitates purification [13]. The protein concentration in the culture supernatant can exceed 10 g L^{-1} [14]. Finally, diverse post-translational protein processing properties that include among others glycosylation and disulfide bond formation in *P. pastoris* are similar to higher eukaryotes, including humans. Consequently, heterologous proteins are more likely to be correctly processed, folded and assembled into functional molecules when produced in *P. pastoris* compared with *S. cerevisiae* or *E. coli* [5].

In the biopharmaceutical industry, over 70% of the therapeutic proteins under preclinical and clinical development are glycosylated and there has been an increasing need for highly efficient glycoprotein expression systems [15]. Mammalian systems such as Chinese hamster ovary (CHO) cells have been most widely used since they have been extensively characterized and are capable of human like glycosylation [16]. However, they typically exhibit low survivability and low recombinant protein productivity unless sophisticated experimental techniques are employed [15]. On the other hand, although yeast systems typically produce hyper-mannosylated proteins with poor bioactivity in humans, advances in yeast glycoengineering, especially for *P. pastoris* enabled the synthesis of humanized glycoproteins with substantially improved bioactivity [17, 18].

Recently, *P. pastoris* was reassigned to the genus *Komagataella*. The commonly used recombinant protein production strains, such as X-33 and GS115, were classified as *Komagataella phaffii* [19]. In the present work, the earlier denomination (*P. pastoris*) is used when referring to the strains X-33 and GS115 since at the time this study was performed all the data banks used the *P. pastoris* name as well.

1.2. Methanol metabolism in *P. pastoris*

A limited number of yeast species is able to utilize methanol as sole energy and carbon source. These methylotrophs include *Hansenula polymorpha* (*Pichia angusta*), *P. pastoris*, *Candida boidinii*, and *Pichia methanolica* [20]. The enzyme alcohol oxidase (AOX) is responsible for the first step of methanol metabolism. The genome of *P. pastoris* contains two genes, *aox1* and *aox2*, whereby activity of AOX1p is responsible for the majority (> 85%) of alcohol oxidase activity in the cell [21]. There are three phenotypes of *P. pastoris* host strains with regard to methanol utilization, Mut^+ (methanol utilization plus) where both *aox* genes are intact and active, Mut^S (methanol utilization slow) which has a disruption in the *aox1* gene and the Mut^- (methanol utilization minus), which is unable to grow on methanol, since these strains have both *aox* genes deleted [22].

All methylotrophic yeasts use a common methanol-utilizing pathway [23]. An outline of methanol metabolism in methylotrophic yeasts is summarized in Figure 1.1. Methanol is first oxidized by alcohol oxidase (AOX) to form formaldehyde and hydrogen peroxide, which are both highly toxic compounds. Formaldehyde is a central intermediate situated at the branch point between assimilation and dissimilation pathways [24]. In the assimilation pathway, a portion of formaldehyde is fixed to xylulose 5-phosphate (Xu_5P) by dihydroxyacetone synthase (DAS) forming dihydroxyacetone (DHA) and glyceraldehyde 3-phosphate (GAP). DHA is phosphorylated by dihydroxyacetone kinase (DAK), and, subsequently, dihydroxyacetone phosphate (DHAP) and GAP form fructose 1,6-bisphosphate which is then utilized for regeneration of Xu_5P and for biosynthesis of cell constituents [25]. Another portion of formaldehyde is further oxidized to CO_2 by the cytosolic dissimilation pathway. Formaldehyde generated by AOX reacts nonenzymatically with the reduced form of glutathione (GSH) to generate S-hydroxymethyl glutathione ($GS\text{-}CH_2OH$). $GS\text{-}CH_2OH$ is then oxidized to CO_2 through the cytosolic GSH-dependent oxidation pathway, which is ubiquitous in nature. NAD^+-linked and GSH dependent formaldehyde dehydrogenase (FLD) uses $GS\text{-}CH_2OH$ as a substrate to yield S-formylglutathione (GS-CHO) and NADH. GS-CHO is then hydrolyzed to formate and GSH by S-formylglutathione hydrolase (FGH). NAD^+-linked formate dehydrogenase (FDH) is the last enzyme involved in the methanol dissimilation pathway and generates

CO_2 and NADH through the oxidation of formate [23]. Methyl formate synthesis by methylotrophic yeasts during growth on methanol has also been considered to play a role in formaldehyde detoxification. An enzyme that catalyses methyl formate synthesis was isolated in *C. boidinii* and suggested to belong to the alcohol dehydrogenase (ADH) family [26].

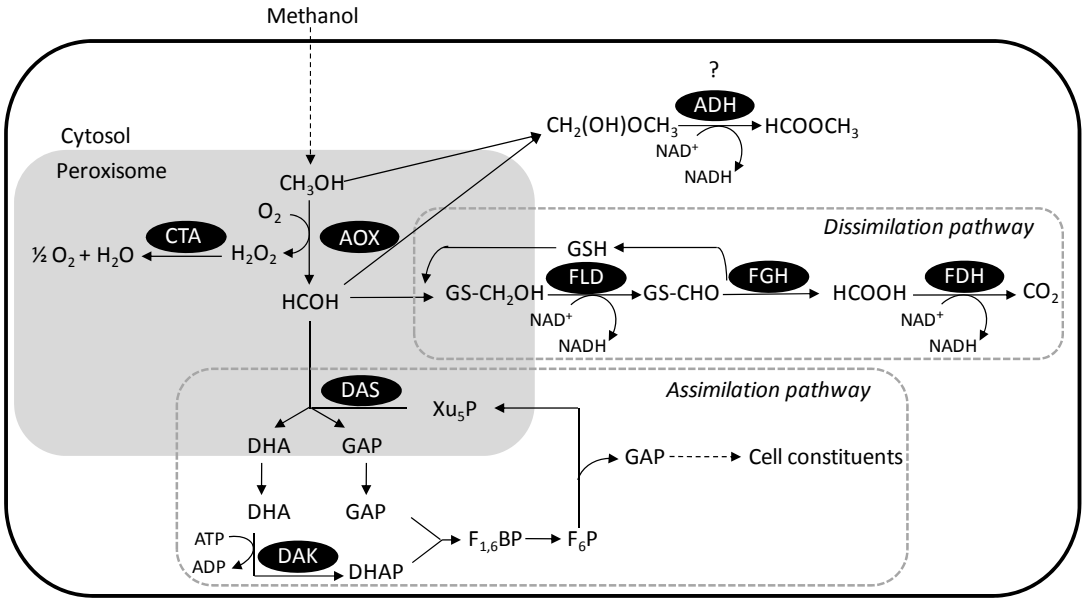

Figure 1.1. Methanol metabolism. Enzymes: AOX, alcohol oxidase; CTA, catalase; DAS, dihydroxyacetone synthase; DAK, dihydroxyacetone kinase FLD, formaldehyde dehydrogenase; FGH, S-formylglutathione hydrolase; FDH, NAD(+)-dependent formate dehydrogenase and ADH, alcohol dehydrogenase. Abbreviations: DHA, dihydroxyacetone; DHAP, dihydroxyacetone phosphate; F_6P, fructose 6-phosphate; FBP, fructose 1,6-bisphosphate; GAP, glyceraldehyde 3-phosphate; GS-CH_2OH, S-hydroxymethyl glutathione; GS-CHO, S-formylglutathione; GSH, reduced form of glutathione; GSSG, oxidized form of glutathione; Xu_5P, xylulose 5-phosphate. This picture was made based on [23, 25, 26].

The methanol pathway has been under rigorous research due to the extensive use of methanol-inducible promoters for commercial production of recombinant proteins [27]. The tightly regulated *aox1* promoter is the most widely utilized in *P. pastoris* for recombinant protein production [22]. *P. pastoris* strains with an engineered methanol utilization pathway have been recently reported [28]. Some key enzymes of the methanol pathway, FLD and DAS, were co-expressed in a producing *P. pastoris* strain and the effect on the growth rate, methanol uptake and productivity was analyzed [28]. The co-expression of DAS increased 2 to 3-fold the conversion of the substrate methanol into product, although the volumetric productivity was

reduced. Nevertheless, the co-expression of FLD not only increased the conversion of methanol to product 2-fold, but also showed an equivalent volumetric productivity compared to the non-engineered strain, pointing a target to improve recombinant protein production [28]. Therefore, it is essential to better elucidate the overall mechanism of methanol metabolism for further application. The methanol metabolic pathway has been attracting scientists also as a source of cofactors, such as NADH, for use in the chemical and drug industry. The improvement of the cofactor regeneration has been reported in *S. cerevisiae, C. boidinii* and most recently in *P. pastoris* strains with an engineered methanol oxidation pathway [29].

Another important area regarding this pathway is the crucial role of the peroxisomes in the methanol metabolism. In the first step of methanol oxidation, which occurs inside the peroxisomes, hydrogen peroxide (H_2O_2) is produced, increasing the intracellular reactive oxygen species (ROS) levels [30]. Although H_2O_2 has no unpaired electrons and thus is not a radical, it is also often qualified as ROS because it can easily convert into the highly reactive hydroxyl radical ($^{\bullet}OH$) [30-32]. The peroxisomal antioxidant enzymes are required to prevent the cell damage caused by these toxic molecules. Thus, when the methylotrophic yeasts are grown on methanol as the sole carbon and energy source, not only the enzymes involved in methanol metabolism are strongly induced, but the membrane-bound organelles, peroxisomes, which contain key enzymes of methanol metabolism, proliferate massively [23]. This means that the regulation of methanol metabolism can be accomplished in part, through control of peroxisome homeostasis. This feature has made methylotrophic yeasts useful model organisms for the study of peroxisome biogenesis and degradation [33, 34].

1.3. Autophagy: adaptation response to nutrient conditions

Autophagy is the process through which proteins and organelles are sequestered and delivered to the vacuole for breakdown and recycling [35, 36]. One of its primary roles is to regulate intracellular homeostasis and to adjust organelle numbers in response to stress such as changes in nutrient availability [35]. Autophagy is a process which is conserved from yeast to man [37]. Autophagic

research has increased significantly in the last years, especially due to the connection with cancer, neurodegenerative disease and various human developmental processes [37, 38]. Autophagy also appears to play an important role in filamentous fungi [37, 39]. The discovery of many of the autophagy genes (termed *ATGs*) and autophagy mechanisms were made in *S. cerevisiae* [40].

For a long time, starvation-induced autophagy has been considered a non-selective pathway [35]. However, numerous recent observations revealed that autophagy can also selectively eliminate specific proteins, protein complexes and organelles [41, 42]. Nonselective autophagy involves random uptake of portions of the cytoplasm (cytosol and organelles) in the vacuole for recycling [43] and during selective autophagy, a specific cargo is exclusively sequestered into the autophagosomes [35].

Autophagy of several organelles has been reported in the last years in yeast. Under starvation conditions, mitochondria [43] and ribosomes [44] were detected in the interior of autophagosomes in yeast cells; fragments of the ER were also enwrapped into autophagosomes and subsequently degraded in the vacuole [45]. The specific degradation of ribosomes is called ribophagy [46]. It has been recently shown that ribosomes are turned over through a selective type of autophagy [35]. Accurate examination of ribosome fate under nutrient starvation conditions in yeast *S. cerevisiae* has revealed that these structures are more rapidly degraded compared to other cytoplasmic components, supporting the notion of a selective degradation process [35]. Ribosome biogenesis and protein translation are among the most energy-consuming cellular processes, and it is therefore not surprising that these pathways are tightly controlled upon nutrient limitation [47].

1.3.1. Pexophagy: autophagic degradation of peroxisomes

Peroxisomes are organelles involved in many aspects of lipid metabolism and the elimination of peroxides. These organelles can be induced or turned over based on the needs of the cell [35]. The balance between biogenesis and degradation is tightly regulated and excess or damaged peroxisomes are degraded by an autophagy-related process called pexophagy [48].

Two forms of autophagy have been described: macroautophagy and microautophagy [32, 49, 50]. During macroautophagy, individual organelles (e.g., peroxisomes) are surrounded by double-membrane structures known as autophagosomes, which fuse with vacuole to deliver autophagic bodies into the vacuole lumen for degradation and recycling [32]. In microautophagy, clusters of organelles (e.g., cluster of peroxisomes) are engulfed by vacuolar sequestering membranes (VSMs), without prior formation of an autophagosome. This occurs either by direct invagination or through formation of finger-like protrusions that sequester cytoplasmic components. Once the engulfment is complete, the membrane and the sequestered material are degraded (Figure 1.2) [32].

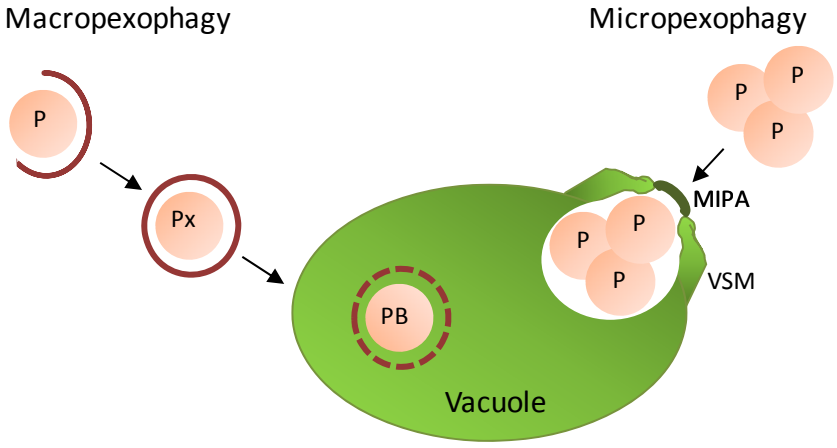

Figure 1.2. Degradation of peroxisomes in yeast by macro- and micropexophagy. Left: Macroautophagy involves sequestration and degradation of peroxisomes by engulfment into autophagosomes. After sequestration is complete, the outer layer of the now formed pexophagosome (Px) fuses with the vacuolar membrane. Upon entry into the vacuole, the resulting pexophagic body (PB) will be degraded by vacuolar hydrolases. Right: Micropexophagy is morphologically characterized by vacuolar extensions (vacuolar sequestration membranes, VSM) and the cup-shaped micropexophagy apparatus (MIPA) that capture the peroxisome cluster. P, peroxisomes; Px, pexophagossomes; PB; pexophagic body. This picture was made based on [32, 40, 49].

In *P. pastoris*, peroxisomes can be induced when cells are grown in media containing methanol, oleate or amines. Transferring cells grown in methanol to ethanol or from oleate or methylamine to glucose without nitrogen induces macropexophagy. Shifting cells from methanol to glucose medium induces micropexophagy [36]. Intriguingly, the two modes of pexophagy can be triggered by different experimental conditions in different yeasts. In *H. polymorpha*

macropexophagy is induced rather than micropexophagy when cells are shifted from methanol medium to glucose [36]. In *P. pastoris*, the choice between induction of either micro- or macropexophagy was suggested to be determined by ATP levels in the cell [51]. High levels of ATP induce micropexophagy while lower levels activate macropexophagy. One explanation for this observation may be that the massive vacuolar re-arrangement during micropexophagy and formation of the MIPA may be a more energy-intensive process than formation of the pexophagosome and thus may demand more energy in the form of ATP from the cell [51]. Some autophagy-related proteins (ATG26, 28 and 30) are required for both micro- and macropexophagy in *P. pastoris* [52-54]. However, ATG35 from *P. pastoris* is specifically required for micropexophagy [55].

Pexophagy has emerged recently as an important process for the vitality of several fungi under different growth conditions. For example, *H. polymorpha* peroxisomes are constitutively degraded by autophagy during the growth of cells in methanol medium despite the continuous induction of peroxisome proliferation [56]. Some of these peroxisomes have decreased activity of peroxisomal catalase that is associated with increased cellular levels of reactive oxygen species (ROS) [56]. Peroxisomal proteolysis and constitutive autophagy of peroxisomes might represent two independent mechanisms protecting cells from accumulation of peroxisomal protein aggregates and ROS under peroxisome proliferation conditions [40].

Despite the advantages of the methylotrophic yeast *P. pastoris*, studies of pexophagy frequently use the model of baker's yeast *S. cerevisiae*. In baker's yeast, peroxisome proliferation is induced only by oleate, while in *P. pastoris*, both oleate and methanol induce peroxisome proliferation; being methanol able to induce much larger peroxisomes [57]. Furthermore, *P. pastoris* possesses two types of peroxisome degradation, macropexophagy and micropexophagy; micropexophagy is induced by glucose in *P. pastoris*. Only macropexophagy is known for baker's yeast [57]. In addition, *P. pastoris* has been frequently used as a model to study the autophagy of peroxisomes during glucose adaptation and ethanol adaptation [58]. However, little is known about peroxisomes biosynthesis and degradation in *P. pastoris* during growth on methanol.

1.4. Stress responses due to recombinant protein production

It is well-known nowadays that the utilization of yeast for recombinant protein production may expose them to several stress conditions and consequently influence the final yield [59]. Regarding the methylotrophic yeasts, oxidative stress caused by methanol degradation is an important issue. Oxidative stress can be simply defined as a state where there is a relative imbalance within cells between generation and removal of reactive oxygen species (ROS) [60]. The methanol metabolism leads to high oxygen consumption resulting in ROS generation which could have detrimental effects on cells in case they can not remove these molecules. To reduce the ROS level in the cell, anti-oxidant enzymes are required and the degradation of peroxisomes also plays a role as previously described. Additionally, the overexpression of recombinant protein can overburden the cell ability to fold them in the endoplasmic reticulum (ER). The resulting accumulation of misfolded or unfolded proteins will elicit the unfolded protein response (UPR) and ER-associated protein degradation (ERAD).

1.4.1. Protein folding and unfolded protein response (UPR)

Protein folding takes place in three main subcellular compartments, cytosol, endoplasmic reticulum (ER) and mitochondria [61]. Each organelle is equipped with a specific set of folding assistants [61].

The ER is the cradle of all cell surface proteins and proteins that are secreted to the extracellular space [62]. Such proteins are synthesized on ER-bound ribosomes and translocated into ER lumen where they attain their native conformation [61]. Most of the proteins leave the organelle once they are fully folded [62]. The ER folding factory sustains a special set of covalent modifications, which include signal sequence processing, disulfide bond formation and N-glycosylation [63]. The mature proteins which could fold into correct structure are coated by transport vesicles, delivered to the secretion pathway of the Golgi apparatus and subsequently transported to the extracellular space, vacuoles or other organelles (Figure 1.3) [64].

Meanwhile, misfolded proteins get accumulated in the ER lumen and are recognized by the quality control (QC) system. As a reaction, many cellular responses are activated simultaneously in a process called "unfolded protein response" (UPR) [61]. In the ER, folding and disulfide bond formation rate is increased by up-regulating chaperones and foldases. Oxidative stress response genes are also activated due to the increased disulfide bond formation activity and the subsequent reactive oxygen species generated [65]. Glycosylation processing elements of the ER and Golgi are also up-regulated to increase processing capacity of the secretory pathway. Trafficking components used in COPI, COPII, and post-Golgi vesicles are up-regulated. The metabolic pathways for lipid and inositol are also up-regulated, to increase the amount of membrane. Membranes, while often not considered to be an active component of the secretory pathway, provide essential surface area that is essential for almost all secretory pathway processes [66].

The initial description and major progress in understanding the molecular mechanisms of the UPR was done using the yeast *S. cerevisiae*. Specifically, this yeast was used for the molecular cloning of the UPR transducer IRE1 and the UPR-specific transcription factor HAC1 [67].

A schematic overview of the protein folding process and unfolded protein stress response in yeast is presented in Figure 1.3.

Under non stress condition, IRE1 is a monomeric protein closely associated with the ER chaperone binding protein (KAR2), IRE1 is then stabilized in an inactive state [68]. KAR2 is the yeast homologue of mammalian BiP, an ER-resident member of the HSP70 family and the expression of *KAR2* gene is up-regulated by the UPR [69]. KAR2 recognizes hydrophobic regions of peptides that are usually buried inside native proteins [70]. IRE1 is a transmembrane protein oriented with the N-terminal in the ER lumen and the C-terminal in the cytosol [68]. When the unfolded protein accumulates in the ER lumen, KAR2 dissociates from IRE1 in order to bind to unfolded proteins [68]. This allows IRE1 to dimerize, be autophosphorylate and to activate its endonuclease activity [68]. The activated IRE1 transmits a signal to cut *HAC1* mRNA at two sites, removing the introns. After the splicing, *HAC1* mRNA is efficiently translated. HAC1 is a transcriptional

activator that up-regulates expression of UPR target genes by binding to the promoter of genes encoding ER-resident chaperones and other proteins [67]. HAC1 is known to activate or repress over 100 genes, including *KAR2*, *PDI* and *ERO1* in *S. cerevisiae* [71]. *HAC1* mRNA is constitutively expressed, but because of the secondary structure of the intron, no protein is produced when the mRNA remains unspliced [72]. The *HAC1* gene and splice event was recently characterized in *P. pastoris* [73]. Nascent glycoproteins are bound by CNE1, a *S. cerevisiae* homologue of the mammalian calnexin [74], which mediates the correct folding and processing of the N-glycans. Prolonged binding to either calnexin or the KAR2 complex targets the polypeptides to degradation [75].

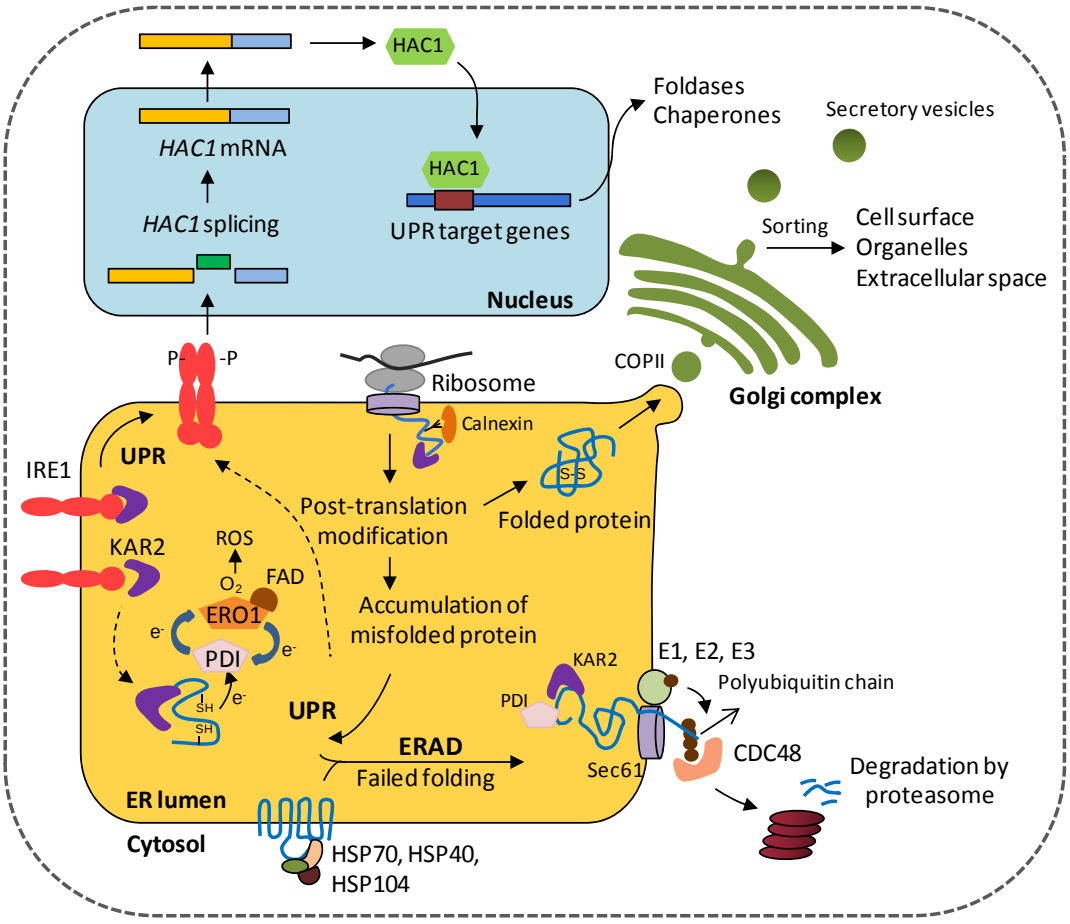

Figure 1.3. Schematic diagram representing folding protein and the unfolded protein response (UPR) in yeast. This picture was made based on [67, 76-79].

The formation of disulfide bonds is an important step in the maturation of the extracellular domains of both membrane and secreted proteins. Protein disulfide bonds are formed in the ER of eukaryotes and this process involves two proteins:

oxidoreductin 1 (ERO1) and protein disulfide isomerase (PDI) [80]. PDI is a multifunctional protein resident in the ER lumen which is responsible for the correct formation of disulfide bonds during oxidative folding and the isomerisation of incorrectly folded disulfides [78]. The disulfide bonds formation requires the transference of electrons from cysteine to PDI which in turn passes the electrons to FAD-bound ERO1 [81]. Finally, ERO1 passes electrons to molecular oxygen, resulting in the production of ROS [76]. The rate of protein folding is dependent upon the complexity of the protein to be folded, the availability of chaperones to assist folding and ATP used by chaperones [76, 81]. This mechanism forms disulfide bridges randomly, and the correct pairings must be found by a trial and error process, involving the repeated oxidation/reduction of cysteines by PDI [66].

If protein repair by ER chaperones is unsuccessful, aberrant proteins are cleared from the ER by a mechanism termed ER-associated degradation (ERAD) [77]. During ERAD, misfolded proteins are translocated, through the ER-membrane protein Sec61, back to the cytosol where they are conjugated to ubiquitin and directed to proteasomal degradation [77]. Ubiquitination is a modification carried out by a set of three enzymes, E1 (ubiquitin-activating enzymes), E2 (ubiquitin-conjugating enzymes) and E3 (ubiquitin ligase) [82]. Retro-translocation of ERAD substrates and their delivery to the proteasome can be catalyzed by a chaperone-like AAA ATPase, known as CDC48, the highly conserved homologue of mammalian p97 in *S. cerevisiae* [83]. As a multiubiquitin-binding protein, it was proposed that CDC48 recognizes multiubiquitin moieties on many proteins, including ERAD substrates and targets them to the proteasome for degradation [83]. The chaperone KAR2 and the isomerase PDI are also important components of the retro-translocation machinery [79]. Prior to the retro-translocation to the cytosol PDI reduces the disulfide bonds present in the protein [84]. KAR2 was suggested to maintain the solubility of ERAD substrates [85].

The degradation of misfolded ER membrane proteins requires a different set of chaperones as compared to ER lumenal proteins, due to the exposure of protein misfolded domain to the cytosol [79]. SSA1, a cytosolic HSP70 in yeast, is required for the ERAD of several membrane proteins [77, 86]. SSA1 probably maintains the solubility of misfolded cytosolic domains on at least some integral membrane ERAD substrates, which would facilitate their delivery to and

degradation by the proteasome [77]. It is also unclear how precisely chaperones act as "decision makers" for the ER quality control system [87]. Distinct chaperone classes have unique effects depending upon the ERAD substrate. For example, BiP/Jem1/Scj1 are required not only for the folding of carboxypeptidase Y (CPY), but also for the degradation of the ERAD target CPY [87]. It has become clear in recent years, that chaperones play a central role in the elimination process of proteins that are either damaged, terminally misfolded or do not fold in a certain time frame [79]. The interaction between chaperone and the unfolded protein keeps the unfolded protein soluble and helps to acquire a native structure [79]. The clearest picture is presently available for the chaperones of the HSP70 family members with their HSP40 co-chaperones [79]. What specifically these chaperones recognize and how they decide whether a protein is properly folded or will be degraded is still unknown [79, 87].

1.4.1.1. Environmental impact on protein folding and secretion

The impact of environmental factors on the productivity of *P. pastoris* cells has been investigated in the past years and the changes in the proteins involved in folding and degradation were always an object to better understand their effect on the final product yield. Among environmental factors that affect protein folding and secretion, especially temperature, high osmolarity and oxidative stress may play important roles [78].

Temperature has a profound impact on cell metabolism and regulation of folding related genes/proteins [78]. The decrease of the cultivation temperature from 30 to 20°C led to a down-regulation of chaperones from the HPS70 family, such as SSA4 and SSB1, as well HSP60 and HSP82. KAR2 was also down-regulated while the PDI did not show any change at lower temperatures [88]. At 20°C, the specific productivity of the human antibody Fab fragment increased 3 fold [88]. The lower temperature may lead to a higher stability of protein and a reduced demand for protein refolding or degradation, resulting in a higher secretion capacity [88].

Although oxygen limitation affects the core metabolism by causing energy deprivation [89], it was shown recently that very low oxygen supply enhances the secretion rate of heterologous proteins in *P. pastoris* [90]. Besides affecting growth and protein production, oxygen also plays a role in cellular redox reactions which

are closely connected with protein folding reactions within the cell [81]. When *P. pastoris* cells were exposed to severe oxygen limitation the stress response was highly activated, which was demonstrated by the up-regulation of the chaperones SSA4 and TSA1 at protein level. At transcript level *HAC1, PDI1* and *ERO1* were significantly increased by hypoxia, while the transcription of *KAR2* and *IRE1* was not affected [89]. It was assumed that the significant induction of some UPR genes under hypoxia could benefit protein folding and secretion, probably by reducing the ROS generation [89].

Response to hyperosmolarity in yeast has also been analyzed in the last years. The adjustment of protein folding machinery in different yeasts was previously reported upon high osmolarity [91, 92]. Proteins from the HSP70 family, such as KAR2, and PDI were found to be up-regulated in a high salt concentration medium as part of a mechanism which alleviates the damaging effects of high salt on protein folding in the yeast *Rhodotorula mucilaginosa* [93]. On the other hand, the heat shock protein SSB was found to be down-regulated in the same study [93]. The major impact of osmolarity on the *P. pastoris* proteome was reported to be on proteins involved in energy metabolism and protein folding [94]. An increased level of some proteins from UPR, such as KAR2, PDI, SSC1, HSP60 and SSA4, was observed in a medium at high osmolarity in a non producing strain, while no change was observed in the producing strain. It has been previously reported that osmotic stress applied prior to induction of protein secretion resulted in higher level of scFv antibody in *P. pastoris* [95], due to the UPR-like response, which makes the cells already conditioned for a better folding response compared to the untreated cells [94].

1.4.1.2. Overcoming folding stress in recombinant protein production

As a straightforward strategy, overexpression of multiple chaperones, PDIs and other folding helpers seemed to be an effective approach [63]. The co-expression of *S. cerevisiae* and more recently *P. pastoris HAC1* has been used successfully as a tool to improve the recombinant protein production [73, 96]. The overexpression of *S. cerevisiae* PDI proved to be functional in *P. pastoris* by enabling the increase of the antibody fragment Fab production level by 1.3-fold [96] and facilitating the secretion of the human parathyroid hormone [97]. The co-expression of KAR2 is

reported to enhance cell growth as well as the production of antithrombic hirudin [98] and, the secretion of human erythropoietin [99] in *S. cerevisiae.* On the other hand, the co-expression of KAR2 could also decrease the yield of the recombinant protein [100]. The effect of coexpression of chaperone and foldase genes strongly depends on the properties of the target protein and, moreover, it seems that fine-tuned (optimal amount) overexpression of these genes is required to generate a functional secretory network to improve foreign protein overproduction [78]. Elevating expression of the chaperones, e.g., KAR2, may also facilitate target protein degradation via the ER-assisted degradation [100] and co-expression of chaperones genes could compete with target genes for transcription, translation and folding in the cell [101].

As a result of a strict QC system in the ER, protein folding often has a tendency to become the bottleneck in heterologous protein secretion. Thus, genetic modification of the ER protein folding and QC system has become the most useful approach in the current strain engineering method to overcome the drawbacks in the cell specific productivities. The wide range of cell specific secretion titers for different proteins in yeast still raises the important question as to whether environment-, host- or protein-based factors limit the cell specific protein secretion levels [63]. Most of the data regarding stress responses come from *S. cerevisiae* studies and are not in a industrial relevant scale [59]. Therefore, there is an urgent demand for research on physiological response on the new yeast generation as *P. pastoris* to bring new insights on the adaptation of the host to stressful situations.

1.5. Proteome analysis

To date, there are only few published studies concerning the physiological adaptations of *P. pastoris* facing different environmental conditions [88, 89, 94, 102]. Additionally, although the *aox1* promoter is the most widely utilized in *P. pastoris* and this yeast has been a successful recombinant protein production platform for decades [11, 22], there is very little known about the intracellular proteome of *P. pastoris* in methanol-induced cultures [103]. Despite the rapid development of many gel-free proteomic techniques, classical combination of two-dimensional electrophoresis (2-DE) and mass spectrometry (MS) is still the workhorse for quantitative proteomic studies [104]. Protein mixtures from cells are

separated by 2-DE. Proteins are separated by charge in the first dimension and then by size in the second dimension, yielding spots on a polyacrylamide gel. The gel is further stained, and each observed protein spot is quantified by its staining intensity. Selected spots are excised, digested into short peptide fragments and analyzed by MS [105].

The term "proteomics" was first introduced in the mid-90s by Wilkins and colleagues [106], and defined as the study of the proteome. After the "transcriptomic era", the field of proteome analysis has gained popularity in various research areas [104]. Although the measurement of transcribed mRNA has proven to be very powerful in the elucidation of functional mechanisms, alone it is not sufficient for the characterization of biological systems as a whole [107]. Examples in which the mRNA and the protein production profiles show only a rather weak correlation are increasing [104]. In a transcriptome and proteome study of *S. cerevisiae* under oxygen deprivation, the data of glycolysis, amino-acyl-tRNA synthesis, purine nucleotide synthesis and amino acid biosynthesis showed a weak connection, leading to a strong evidence for post-transcriptional regulation of these key cellular processes [108]. Control of biological systems not only involves transcription and mRNA stability, but also control at other levels such as mRNA processing, nuclear export, translation and protein degradation [109]. Therefore, the disparities between mRNA and protein abundance are not unexpected [109]. Integration of transcriptome and proteome data leads to new insights into the physiology of growing yeast and it is fundamental to understand the entire network of reactions in the living cell.

The public genome sequences of *P. pastoris* GS115 and DSMZ 70382 are now available. A total of 5,313 and 5,450 predicted ORFs were identified in GS115 and DSMZ 70382, respectively [110, 111]. These two databases provide a powerful tool to study and pinpoint global cellular responses derived from recombinant protein production in *P. pastoris* under bioprocess-relevant conditions [112].

One major obstacle towards directed strain engineering in alternative host systems seems to be the lack of detailed knowledge of host physiology, molecular biology and biochemistry. The aim of this work was to perform a comprehensive analysis of the intracellular proteome of *P. pastoris* GS115 and X-33 throughout fed-batch

cultivation, producing high level of recombinant hepatitis B virus surface antigen (HBsAg) and insulin precursor (IP) under the control of the methanol-regulated promoter (*aox1*). The analyses were focused on the stress caused to the cell by methanol degradation and recombinant protein production leading to the induction of oxidative stress and unfolded protein response pathway.

The insights gained in this study will enable us to better understand the global cellular physiology of *P. pastoris,* essential for further development of metabolic and cellular engineering strategies.

2. Aim of this work

The yeast *Pichia pastoris* has been recognized as an effective host for recombinant protein production and has been widely used to produce high yield of proteins for both basic research and industrial use. Unfortunately, the current knowledge of the changes in physiology of this yeast under bioprocess-relevant conditions is still scarce.

The aim of the present study is to analyze the physiological response of *P. pastoris* to overproduction of intracellular hepatitis B virus surface antigen (HBsAg) and secreted insulin precursor (IP) in large scale cultivation under the control of a methanol-regulated promoter (*aox1*). The cell adaptation facing a carbon source transition from glycerol (growth phase) to methanol (production phase), as well as stress responses such as oxidative stress and unfolded protein response will be analyzed. Additionally, autophagic responses of the cells to nutrient conditions throughout cultivation processes will be also investigated in this work. The new insights into the global mechanisms connecting protein production to environmental conditions gained in this study can serve as a valuable basis for future rational strain engineering.

For this purpose, samples from two different cultivations of *P. pastoris* producing the HBsAg and IP will be analyzed. Sample at different time points will be collected and the protein identification and analysis of changes in the proteome will be done using 2D gel electrophoresis combined with MALDI-TOF. Also, electron microscopic studies of the cells will be used in order to analyze the adaptation response, such as autophagy, to the environmental nutrient conditions.

3. Physiological response of *Pichia pastoris* GS115 to methanol-induced high level production of the Hepatitis B surface antigen: catabolic adaptation, stress responses, and autophagic processes

In the first part of this work the proteome profile of *Pichia pastoris* GS115 producing high level of the hepatitis B surface antigen (HBsAg) under the control of *aox1* promoter was analyzed. 2D gel electrophoresis was employed to measure the relative changes in protein abundance during the cultivation. These results were combined with electron microscopy to better understand the physiological response of the cell under a relevant bioprocess condition. The stress caused to the cell by protein overproduction as well by using methanol as a carbon source during the induction phase are described in the published work integrated in this thesis.

The present chapter is reprinted from the following article [113] and it is a courtesy of BioMed Central. It is an open acess publication.

Vanz AL, Lünsdorf H, Adnan A, Nimtz M, Gurramkonda C, Khanna N, Rinas U. Physiological response of *Pichia pastoris* GS115 to methanol-induced high level production of the Hepatitis B surface antigen: catabolic adaptation, stress responses, and autophagic processes. Microb Cell Fact 2012, 11(1):103

3.1. Abstract

Background

Pichia pastoris is an established eukaryotic host for the production of recombinant proteins. Most often, protein production is under the control of the strong methanol-inducible *aox1* promoter. However, detailed information about the physiological alterations in *P. pastoris* accompanying the shift from growth on glycerol to methanol-induced protein production under industrial relevant conditions is missing. Here, we provide an analysis of the physiological response

of *P. pastoris* GS115 to methanol-induced high-level production of the Hepatitis B virus surface antigen (HBsAg). High product titers and the retention of the protein in the endoplasmic reticulum (ER) are supposedly of major impact on the host physiology. For a more detailed understanding of the cellular response to methanol-induced HBsAg production, the time-dependent changes in the yeast proteome and ultrastructural cell morphology were analyzed during the production process.

Results

The shift from growth on glycerol to growth and HBsAg production on methanol was accompanied by a drastic change in the yeast proteome. In particular, enzymes from the methanol dissimilation pathway started to dominate the proteome while enzymes from the methanol assimilation pathway, e.g. the transketolase DAS1, increased only moderately. The majority of methanol was metabolized via the energy generating dissimilatory pathway leading to a corresponding increase in mitochondrial size and numbers. The methanol-metabolism related generation of reactive oxygen species induced a pronounced oxidative stress response (e.g. strong increase of the peroxiredoxin PMP20). Moreover, the accumulation of HBsAg in the ER resulted in the induction of the unfolded protein response (e.g. strong increase of the ER-resident disulfide isomerase, PDI) and the ER associated degradation (ERAD) pathway (e.g. increase of two cytosolic chaperones and members of the AAA ATPase superfamily) indicating that potential degradation of HBsAg could proceed via the ERAD pathway and through the proteasome. However, the amount of HBsAg did not show any significant decline during the cultivation revealing its general protection from proteolytic degradation. During the methanol fed-batch phase, induction of vacuolar proteases (e.g. strong increase of APR1) and constitutive autophagic processes were observed. Vacuolar enclosures were mainly found around peroxisomes and not close to HBsAg deposits and, thus, were most likely provoked by peroxisomal components damaged by reactive oxygen species generated by methanol oxidation.

Conclusions

In the methanol fed-batch phase *P. pastoris* is exposed to dual stress; stress resulting from methanol degradation and stress resulting from the production of the recombinant protein leading to the induction of oxidative stress and unfolded protein response pathways, respectively. Finally, the modest increase of methanol assimilatory enzymes compared to the strong increase of methanol dissimilatory enzymes suggests here a potential to increase methanol incorporation into biomass/product through metabolic enhancement of the methanol assimilatory pathway.

Keywords

Pichia pastoris, Proteome, *Aox1* promoter, Carbon metabolism, ER stress, Autophagy

3.2. Background

The methylotrophic yeast *Pichia pastoris* is nowadays a well-established eukaryotic host for the heterologous production of technical enzymes and also for protein pharmaceuticals [10, 114]. *P. pastoris* naturally possesses two different genes (*aox1* and *aox2*) encoding alcohol oxidases for oxidation of methanol, the first step in methanol degradation [115]. *Aox1* is highly expressed during growth on methanol, thus the strong *aox1* promoter is utilized most often to drive the production of foreign proteins. Another attempt to enhance the yield of the target protein is to increase its chromosomal gene dosage which - up to a certain target-protein dependent extent - can further increase product levels [116-119]. However, increasing the gene copy number beyond a target protein-dependent threshold can have a severe impact on cell growth and viability including a reduced level of the target protein [117, 120-122]. In particular, overburdening the cellular protein export machinery for production of extracellular proteins can cause severe stress responses [78]. The passage of export-destined proteins through the secretory pathway often presents a bottleneck leading in many cases to partial retention of the target protein in the endoplasmic reticulum (ER) and a transcriptional up-

regulation of the Unfolded Protein Response (UPR) and the ER-Associated Degradation (ERAD) pathway [123, 124].

In this study we investigated the physiological changes accompanying the methanol-induced high-level production of HBsAg, the major surface antigen of the Hepatitis B virus (HBV) employed for vaccination against HBV, in *P. pastoris* under industrially relevant conditions. The antigen is a very stable and also a very hydrophobic protein and not secretable in yeast expression systems [125]. Thus, production occurs as intracellular protein in *P. pastoris* GS115 carrying 8 copies of the gene encoding mature HBsAg without employing yeast-derived secretory signals [116]. Cells are grown on defined medium in a controlled fed-batch procedure maintaining the methanol concentration at 6 g L^{-1} through continuous methanol feeding during the production phase [126]. Although not destined for export the HBsAg is translocated into the ER where it is retained leading to a bulging of the ER into cloud-shaped irregular formations [125]. The very hydrophobic HBsAg is not further passaged in the secretory pathway but assembles into well-ordered multi-layered lamellar structures in the ER which are transformable into virus-like particles (VLPs) during down-stream processing [125]. The high-level production and the retention of the protein in the ER are supposedly of major impact on the cell physiology. For a more detailed understanding of the cellular response to methanol-induced high level HBsAg production, we followed the changes in the yeast proteome and the ultrastructural cell morphology during the HBsAg production process.

3.3. Results and discussion

The physiological alterations accompanying the adaption of recombinant *Pichia pastoris* to methanol-induced high-level production of HBsAg were followed by proteome analysis and electron microscopy. Cells were grown initially on glycerol, and after depletion of glycerol, methanol was added to a final concentration of 6 g L^{-1} to initiate HBsAg production. This methanol concentration was kept constant through appropriate methanol feeding for the remaining fed-batch phase of the cultivation [126]. After an initial growth arrest and a short period of adaptation to methanol (~3-4 h), cells started to consume methanol and the biomass

increased from 60 to 100 g L^{-1} cell dry mass during the first 90 - 100 h of the methanol feeding phase [126]. During this period, the intracellular HBsAg levels increased strongly reaching a final maximum of 6 - 7 g L^{-1} (thereof 30% soluble HBsAg competent for assembly into VLPs). Beyond this period, cell viability declined concomitant with a decrease of the soluble fraction of HBsAg [126]. Thus, this production process is characterized by four distinct phases: *i*. glycerol batch phase, *ii*. adaptation phase to methanol, *iii*. production phase, and *iv*. decline phase. From all these phases representative samples were taken for proteome analysis. The complete list of all identified proteins with their corresponding changes and classified into functional categories and a 2D gel image indicating all identified proteins are found in the Additional file 1. Moreover, cell physiological changes were also followed by ultrastructural analysis using transmission electron microscopy.

3.3.1. Carbon metabolism: cell adaptation to carbon source change from glycerol to methanol

The intracellular proteome of *Pichia pastoris* exhibited a dramatic change in response to the shift from growth on glycerol to production and growth on methanol (Figure 3.1 A and B).

3.3.1.1. Methanol metabolism

In particular, proteins required for methanol utilization which were only present in minor amounts during growth on glycerol started to dominate the proteome after the onset of the methanol feeding phase. Surprisingly, a major protein which accumulated during growth on methanol was identified as alcohol oxidase 1 (AOX1) (Figures 3.1 A-C, 3.2 and Additional file 2). This HBsAg producing strain was first classified as Mut^s [116], hence the presence of *aox1* and the accumulation of AOX1 unexpected. A comprehensive analysis verified the formation of AOX1 as well as the presence of the intact encoding gene *aox1* (for details please refer to Additional file 2). Thus, high level recombinant protein production may lead to impaired growth on methanol despite the presence of functional *aox1*.

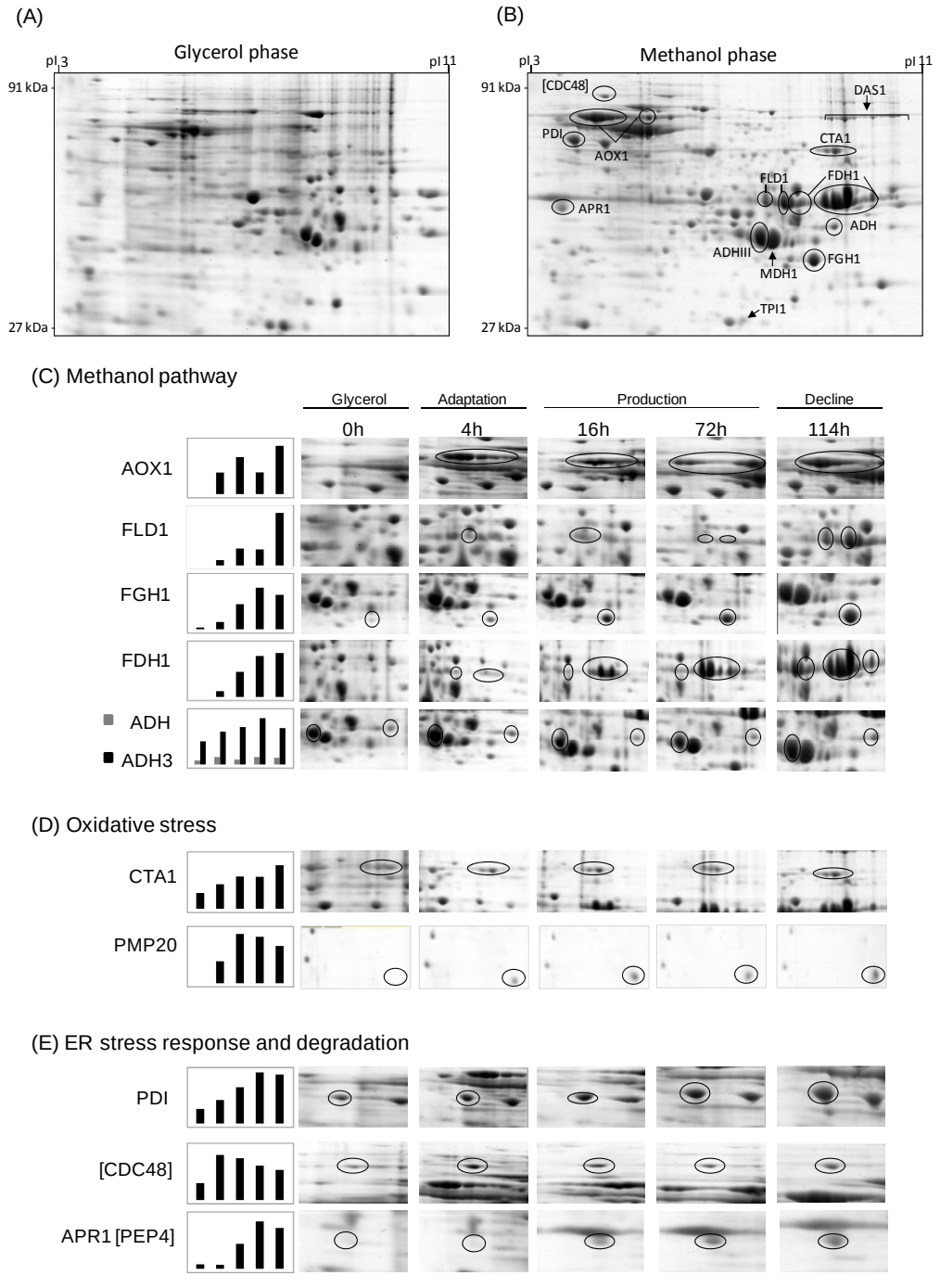

Figure 3.1. Change of the intracellular proteome of *P. pastoris* GS115 in response to methanol-induced high-level production of the Hepatitis B surface antigen. Sections of 2D gels representing parts of the intracellular proteome (A) at the end of the glycerol batch phase and (B) 114 hours after the onset of methanol feeding. For encircled protein spots (dark lines) time-dependent changes are given below. Magnified 2D gel sections from samples taken at the end of the glycerol batch phase and 4, 16, 72 and 114 hours after the onset of methanol feeding with representative proteins involved in (C) methanol metabolism and (D) oxidative and (E) ER stress responses (including also vacuolar degradation).

In addition to AOX1 also the NAD^+-dependent formate dehydrogenase (FDH1), the enzyme catalyzing the last step in the methanol dissimilation pathway increased to very high levels in the methanol feeding phase (Figures 3.1 A-C and 3.2). The other two enzymes of the methanol dissimilation pathway, the S-(hydroxymethyl)-glutathione dehydrogenase (FLD1) and S-formylglutathione hydrolase (FGH1), also increased strongly but not as pronounced as AOX1 and FDH1 (Figures 3.1 A-C and 3.2).

Interestingly, AOX1 already accumulated to high levels during the adaption phase to methanol (Phase II), while the subsequent enzymes of the methanol dissimilation pathway reached their highest concentrations in the production phase (Phase III) or even later in the decline phase (Phase IV) (Figure 3.1 A-C). Methanol is not only oxidized by *Pichia pastoris* in the dissimilation pathway for potential energy generation through reoxidation of NADH in the respiratory chain but can also be incorporated into biomass in the assimilation pathway. In this case, formaldehyde, which is formed through oxidation of methanol by AOX1 (or AOX2), is not further converted to carbon dioxide, but condensed with xylulose 5-phosphate (Xu_5P), through the action of dihydroxyacetone synthase (DAS1), a special transketolase which converts formaldehyde and Xu_5P into the central C3-compounds dihydroxyacetone (DHA) and glyceraldehyde 3-phosphate (GAP) [25] (Figure 3.2).

In contrast to the strong increase of the enzymes from the methanol dissimilation pathway, the level of DAS1 increased only moderately during the production phase (Figures 3.1 A, B and 3.2) suggesting that the majority of methanol is processed through the dissimilation pathway leading to the generation of NADH and carbon dioxide. In fact, a carbon mass balance analysis revealed that 70 - 80% of the methanol metabolized is converted into carbon dioxide in the methanol fed-batch phase (data not shown). Interestingly, the mitochondrial area within cellular cross sections increased significantly during the methanol fed-batch phase (Figure 3.3) probably as a result of the elevated NADH supply from methanol dissimilation and the enhanced energy demand for growth, production and cell maintenance (e.g. repair and recycling).

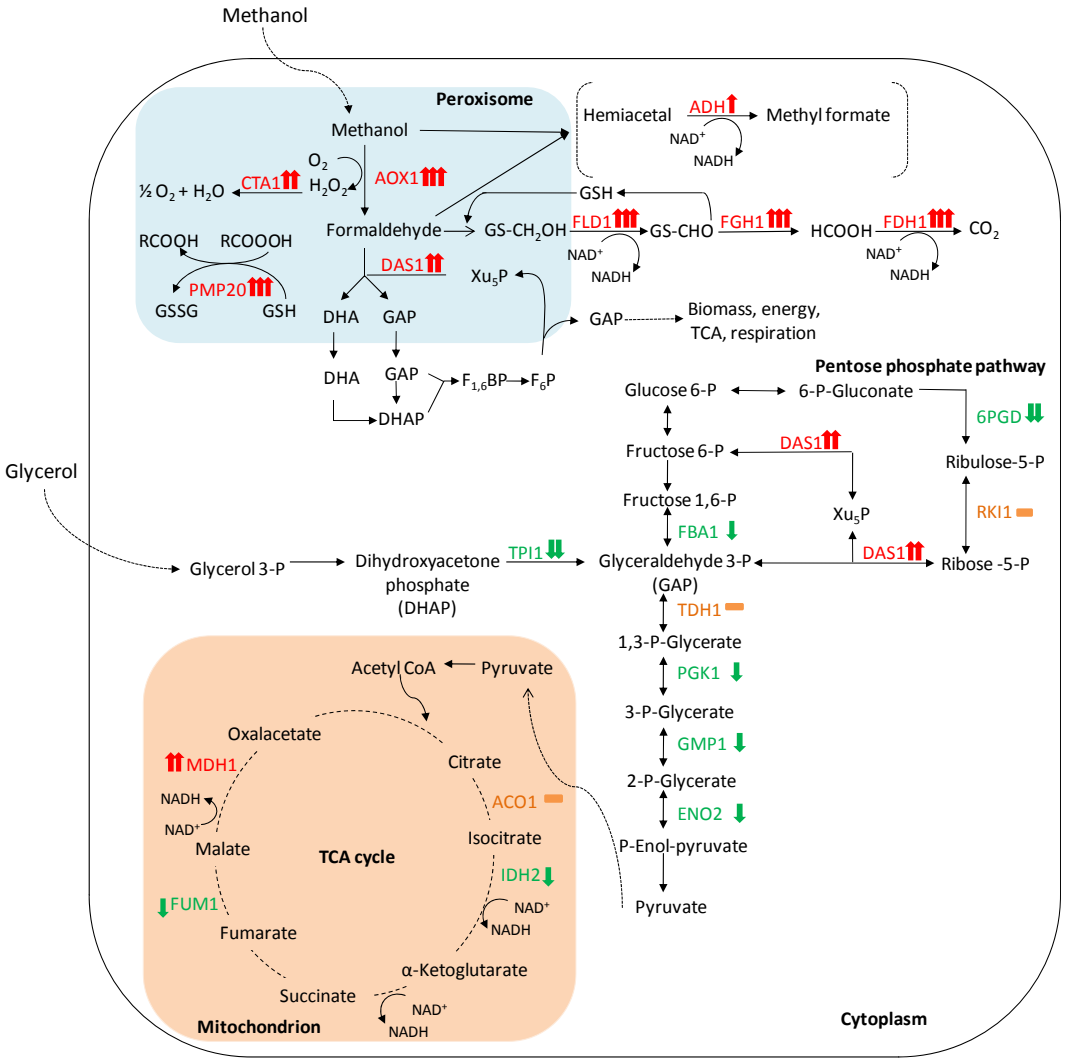

Figure 3.2. Simplified carbon metabolic network. Identified enzymes from pathways involved in glycerol and methanol metabolism, from the glycolytic and pentose phosphate pathway, and TCA cycle and their changes in response to the shift from growth on glycerol to growth and HBsAg production on methanol. The red arrow (↑) indicates an increasing and the green arrow (↓) a decreasing amount of the enzyme in the methanol fed-batch phase. An orange dash (−) indicates no significant change. One arrow indicates small (0.6-1 log2 change), two arrows strong (1–4 log2 change) and three arrows very strong changes (> 4 log2 change). Abbreviations (enzymes): AOX1, alcohol oxidase 1; CTA1, catalase; PMP20, peroxiredoxin; FLD1, formaldehyde dehydrogenase; FGH1, S-formylglutathione hydrolase; FDH1, NAD(+)-dependent formate dehydrogenase; ADH, alcohol dehydrogenase; DAS1, transketolase (dihydroxyacetone synthase); TPI1, triose phosphate isomerase; FBA1, fructose 1,6-bisphosphate aldolase; TDH1, glyceraldehyde-3-phosphate dehydrogenase; PGK1, 3-phosphoglycerate kinase; GMP1, tetrameric phosphoglycerate mutase; ENO2, enolase; 6PGD, 6-phosphogluconate dehydrogenase; RKI1, 1- ribose-5-phosphate ketol-isomerase; ACO1, aconitase; IDH2, subunit of mitochondrial NAD(+)-dependent isocitrate dehydrogenase; FUM1, fumarase; MDH1, mitochondrial malate dehydrogenase.

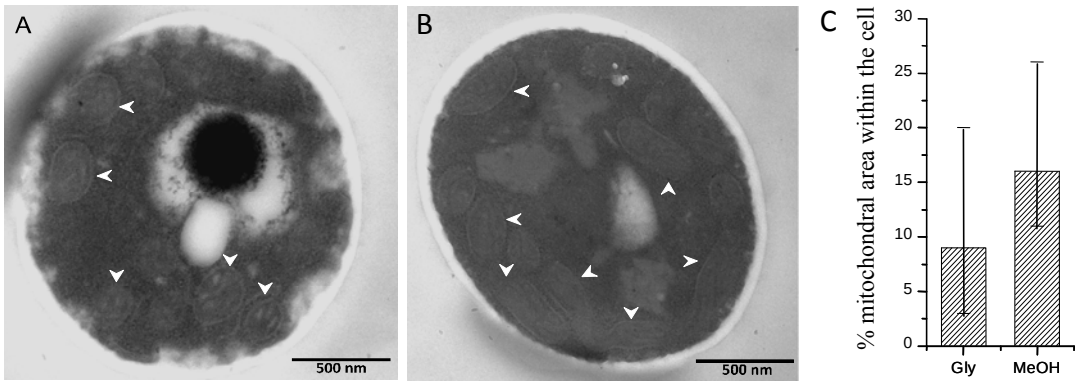

Figure 3.3. Mitochondrial morphology and size changes during methanol-induced high-level production of the Hepatitis B surface antigen. Transmission electron micrographs of *P. pastoris* GS115 (A) at the end of the glycerol batch phase and (B) 112 hours after the onset of methanol feeding. White arrow heads indicate mitochondria. (C) Quantification of the average total mitochondrial area within the cross sectional average cell area. The vertical bars encompass individual cell variance, e.g. the lowest and highest total mitochondrial area observed in a single cell in each growth phase; (left column) at the end of the glycerol batch phase and (right column) 112 hours after the onset of methanol feeding.

3.3.1.2. Glycolysis, pentose phosphate pathway, and tricarboxylic acid (TCA) cycle

In contrast to the strong increase of the enzymes from the methanol utilizing pathways, in particular enzymes from the methanol dissimilation pathway, the enzymes from the glycolytic and the pentose phosphate pathway either decreased during the methanol fed-batch phase or did not show significant changes (Figure 3.2). A more pronounced decrease was observed for the triose phosphate isomerase (TPI1), the glycolytic enzyme required for channeling glycerol into the central carbon metabolic pathways (Figures 3.1 A, B and 3.2 and Additional file 1). The enzymes of the TCA cycle did not show significant changes except for the mitochondrial malate dehydrogenase (MDH1) which increased strongly during the methanol feeding phase (Figures 3.1 A, B and 3.2 and Additional file 1). MDH1 was already a prominent component of the intracellular proteome during growth on glycerol but increased even further in the methanol feeding phase (Figure 3.1 A and B). Interestingly, the corresponding homolog in *A. niger* was also identified as major part of the intracellular proteome in well-aerated bioreactor cultures [127].

3.3.1.3. Ethanol metabolism

P. pastoris is generally classified as Crabtree-negative yeast and glycerol and methanol are not considered as fermentable carbon sources. However, two alcohol dehydrogenases (ADH and mitochondrial ADHIII) were identified in the proteome during growth on glycerol with ADHIII as a prominent component of the intracellular proteome (Figure 3.1 A and C). The presence of alcohol dehydrogenases indicated the formation of ethanol in the glycerol batch phase which was confirmed by gas chromatography (1.3 g L^{-1} ethanol at the end of the glycerol batch phase). Previous reports also documented ethanol formation by *P. pastoris* during growth on excess glycerol [128, 129]. Surprisingly, the amount of both enzymes increased even further in the methanol fed-batch phase (Figure 3.1 A-C; ethanol concentration: 0.3 g L^{-1} after 112 hours of growth on methanol) indicating a potential involvement in metabolic activities beyond ethanol metabolism. In fact, it has been suggested that proteins of the ADH family from other methylotrophic yeasts (e.g. *C. boidinii*) are involved in fomaldehyde detoxification through formation of methyl formate [26]. A similar role may be also attributable to ADHs in *P. pastoris.*

3.3.2. Stress responses

In the methanol fed-batch phase the cells are exposed to dual stress; stress resulting from methanol degradation and stress resulting from the production of the recombinant protein. The first, AOX catalyzed step during methanol utilization generates formaldehyde and hydrogen peroxide, both toxic compounds [25]. The delayed accumulation of formaldehyde processing enzymes compared to the rapid accumulation of AOX after the onset of methanol feeding (cf. preceding paragraph and Figure 3.1 A-C) suggests a considerable negative impact of formaldehyde on the cells, in particular in the beginning of the methanol fed-batch phase.

3.3.2.1. Oxidative stress response

Methanol metabolism is mainly localized in the peroxisomes, membrane surrounded organelles which harbor the enzymes required for the initial steps of methanol metabolism (e.g. AOX, DAS1). During oxidation of methanol reactive oxygen species such as hydrogen peroxide but also peroxidated molecules are

generated which need to be removed to prevent or minimize corresponding cell damage. At least two peroxisomal enzymes which are involved in the removal of reactive oxygen species, catalase (CTA1), which removes hydrogen peroxide [25, 30, 130], and a glutathione peroxidase or peroxiredoxin (PMP20), which removes peroxidated molecules, e.g. lipid hydroperoxides [25, 130, 131], increased strongly in the methanol fed-batch phase (Figures 3.1 D and 3.2). CTA1 was already present in significant amounts during growth on glycerol and increased further in the adaptation and production phases (Figures 3.1 A, B, D and 3.2). In contrast to CTA1, PMP20 was virtually absent during growth on glycerol but increased immediately in the methanol adaptation phase (Figures 3.1 A, B, D and 3.2) indicating a more important role in methanol-related detoxification of reactive oxygen species. In fact, deletion of *pmp20* was more deleterious than deletion of *cta1* in methylotrophic yeast knockout strains (*C. boidinii* and *P. pastoris*) exposed to methanol [131, 132]. It has been suggested that the presence of PMP20 is essential for maintaining peroxisomal membrane integrity during growth on methanol through removal of oxidized lipids [133]. Cyclophilin B, a cytoplasmic peptidyl-prolyl *cis-trans* isomerase (Cpr1), reported as environmental (oxidative)-stress responsive protein in *Saccharomyces cerevisiae* [134], also increased immediately in the methanol adaptation phase (Additional file 1) suggesting a stress-responsive function also for *P. pastoris.*

3.3.2.2. Induction of UPR and ERAD pathway

HBsAg is a very stable and also a very hydrophobic protein able to form VLPs during downstream processing [126]. The VLPs are further stabilized by intra- and intermolecular disulfide bonds [135]. During its methanol-induced high-level production HBsAg is translocated into the ER but not further processed in the secretory pathway [125]. The accumulation of HBsAg in the ER is leading to an expansion of the ER which bulges into cloud-shaped irregular formations. Thus, an induction of the UPR and a corresponding increase of ER resident chaperones or foldases would not be surprising. In fact, the amount of the UPR-inducible and ER-resident disulfide isomerase (PDI) increased strongly in the methanol fed-batch phase (Figure 3.1 A, B, and E). Moreover, other UPR-induced proteins such as the mitochondrial chaperone SSC1 [136] also increased significantly during HBsAg production (Additional file 1). In addition, two cytosolic chaperones and members

of the AAA ATPase superfamily (ClpB=hsp104 and the AAA ATPase PAS_FragD_0026=Cdc48) also revealed a strong increase in the methanol fed-batch phase (Figure 3.1 A, B, E and Additional file 1) indicating an activation of the ERAD pathway. In *S. cerevisiae*, the homologs of both proteins have been identified as ER-stress responsive proteins, which participate in energy-driven disaggregation and degradation of ERAD substrates [137-139]. Hsp104 cooperates with hsp70 and hsp40 in disassembling protein aggregates for either proper refolding or degradation [137, 139, 140]. The AAA ATPase Cdc48 operates on the cytosolic part of the ER membrane actively involved in dragging misfolded proteins from the ER for subsequent degradation by the proteasome [83, 141, 142]. Here, their increase in response to ER stress was also verified for *P. pastoris*.

3.3.2.3. Induction of other degradation pathways and autophagic processes

Moreover, a strong increase of the vacuolar aspartyl protease APR1 (PEP4 in *S. cerevisiae*) was observed in the methanol fed-batch phase (Figure 3.1 A, B, E and Additional file 1) suggesting the induction of vacuolar degradation pathways in addition to ERAD. An electron microscopic examination of the cells revealed a drastic change in vacuole morphology after the start of the methanol fed-batch phase (Figure 3.4). At the end of the glycerol batch phase, the majority of cells possessed large spherical vacuoles of which many contained autophagic bodies. The appearance of spherical vacuoles with autophagic bodies indicate the onset of nutrient limiting conditions and the accompanying recycling of cell material [143]. After the start of methanol feeding, the number of cells with spherical vacuoles declined strongly and, instead, cells with irregularly shaped vacuoles increased in number (Figure 3.4).

A closer electron microscopic examination revealed invagination of vacuoles (Figure 3.5) as is typically observed during peroxisome degradation by microautophagy (micropexophagy) [36, 144]. Micropexophagy requires high levels of ATP [51] most likely available in the methanol fed-batch phase through primarily dissimilatory methanol catabolism. Interestingly, vacuolar enclosure was mainly related to peroxisomes (for details see Figure 3.5) and not to HBsAg deposits suggesting that vacuolar degradation pathways were not induced by

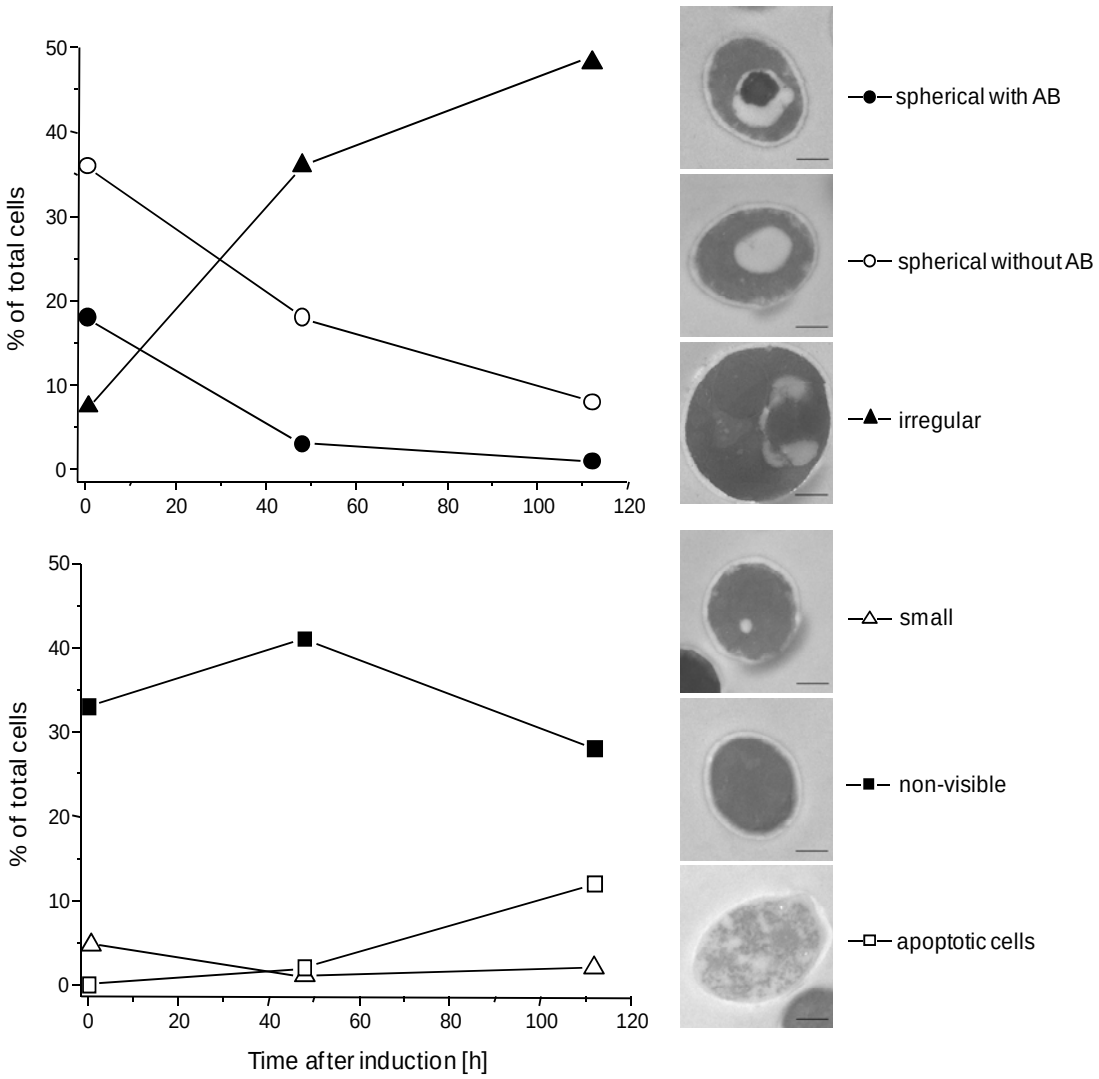

Figure 3.4. Vacuole morphology changes in *P. pastoris* GS115 during methanol-induced high-level production of HBsAg. Time-dependent change in the percentage of cells containing large spherical vacuoles with autophagic bodies (AB, ●), cells containing large spherical vacuoles without autophagic bodies (○), cells containing irregular vacuole (▲), cells with small vacuoles (Δ), cells without any visible vacuoles (■), and apoptotic cells (□). The bar in the electron micrographs of representative cells corresponds to 500 nm.

HBsAg accumulation but most likely by damaged peroxisomes. In other cases, activation of autophagic processes have been reported in *S. cerevisiae* and mammalian cells upon induction of ER stress through addition of reducing agents [42] and tunicamycin and thapsigargin [145], respectively. Moreover, the analysis of the interactome of a degradation-prone and secreted Fab fragment in *P. pastoris* revealed mainly proteasomal degradation but also degradation via vacuolar pathways [64]. Also, analysis of the effects of producing folded-state stability

variants of human lysozyme on the activation of stress responsive pathways revealed a reverse correlation of protein stability versus activation of degradative processes such as ERAD and ER-phagy, apparent through enhanced expression of e.g. *sec61* and e.g. *atg1*, respectively [123]. However, in our case invaginated vacuoles were either closely connected to peroxisomes (Figure 3.5) or otherwise did not show any clear connection to other organelles (e.g. mitochondria or ER).

Autophagy of peroxisomes (pexophagy) has been previously reported for *P. pastoris* upon shifting from methanol to ethanol or glucose but not during growth on methanol. Our findings suggest that constitutive autophagic recycling of peroxisomes might be part of the house-keeping machinery of *Pichia pastoris* also under methanol growth conditions helping cells to deal with damage caused by reactive oxygen species created through methanol oxidation. Vacuolar enclosure of peroxisomes was already apparent in the middle of the production phase (Figures 3.4 and 3.5 D) and increased further during the ongoing methanol fed-batch phase (Figure 3.4 and 3.5). Indeed, it has been shown for the methylotrophic yeast *Hansenula polymorpha* that constitutive pexophagy is vital during growth on methanol as mutant cells with defects in autophagy displayed reduced vitality [56] and damaged peroxisomes are rapidly subjected to autophagic degradation in *H. polymorpha* [146]. Thus, the strong increase in the vacuolar protease APR1 during the methanol fed-batch phase might not be related to HBsAg production but to vacuolar degradation of damaged peroxisomes.

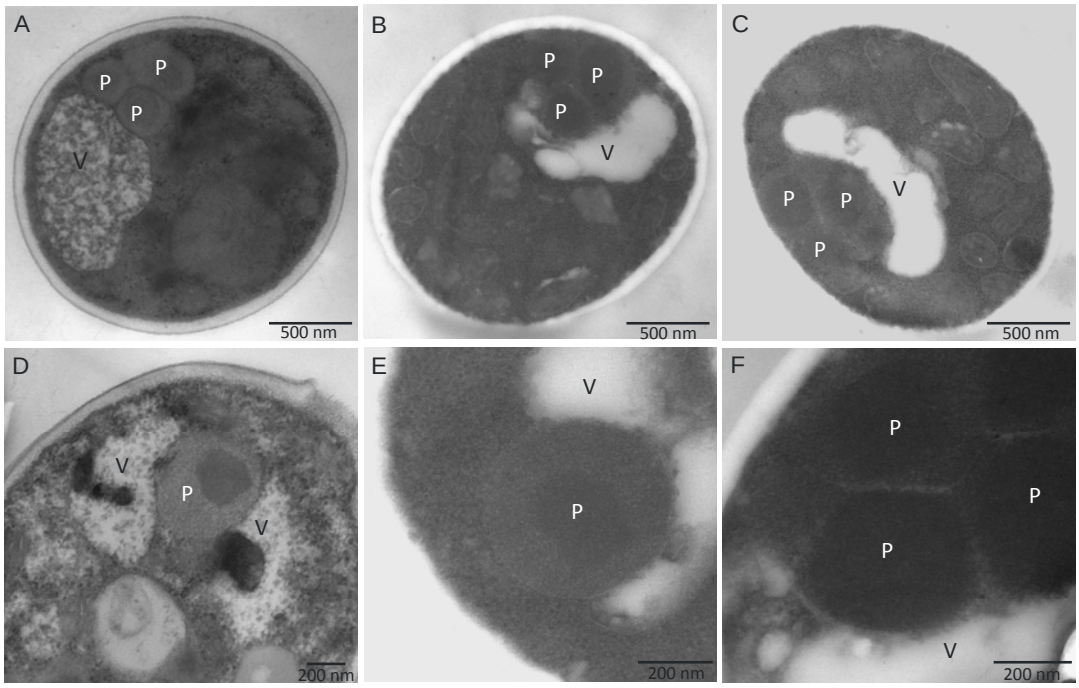

Figure 3.5. Peroxisome sequestration via micropexophagy during methanol-induced high-level production of HBsAg. (A-C) Representative transmission electron micrographs of ultrathin sectioned cells of *P. pastoris* GS115 growing for 112 hours on methanol. (D-F) Close-up views of vacuoles sequestering peroxisomes in cells growing for (D) 48 and (E, F) 112 hours on methanol. Abbreviations: V, vacuole; P, peroxisome.

3.4. Conclusions

The shift from growth on glycerol to growth and production on methanol leads to a drastic change in the yeast proteome. In particular, enzymes from the methanol dissimilation pathway start to dominate the proteome while enzymes from the methanol assimilation pathway, e.g. the transketolase DAS1, only show a moderate increase during the production phase suggesting this pathway as a potential target for metabolic engineering to enhance methanol assimilation, e.g. though enhanced expression of genes from the methanol assimilatory pathway [28]. Moreover, the strong increase of alcohol dehydrogenases, ADHs, in the methanol-fed batch phase indicate that ADHs may play an important role in formaldehyde detoxification in *P. pastoris.*

The accumulation of HBsAg in the ER of *P. pastoris* leads to the induction of the UPR and the ERAD pathway suggesting that potential degradation of HBsAg may proceed via the ERAD pathway and through the proteasome. On the other hand,

there is no significant decrease in the concentration of HBsAg even after prolonged cultivation [126] suggesting that the (lamellar) HBsAg deposits in the ER [125] are well protected from proteolytic degradation. Electron microscopic investigations revealed autophagic processes mainly related to peroxisome degradation and not to degradation of HBsAg deposits. Thus, the activation of autophagic processes also by ER-derived misfolded proteins as reported for mammalian [145] but also for fungal systems [147] might depend on specific protein properties and also on environmental conditions. During methanol-induced production of HBsAg in *P. pastoris*, autophagic processes are clearly related to peroxisome turnover most likely provoked by peroxisomal proteins and components damaged by reactive oxygen species.

3.5. Methods

3.5.1. Strain and growth conditions

The construction of the *P. pastoris* strain GS115 carrying 8-copies of the HBsAg structural gene under the control of the *aox1* promoter and displaying a Mut^S phenotype was described before [116]. Cells were grown on defined medium in a fed-batch procedure as described earlier [126]. High-level production of HBsAg was started after batch growth on glycerol through the addition of methanol to a final concentration of 6 g L^{-1}. This methanol concentration was kept constant by continuous methanol feeding throughout the entire production phase [126].

3.5.2. Sample preparation

Cells were harvested by centrifugation and washed with phosphate buffered saline to remove extracellular proteins and other contaminants. The remaining pellet was resuspended in extraction buffer (20 mmol L^{-1} Tris–HCl, pH 7.6, 10 mmol L^{-1} NaCl, 0.5 mmol L^{-1} deoxycholate, 1 μg mL^{-1} pepstatin). Cell disruption was accomplished by grinding in liquid nitrogen using a Mortar Grinder (RM 100, Retsch Gmbh & Co. KG, Germany). The cell debris was removed by centrifugation (22 000 × g, at 4°C for 30 min) and 1 mL of the subsequent supernatant treated for 15 min with 7 μL of nuclease mix (0.5 mg mL^{-1} DNase, 0.25 mg mL^{-1} RNase, 50 mmol L^{-1} $MgCl_2$). Protein was precipitated with 30% TCA. Finally, the protein

pellets were air-dried and dissolved in a solubilization buffer containing 7 mol L^{-1} urea, 2 mol L^{-1} thiourea, 4% (w/v) CHAPS, 1% (w/v) dithiothreitol (DTT), 20 mmol L^{-1} Tris, and 1% (v/v) Pharmalyte™ pH 3–10 (Amersham Biosciences). The total soluble protein concentration was determined using the BIO-RAD protein assay (BIO-RAD Lab., Hartfordshire, USA). The solubilized proteins were stored at −70°C until further analysis.

3.5.3. Two-dimensional gel electrophoresis

Two-dimensional (2-D) gel electrophoresis was essentially carried out as described previously [127]. Briefly, the first-dimension using isoelectric focusing (IEF) was run with the IPGphor™ Isoelectric Focusing System (Amersham Biosciences) loading 300 µg protein sample onto Immobiline DryStrip gels of pH 3–10 (IPG strips, Amersham Biosciences) by in-gel rehydration. IEF was performed with the following setting: 30 V×12 h, 300 V×3 h, 600 V×2 h, 1000 V×1 h, gradient from 1000 V to 5000 V within 2 h, 5000 V×2 h, gradient from 5000 V to 8000 V within 2 h, then 8000 V×10 h. Prior to the second dimension (SDS-PAGE), the IPG strips were equilibrated and then transferred onto lab cast SDS-polyacrylamide gels (DALT multiple gel caster and DALT gradient maker, Amersham Biosciences). Proteins were separated on 12-16% linear gradient gels using the vertical separation unit Hoefer™ System (Amersham Biosciences). Subsequently, gels were stained using colloidal Coomassie Blue G-250 according to the "Blue silver" protocol [148]. The gels were then scanned (ScanMaker 9800 XL, Umax System GmbH, Germany) at 300 dpi resolution. Image analysis, namely protein spot detection, matching and quantification were performed using Proteomweaver™ 3.0 (Definens AG, Germany).

3.5.4. In-gel trypsin digestion and peptide extraction

The intracellular proteome was analyzed at different cultivation time points by 2-D gel electrophoresis combined with MALDI-TOF analysis. A total of 136 protein spots were excised manually from Coomassie brilliant Blue stained 2-D gels, each spot was washed several times with 200 µl water, dehydrated in 50 µl acetonitrile, and dried in a vacuum concentrator (Eppendorf ® Vacufuge Concentrator 5301, Eppendorf AG, Hamburg). The gel pieces were treated with 100 mmol L^{-1}

ammonium bicarbonate containing 20 mmol L^{-1} DTT at 56°C for 30 min and then with 100 mmol L^{-1} ammonium bicarbonate containing 55 mmol L^{-1} iodoacetamide in the dark at room temperature for 30 min. Acetonitrile was added in between the treatments to dehydrate the gel pieces. Finally, the gel pieces were washed twice with 100 mmol L^{-1} ammonium bicarbonate, dehydrated with acetonitrile and dried in the vacuum concentrator. In-gel digestion was carried out by incubation with 2 ng μL^{-1} trypsin (sequencing grade modified, Promega Corp.) in 50 mmol L^{-1} ammonium bicarbonate at 37°C overnight. Obtained peptides were extracted and then desalted with reversed-phased C-18 ZipTips (Millipore, Billerica, MA, USA) before application to the MALDI-TOF sample plates.

3.5.5. MALDI-TOF MS analysis

Matrix-assisted laser desorption ionization time-of-flight mass spectrometry (MALDI-TOF MS) was employed to obtain the peptide mass fingerprint of a given protein. The concentrated peptide solution was mixed (1:1, v/v) with the MALDI loading solution (10 mg α-cyano-4-hydoxycinnamic acid, 400 μL acetonitrile and 600 μL 0.1% trifluoroacetic acid), loaded on the target and dried at room temperature. The molecular masses of the tryptic peptides were determined on a Bruker Ultraflex time-of-flight mass spectrometer (Bruker Daltonics GmbH, Germany).

3.5.6. Data analysis

Peptide mass fingerprints obtained by the MALDI-TOF MS were processed using FlexAnalysis 2.0 (Bruker Daltonics GmbH, Germany) and used to search NCBInr database by using Mascot 2.10 software (http://www.matrixscience.com). The parameters used for the search were as follows: taxonomy: other Fungi, tryptic digestion, modifications were allowed for carbamidomethylation of cysteine (fixed modification) and methionine oxidation (variable modification), one missed cleavage site was allowed, all peptides monoisotopic, peptide tolerance at 100 ppm. Mascot scores (probability based MOWSE scores) and expect values were generated from the Mascot search program. All proteins with a Mowse score ≥ 70 were regarded as significant ($p < 0.05$). Protein identification was based on the recently annotated *P. pastoris* GS115 genome sequence [110] and the gene name

used in this study is according to *Pichia pastoris* strain GS115 (http://www.uniprot.org/). If no gene name was given for this strain the gene name is according to *Pichia pastoris* strain ATCC 76273 / CBS 7435 / CECT 11047 / NRRL Y-11430 / Wegner 21–1 or general *Pichia pastoris* (yeast) in case of 100% sequence identity (http://www.uniprot.org/). Image analysis from the scanned gels, namely protein spot detection, matching and quantification were performed using Proteomweaver™ 3.0 (Definiens AG, Germany). The spot volumes were computed and normalized for each spot on each gel in relation to the total spot volume of each 2D gel. To obtain comparable data, spot intensities were normalized using the log2 ratio of induced samples *versus* uninduced sample. Log2 fold changes above 0.6 (equivalent to a 1.5 fold changes) were considered significant.

3.5.7. Ethanol analysis

Ethanol concentrations were determined by gas chromatography (Shimadzu 14B GC, Kyoto, Japan) using a column packed with Carbograph 1AW (20/120; 5% carbowax 20 M) (Alltech Associates Inc., Deerfield, IL, USA), column temperature 160°C, detector: flame ionization detector.

3.5.8. Electron microscopy and image analysis

Electron microscopic studies were carried out essentially as described previously [125]. Mitochondrial and total cell area were determined from randomly chosen cells at the end of the glycerol batch phase (in total: 55 mitochondria in 12 cells) and after 112 hours of growth on methanol (in total: 67 mitochondria in 8 cells) using Image J Software (National Institutes of Health, Bethesda, Maryland, USA). For analysis of vacuolar morphology, 520 cells were randomly chosen for analysis (224 cells at the end of the glycerol batch phase, 160 cells 48 hours and 136 cells 112 hours after the onset of methanol feeding).

Competing interests

The authors declare that they have no competing interests.

Authors' contributions

AV identified the proteins by MALDI-TOF, analyzed the data and prepared a first draft of the manuscript. HL prepared the electron micrographs. AA and CG carried out the cultivation. AA also prepared the 2D gels. MN contributed to protein identification by MALDI-TOF. NK was involved in the initial outline of the project. UR conceived and directed the study and prepared the final manuscript. All authors read and approved the final manuscript.

Acknowledgements

Ana Letícia Vanz would like to acknowledge the Federal Agency for the Improvement of Higher Education, Brazil (CAPES) for providing a PhD fellowship. Ahmad Adnan wishes to express his gratitude to the Higher Education Commission (HEC) of Pakistan for a post-doctoral fellowship. Partial support through an Indo-German program funded by DBT (India) and BMBF (Germany) is also gratefully acknowledged. We are also grateful to Ingeborg Kristen and Anja Meier for skilful support in TEM and MS sample preparations (VAM and CPRO, HZI). Moreover, we thank Frank Stahl for helpful support and discussions concerning primer design and PCR analysis.

Appendix I

Additional file 1 All identified intracellular proteins. The complete list of all identified proteins classified into functional categories and their log2 changes in response to methanol-induced high-level production of the HBsAg and a representative 2D gel image indicating the spots of all identified proteins are given.

Appendix II

Additional file 2 Identification of AOX1 in *P. pastoris* GS115 with a "Mut^s phenotype". Unexpectedly AOX1 was identified in the supposedly Mut^s strain of *P. pastoris* GS115 producing high levels of HBsAg. Background information on AOX1 identification and discussion about Mut^S behavior of Mut$^+$ strain is given

4. *Pichia pastoris* cellular response to overproduction of secretory insulin precursor under methanol induction: morphological and proteomic analysis

4.1. Background

The secretion of properly folded proteins is one of the major factors taken into account when considering yeast as the preferred host for recombinant protein production [11, 13, 149]. Secretion requires the presence of a signal sequence at the N-terminus of the foreign protein to target it to the secretory pathway. The secretion signal sequence from the *S. cerevisiae* α-factor-prepro peptide, which is located downstream of the *aox1* promoter and upstream of the heterologous protein gene, has been used with success to facilitate the secretion of numerous heterologous proteins [22, 150], including proinsulin [10]. The *S. cerevisiae* α-factor prepro-leader consists of a 19-residue signal (pre) sequence followed by a 66-residue pro-sequence containing three consensus N-linked glycosylation sites and a dibasic Kex2 endoprotease (an endopeptidase processing *S. cerevisiae* α-factor precursor) processing site [151].

In the methylotrophic yeast *Pichia pastoris*, heterologous proteins can either be produced intracellular or secreted into the medium. Since *P. pastoris* secretes only a small amount of endogenous proteins, the secreted product of interest can comprise more than 80% of the total protein in the medium [11]. Thus, secretion serves as a major first step in purification and eliminates the need for high-cost and low-yielding cell disruption or refolding processes [152].

However, not all recombinant proteins can be efficiently secreted in yeast, and endoplasmic reticulum (ER) retention of highly expressed proteins is still a problem [112]. The successful high level secretion of recombinant protein can be limited by a number of different steps, such as folding, disulfide bridge formation, glycosylation, transport within the cell and release from the cell [124]. The

physical properties of the target protein can also play an important role on the final protein yield [63]. As reviewed in the introduction chapter, the accumulation of unfolded proteins in the ER is sensed and leads to initiation of the unfolded protein response (UPR) and the ER-associated degradation (ERAD) process. In the yeast *S. cerevisiae*, nearly 400 genes are transcriptionally affected by the UPR and a similar proportion of genes has been also reported to be affected by the UPR in other yeasts and filamentous fungi [153]. To explore this complex field involving protein secretion and degradation, yeasts such as *P. pastoris* have been used as model organism [124, 154].

Insulin is synthesized as preproinsulin in the pancreatic β-cells and is composed of two polypeptide chains, A (21 amino acids) and B (30 amino acids), with three disulfide bonds [155]. In this work, the expression of insulin precursor in *P. pastoris* was performed in the following configuration: α-factor leader – KR – spacer - insulin precursor, where KR is the Kex2 dibasic endoprotease processing site [156]. The Kex2 endoprotease cleaves the leader-insulin precursor fusion protein in the late secretory pathway and the folded insulin precursor is secreted to the culture supernatant. The spacer peptide (EEAEAEAEPK) localized between the leader and the insulin precursor was integrated to optimize Kex2 endoprotease processing and insulin precursor yield [157]. The mature insulin precursor is secreted as a single-chain N-terminally extended proinsulin-like polypeptide consisting of the insulin A chain with 21 amino acids and B chain with 29 amino acids (lacking the C terminal B30 threonine) linked via a short synthetic C peptide (AAK). It is predicted to be 63 amino acids long with a molecular weight of ~ 7 kDa [156]. After purification of the insulin precursor and proteolytic removal of spacer and C-peptides with trypsin, the amino acid Thr^{B30} can be added to Lys^{B29} by trypsin-mediated transpeptidation to generate insulin [156-158].

In this study, the intracellular proteome of *P. pastoris* was analyzed combined with ultrastructural analysis to better understand the response of the cell factory forced to produce the recombinant secreted insulin precursor (IP) under the control of the *aox1* promoter. Besides the unfolded protein response, other cell responses/adaptation to the carbon feeding condition, such as autophagy, were also analyzed throughout the cultivation.

4.2. Results and discussion

To evaluate the cell response to production of the secreted synthetic insulin precursor in *P. pastoris* strain X-33, the global intracellular protein production profile combined with electron micrographs was analyzed. The recombinant strain was grown to high-cell density in a batch procedure using a defined medium with low salt and high glycerol concentrations [156]. Following batch growth, the production of IP was carried out by addition of 1.0 g L^{-1} of methanol. After the first pulse, the methanol concentration was increased to 1.5 g L^{-1} and further to a final concentration of 2 g L^{-1}, which was kept constant throughout the remaining production phase. Samples for proteomic analysis were taken at 0 h (immediately before induction), and at 6, 18, 48 and 120 hours after methanol induction.

4.2.1. Evaluation of the *P. pastoris* intracellular proteome

Glycerol and methanol were the only carbon sources during the growth and production phase, respectively. As expected, the proteins related to carbon metabolism showed the most relevant changes upon methanol induction. The global view of the protein profile changes upon the shifting from glycerol to methanol is schematically represented in Figure 4.1. All identified proteins according its functionality and log2 fold change in response to methanol-induced high-level production of the IP are detailed in Appendix III.

The enzymes related to methanol metabolism were significantly up-regulated after induction with methanol. Most of the enzymes from methanol pathway, such as AOX1, CTA1, DAS1, DAK, FLD1, FGH1 and FDH1 were identified and represent the majority of the produced proteins during the production phase (Appendix III). Some protein spots were identified as being fragments of the full-length proteins AOX1 and FDH1 (see details in Appendix III). These proteins fragments showed an increase in abundance along the production phase. The enzymes from the dissimilation pathway showed a significant up-regulation already at 6 h after induction with methanol and increased its level along the cultivation (e.g., FDH1, 10.7 and 12.3 log2 fold change at 6 and 120 h after induction with methanol, respectively). Whereas, the abundance level of the enzymes from assimilation pathway were much lower during whole methanol phase (e.g., DAK, 6.5 and 8.7 log2 fold change at 18 and 120 h after induction with methanol,

respectively). According to the mass balance analysis the majority of methanol (~70%) was metabolized through the dissimilation pathway and converted into carbon dioxide in the methanol fed-batch phase (data not shown).

In line with the previous chapter, the alcohol dehydrogenase (ADHIII) was detected in the proteome of *P. pastoris* X-33 during growth on glycerol and throughout the entire methanol fed-batch phase (Appendix III). The ADH abundance was slightly lower than observed during HBsAg cultivation. This is probably due to the lower methanol concentration used for IP production in comparison to that for HBsAg. This data support the idea about the involvement of alcohol dehydrogenases on methanol metabolism as part of the formaldehyde detoxification process [26].

The proteins related to the glycerol, pentose phosphate pathway and TCI cycle were mostly down-regulated or kept their level constant after induction with methanol (Figure 4.1 and for details see Appendix III).

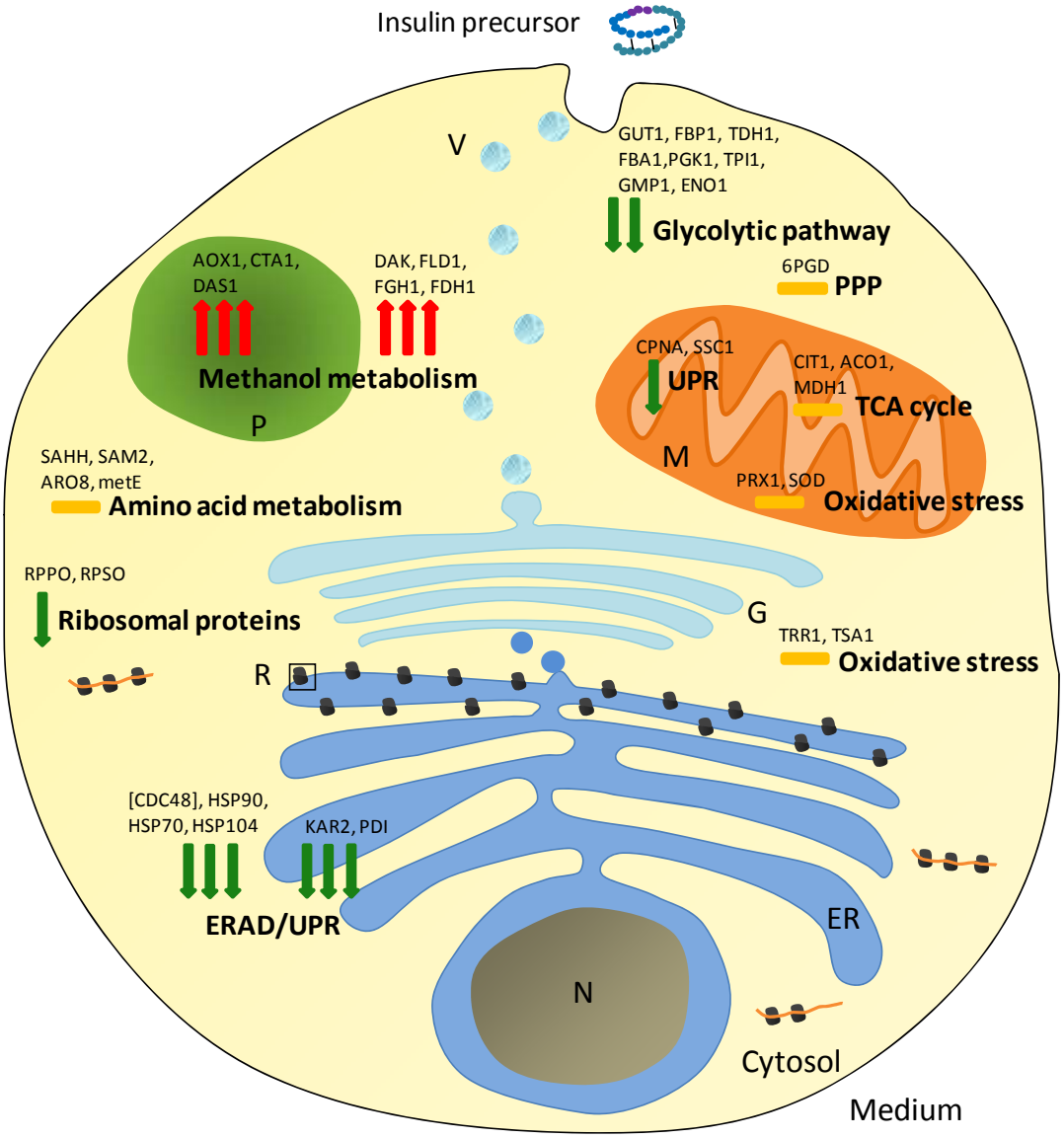

Figure 4.1. The global view of the intracellular proteome profile change upon shifting from glycerol to methanol in *P. pastoris* X-33 producing secretory insulin precursor. The red arrow (↑) indicates an increasing and the green arrow (↓) a decreasing amount of the enzymes in the methanol fed-batch phase. An orange dash (−) indicates no significant change. One arrow indicates small (0.6-1 log2 change), two arrows strong (1–4 log2 change) and three arrows very strong changes (> 4 log2 change). The arrows correspond to the average of log2 fold change from each functional group. The position of the arrows is according to the proteins location in the cell. Only some proteins from each functional group are indicated in this figure. The complete list of the identified protein is in Appendix III. Abbreviations: TCA, tricarboxylic acid cycle; PPP, pentose phosphate pathway; ERAD, endoplasmic reticulum associated degradation; UPR, unfolded protein response; P, peroxisome; R, ribosome; ER, endoplasmic reticulum; V, vesicle; M, mitochondria; N, nucleus; G, Golgi complex.

4.2.1.1. Cellular response to secretory insulin precursor production in *P. pastoris*

Most of the identified proteins involved in ER stress showed a down-regulation throughout the IP production phase (Figure 4.2). Two ER-resident chaperones, KAR2 and PDI were identified. The KAR2, also known as BiP in mammalian cells, is the central player in folding assistance in the ER. KAR2 plays a role in all known functions of the ER, including gating the translocon, folding nascent proteins, targeting misfolded proteins for degradation and regulating the unfolded protein response [63, 159]. The cytosolic chaperones from the HSP70 family (SSA1, SSA3 and SSB), HSP90 and members of the AAA ATPase superfamily (ClpB and the AAA ATPase PAS_FragD_0026, named as HSP104 and CDC48 in *S. cerevisiae*, respectively), as well the mitochondrial chaperones CPNA (HSP60 family) and SSC1 (HSP70 family), which are classical UPR targets [136], were also identified and showed a down-regulation during the production phase. The ubiquitin-activating enzyme, also known as E1 enzymes (UBA1), which catalyzes the first step in the ubiquitination reaction and targets a protein for degradation via a proteasome [82] also showed a down-regulation. Additionally, one protein spot identified as fragment of the heat shock protein SSA3 with a molecular weight of approximately 25 kDa showed a significant increasing level along the cultivation. This fragment is probably derived from a degradation process.

Comparable results were also observed in a second bioreactor cultivation performed at similar conditions (Figure 9.1, Appendix III).

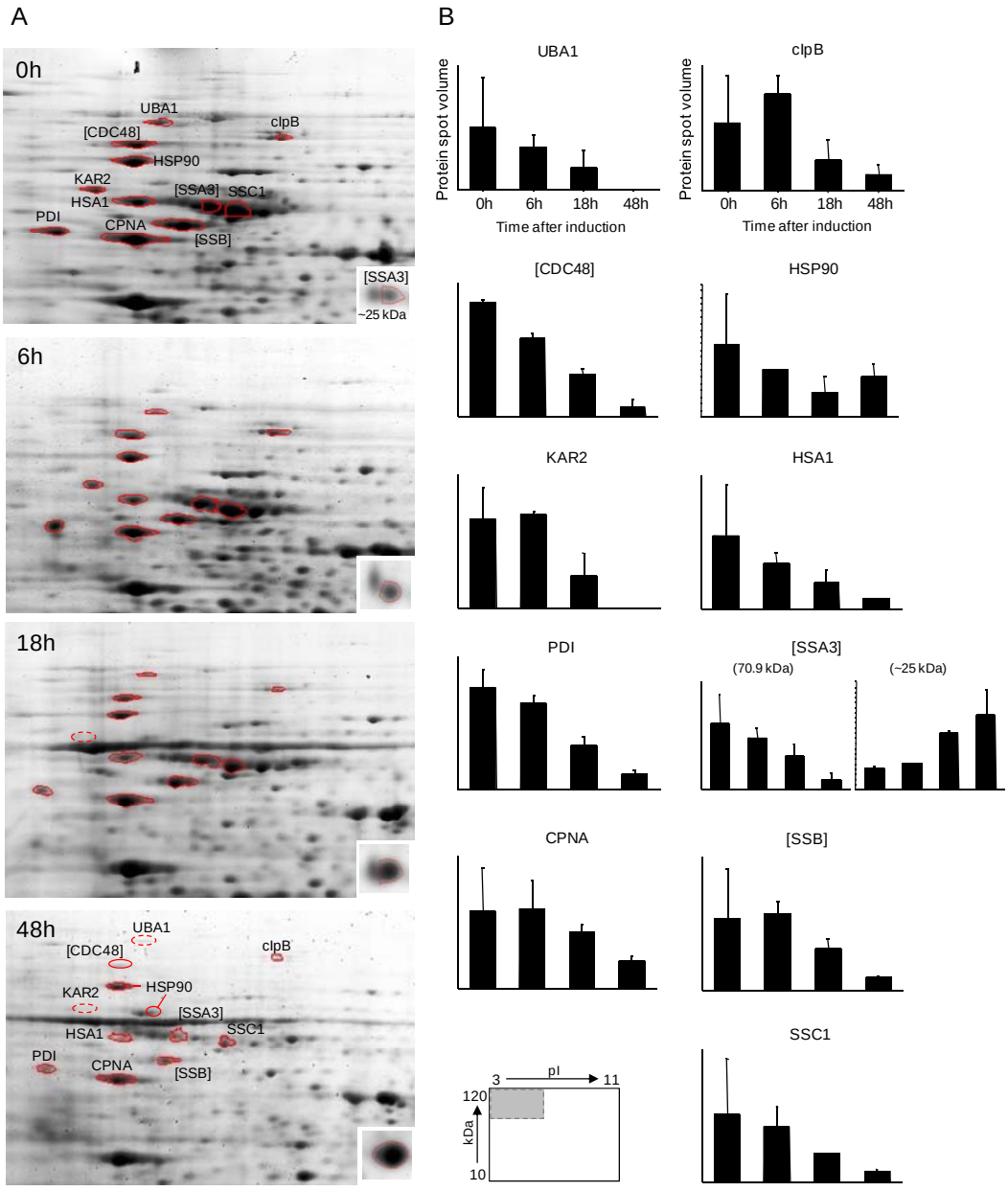

Figure 4.2. Changes of the intracellular proteome of *P. pastoris* X-33 in response to secretory insulin precursor production containing most of the identified ERAD and UPR related proteins. The proteome analysis was done using duplicate 2D gel electrophoresis and the average of each spot intensity was calculated. Here only one of the duplicate gels used for the analysis is shown. (A) Sections of 2D gels representing parts of the intracellular proteome and containing most of ERAD and UPR related proteins, at 0, 6, 18 and 48h after methanol induction. (B) Representative graphs of the abundance changes of each protein spot shown in A. The protein abundance corresponds to an average of the resulting value from the duplicate gels used. The bar on the columns in the graphs represents the standard deviation. The spot related to fragment SSA3 ~25 kDa is shown in the small box. The small map indicates the position of the 2D sections in the entire 2D gel.

Although the final yield of IP was approximately 4 g L^{-1} of cell-free culture supernatant [156], the amount of protein which could be retained into the cell was not analyzed up to that time. It is known that the up-regulation of ERAD and UPR related proteins is caused by unfolded proteins retained in the ER [67]. Since it was observed a down-regulation of such proteins, the amount of the IP which was secreted to the media and the amount which was retained inside the cells were evaluated. It was observed that less than 5% of the insulin precursor stacked inside the cell (Figure 9.2, Appendix III). This result confirms a functioning secretory pathway and could explain the down-regulation or no stimulation of the UPR and ERAD responses.

With the purpose to compare the proteome profile of the insulin producing strain (X-33-IP) with the *P. pastoris* host strain X-33 (X-33-host), regarding specially the proteins related to ERAD and UPR, parallel shake flask cultivations were performed and the samples were analyzed by SDS-PAGE. It is important to highlight that most of the proteins, until now, related to unfolded protein stress have a high molecular weight, i.g. KAR2, 74 kDa; UBA1, 115 kDa; Hsp90, 80 kDa and clpB, 100 kDa. In an overview of SDS-PAGE of the crude extract of the intracellular proteins of the strain X-33-IP and the X-33-host it is clearly observed that the proteins from the upper part of the gel decreased their level during the production phase (Figure 4.3). To assure the identity of the referred proteins in the SDS-PAGE, some protein bands from the upper part of the gel were analyzed by MALDI-TOF. One of the protein bands was identified as clpB and it is indicated by the black arrow in Figure 4.3. In the previous chapter, a ER stress caused by the recombinant protein production was reported and the clpB showed an up-regulation during the production phase of the recombinant protein HBsAg [113]. In a general view, the insulin producing strain has a similar proteome profile comparing with the host strain which suffers no stress related to recombinant protein overproduction.

To verify if this effect is not strain dependent, the *P. pastoris* host strain GS115 (GS115-host) was also analyzed at the same conditions. The shake flask cultivation of the GS115 cells harbouring 4 copies of HBsAg gene and 1 copy of chimeric protein possessing envelope domain III of dengue virus serotype 2 fused with HBsAg (Den2EDIII- HBsAg) was also performed in parallel. The same proteome

profile of strains X-33, i.e., the decreasing level of UPR related proteins, was observed in the strain GS115-host, confirming that this profile is not strain dependent (Figure 4.3). On the other hand, in the GS115-Den2EDIII-HBsAg, the same group of protein showed a constant or even higher level in the production phase compared to the growth phase. This effect is probably due to the unfolded protein response.

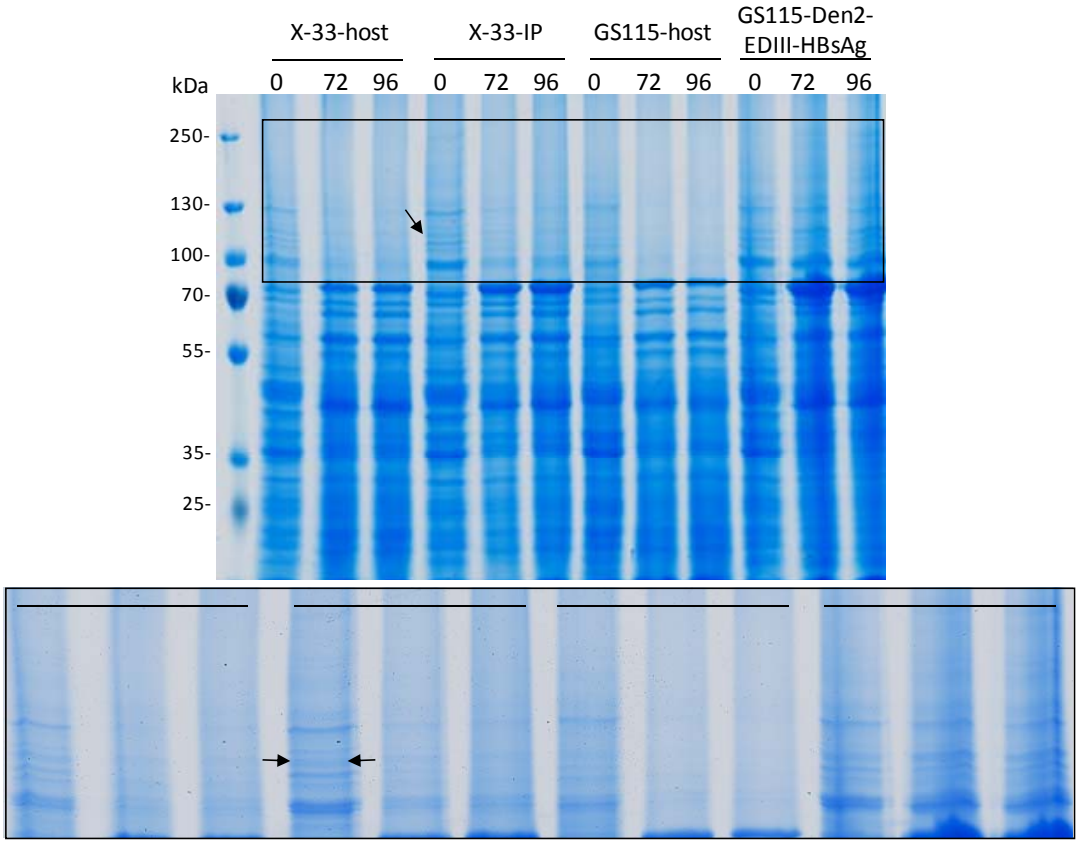

Figure 4.3. UPR and ERAD related proteins profile in *P. Pastoris* X-33 and GS115 producing and host strains. Crude extracts of the intracellular proteins of the *P. pastoris* insulin precursor producing strain (X33-IP), X-33 host strain (X33-host), chimeric protein hepatitis B surface antigen with the envelope domain III of the dengue virus (GS115-Den2 EDIII-HBsAg) and GS115 host strain (GS115-host) were analyzed by SDS-PAGE. Samples at the end of the growth phase directly before induction with methanol (0) and at 6, 72 and 96 h after induction with 1% methanol were disrupted and analyzed. The black arrow indicates the protein clpB identified by MALDI-TOF. Marker: Thermo Scientific, Page Rule Plus 26619.

In order to better examine the changes in abundance of these proteins from the growth to production phase, Western blot analysis was performed. Due to the lack

of specific antibodies against *P. pastoris* proteins, an anti-HDEL antibody was used. Resident proteins of the lumen of ER, such as KAR2 and PIB, carry the HDEL C-terminal retention signal [160] and these antibodies have been used to detect these proteins [88, 161]. It could clearly be demonstrated that after induction with methanol, the proteins recognized by the antibody, KAR2 and PDI, showed a lower level in both strains X-33-IP and X-33-host when compared to the growth phase (Figure 4.4). However, this decreasing level is stronger in the host strain compared to the producing strain. This is probably due to the recombinant protein production. On the other hand, the same proteins showed a constant level or even a higher level during the production phase of the GS115-Den2EDIII-HBsAg strain (Figure 4.4). The ER stress response caused in this strain is probably due to the recombinant protein production. In conclusion, although no significant ER stress was observed during the production of the secreted insulin precursor, the UPR related proteins are still required for the recombinant protein production at certain level.

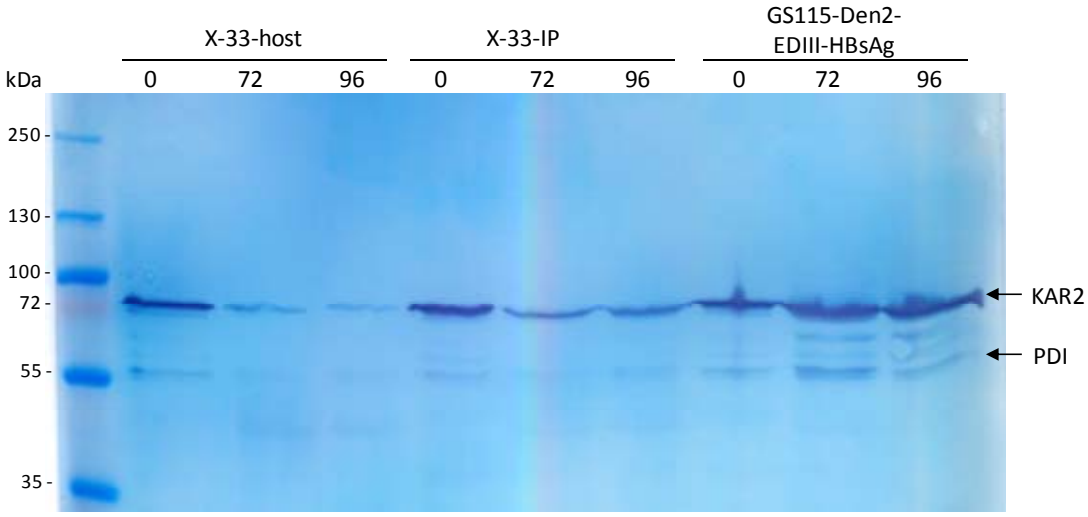

Figure 4.4. Western Blot analysis with anti-HDEL. Crude extracts of the intracellular proteins of the *P. pastoris* insulin precursor producing strain (X-33-IP), X-33 host strain (X-33-host), chimeric protein hepatitis B surface antigen with the envelope domain III of the dengue virus (GS115-Den2-EDIII-HBsAg) were analyzed. Samples at the end of the growth phase directly before induction with methanol (0) and at 72 and 96 h after induction with 1% methanol were disrupted and analyzed. The proteins detected by this antibody are indicated with arows. KAR2 has 74 kDa and PDI has 58 kDa. Marker: Fermentas, Page Rule Plus Prestained SM1811.

Secretion efficiency is not dictated solely by a signal sequence, but in part, it depends on the nature of the protein [10]. One limiting factor for a successful secretion to the medium could be the tertiary structure of the protein. The protein β-glucosidase from *Pyrococcus furious* has a tetrameric nature and it was reported to be retained in the ER of *S. cerevisiae.* The possibility that such retention was provoked by a tetrameric missassociation was not exclude [162]. Furthermore, copy number was also reported to cause a bottleneck during protein secretion [163]. Parekh et al. [163] used bovine pancreatic trypsin inhibitor (BPTI), a small polypeptide with 58 aa, as a model for studying secretion and the role of folding in the ER. It was found that the level of protein secretion driven by multiple copies of the expression cassette compared to a single copy was very similar. Gene transcription was higher in the multicopy strain, as expected, but the binding of conformation-specific antibodies showed that the majority of BPTI was improperly folded and retained in the ER lumen. It was suggested that the limitation for the secretion may be the maintenance of correct tertiary structure of the recombinant protein or insufficient levels of ER-resident protein folding chaperones.

Given that the produced insulin precursor is a small protein composed of 63 aa, it has only three disulfide bonds and it is not glycosylated, it is assumed that such non complicated structure facilitates protein folding, transport through the secretory pathway and consequently does not provoke folding stress to the cells. Additionally, as previously described, the IP gene sequence was constructed to improve the secretion of the IP to the culture supernatant with the replacement of the human proinsulin C-peptide with a small C-peptide (AAK) and insertion of the spacer peptide between leader and the insulin precursor. Moreover, the clone carries only one copy of insulin precursor gene which probably does not overburden the protein folding assistants.

In line with the obtained data, it was recently reported the influence of the protein physical features, such as size and number of disulfide bonds, on the dysfunction of the secretory pathway in the yeast *S. cerevisiae* [81]. The secretion of the small insulin precursor was compared with the large protein α-amylase and although a higher level on mass basis of α-amylase was secreted, six-fold more insulin molecules were secreted to the medium. This result shows that the protein properties influence the amount of protein secretion. The oxygen and ATP

consumption was lower in cells producing insulin then in cells producing α-amylase, likely because IP is shorter and has less disulfide bonds. For a successful recombinant protein production, the transcription should be as high as possible without overburding the ER folding capacity, bringing the cell to an oxidative stress condition. However, this optimal expression level will be different according to the protein, since protein folding rates will vary according to the protein size and structure [81].

In addition, the higher amount of proteins related to the UPR and ERAD detected at the end of the growth phase when compared to the production phase (Figure 4.2, 4.3 and 4.4, at 0h) might be related to the environmental condition. The same abundance level of those proteins was also observed in the middle of the growth phase (data not shown). For the growth phase a high amount of glycerol (95 g L^{-1}) was used and the cultivation was performed at 30°C. As described previously in the introduction chapter, high temperature [88] and high osmolarity (140 mOsm Kg^{-1} was considered a low and 1350 mOsm Kg^{-1} a high osmolarity) [94] result in the induction of proteins from UPR. Generally, the induction of the UPR may not be only a result of high concentration of ionic solutes but it is also triggered by high osmotic pressure induced by other substances [94]. It has been reported for mammalian cells that high hexose concentration can lead to UPR induction [164]. The osmolarity of the culture supernatant of the bioreactor samples was analyzed. It was approximately 1780 mOsm Kg^{-1} at the beginning of the growth phase, 822 mOsm Kg^{-1} at the end of the growth phase and 560 mOsm Kg^{-1} at the end of production phase. It is assumed that the higher level of the UPR related proteins during the growth phase may be caused by the high osmolarity in the medium and the high temperature used. It has been reported that osmotic stress applied prior to the induction of protein secretion resulted in higher level of scFc antibody in *P. pastoris* [95]. Therefore, the presence of high amount of chaperones and folding helpers at the beginning of the induction phase may also explain the fine folding competence of the cells leading to an efficient IP production and secretion.

4.2.2. Autophagic processes in *P. pastoris:* a cell adaptation response

Cells were first grown in a batch procedure on defined medium with glycerol as carbon substrate. After depletion of glycerol, the production of insulin precursor was induced by the addition of methanol in gradually increasing steps for a better cell adaptation [156]. First methanol was added to a final concentration of 1 g L^{-1}. About 24 h after the initial methanol pulse, the concentration of methanol in the bioreactor was further increased to 1.5 and later (~30 h) to 2 g L^{-1}, and it was kept constant for the remainder of the cultivation. At the transitional phase from glycerol to methanol, the cells were subjected to a short carbon starvation condition. With the help of electron microscopy, autophagic processes could be observed at the end of the growth phase. Upon nutritional deficiency, fractions of the cytoplasm are consumed via autophagy and the resulting catabolic products are used as sources of energy or as building blocks for the synthesis of new macromolecules [46].

In the electron micrographs of samples at the end of growth phase, directly before induction with methanol, a great number of autophagic vacuoles were observed (Figure 4.6 A-C and E). Autophagic bodies (Figure 4.6 A and E) and multilamellar membrane structures (Figure 4.6 B and C) were observed inside the vacuoles which could be part of a degradation process. The nature of these multilamellar structures is not fully understood. Apparently forming autophagosomes could also be observed in the cytosol near to the vacuole (Figure 4.6 A and C-E). These vesicles seem to contain structures with similar appearance as the ribosomes from the cytosol (Figure 4.6 A). However, the classical double membrane of the autophagosome [165, 166] was not found. Considering that the cells are not in an extreme and long starving situation and the cell response was analyzed in a "normal" bioprocess condition (i.e., the autophagy was not intentionally induced), it is not an easy task to find autophagosomes, specially when they have a short half-life (5-10 min) [166]. Ribosomes entering in the vacuole were also observed (Figure 4.6 B). The autophagy of ribosomes, a process called ribophagy, in *S. cerevisiae* cells under nitrogen starvation condition has been reported [47]. A dense area was always present in the vacuole (Figure 4.6 A, C and E). Some similar

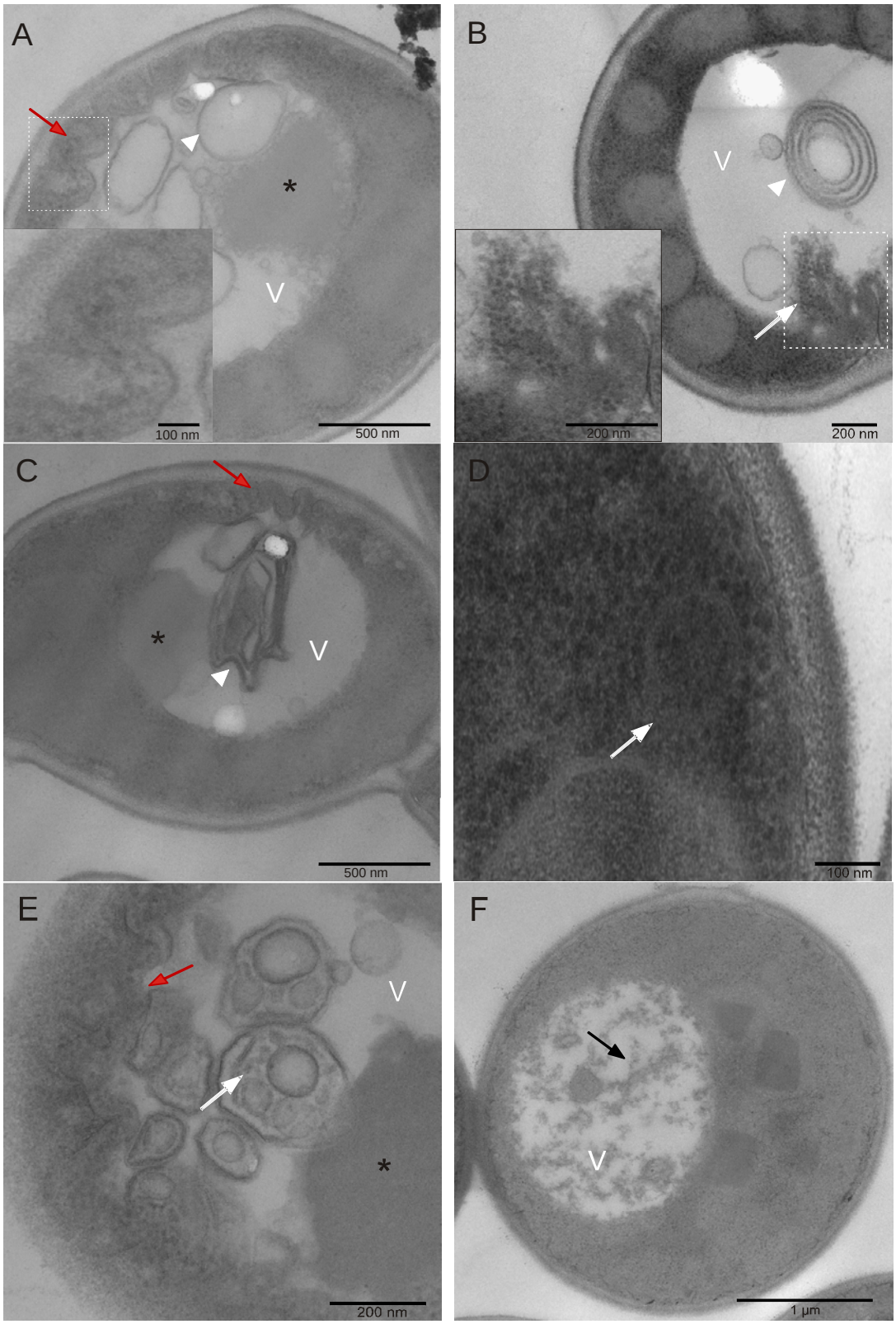
A
V
*
100 nm
500 nm
B
V
200 nm
200 nm
C
*
V
500 nm
D
100 nm
E
V
*
200 nm
F
V
1 µm

Figure 4.6. Representative transmission electron micrographs of ultrathin sectioned cells of *P. pastoris* X-33 in the transitional phase from glycerol to methanol. (A-E) Cells at the end of growth phase, directly before induction with methanol, containing autophagic vacuoles were observed. The red arrow in pictures A, C and E indicates the probable forming autophagosomes (close view in picture A). In picture A, the white arrowhead indicates an empty vesicle; probably the material was already digested. In picture B the white arrow indicates probable ribophagy as a consequence of the C-starvation condition. In pictures B and C, the white arrowheads indicate multilamellar structures. In picture D, the white arrow indicates a probable autophagosome with apparent ribosome inside. In picture F, cells are at 48 h after methanol induction and the black arrow indicates fragments of the membrane of autophagic bodies. In pictures A, C and E the (* symbol) points to a dense area containg material for digestion. V, vacuole.

structures have been already described as autophagic bodies containing ribosomes of high density and it was suggested they were condensed ribosomes [43]. These dense areas were analyzed and, in this sample, the presence of ribosomes could not be neither confirmed nor exluded (data not shown). Further analysis should be done to clarify the presence of the autophagosomes in the cytosol and its contents. At the beginning of the production phase (at 48 h), where the cells were being adapted to the new carbon source (methanol), some intact autophagic bodies were still present inside the vacuole, but in most of the cells fragments of autophagic bodies were detected representing the degradation of the vesicle membrane (Figure 4.6 F).

An examination of ribosomes in yeast *S. cerevisiae* under nitrogen starvation conditions has revealed that these structures are more rapidly degraded compared to other cytoplasmic components, supporting the idea of a selective degradation process [47]. As ribosomes constitute about half of the total cellular protein [46], their degradation may be a major amino acid source under nutrient limiting conditions. Furthermore, by the fact that both ribosome biogenesis and protein translation are highly energy consuming processes, ribophagy might contribute to the rapid down-regulation of these processes and effectively save energy [47].

Up to this date, most of the researches regarding ribosome degradation were based on *S. cerevisiae* under N-starvation condition. Since the typical strategy to produce recombinant protein in *P. pastoris* is based on two steps process (growth phase and induction phase) using glycerol and methanol as carbon source, it seems to be

relevant to perform further studies to elucidate how the carbon starvation period during this transition phase is overcame by the cells and which influences it could bring to cell viability and protein production.

4.2.2.1. Pexophagy: degradation of peroxisomes

P. pastoris is a valuable model system for the study of methanol metabolism [23, 25], peroxisome biogenesis [34] and pexophagy [144]. In the recent ultrastructural analysis of *P. pastoris* GS115 producing high-level of intracellular HBsAg, pexophagy was described. In that study, cells were first grown to high-cell density in a batch process, using a simple defined medium and high glycerol concentrations. After batch growth, induction of high-level product formation was achieved by adding methanol to a final concentration of 6 g L^{-1} and keeping this high concentration for the remainder of the production phase [126]. From 48 h after methanol induction, the pexophagy process was already observed and it seemed to become more intense along the cultivation. Approximately 9% and 12% of the total cells randomly counted from overview images, at 48 h and 112 h after induction with methanol, respectively, showed peroxisomes clearly been engulfed by vacuoles in the cells producing HBsAg (Figure 4.7 A and C).

The strategy to produce the secretory HBsAg was modified and the methanol amount was decreased to a final constant concentration of 2 g L^{-1} to produce the secretory IP [156]. In the ultrastuctural analysis of cells from this new condition, it was noticed that although the peroxisomes were already present in large amount at 48 h after methanol induction, no peroxisome degradation was observed (Figure 4.7 A and B). Just from the next time point analyzed, at 96 h after methanol induction, pexophagy could be observed (Figure 4.7 A and B). Nevertheless, comparing with HBsAg production, only in 6% of the total cells a clear pexophagy process could be observed (Figure 4.7 A). The average of the methanol consumption rate throughout the induction phase was lower in the cells producing IP (2.6 g L^{-1} h^{-1}) compared to the cells producing HBsAg (4.1 g L^{-1} h^{-1}). The difference on the initiation and intensity of pexophagy in the cells under these two different methanol feeding strategies is probably due to the amount of ROS generated related to the methanol consumption rate along the induction phase.

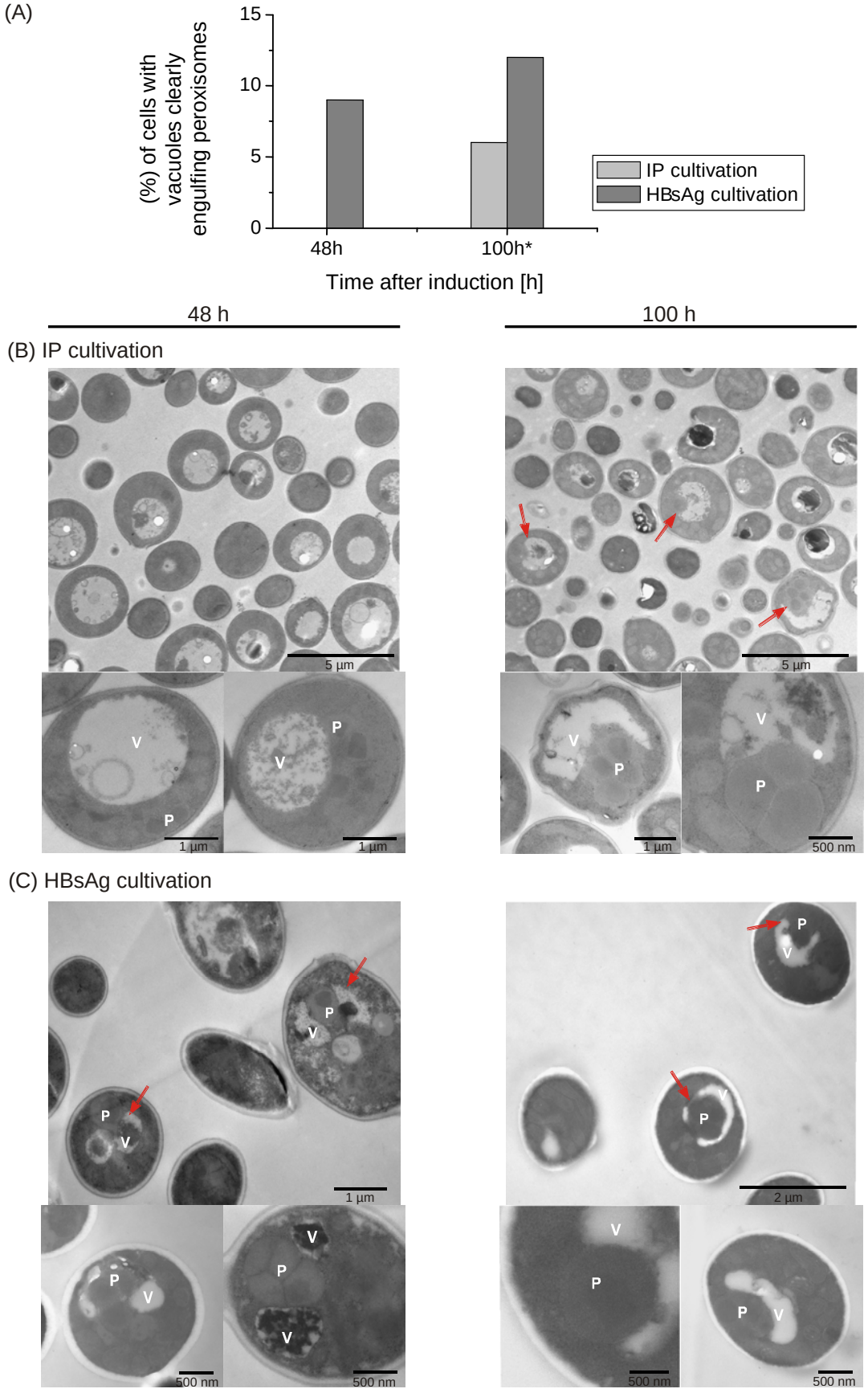
(A)
(%) of cells with vacuoles clearly engulfing peroxisomes
15
10
5
0
48h
100h*
Time after induction [h]
IP cultivation
HBsAg cultivation
48 h
100 h
(B) IP cultivation
5 µm
5 µm
V
P
1 µm
1 µm
1 µm
500 nm
(C) HBsAg cultivation
1 µm
2 µm
500 nm
500 nm
500 nm
500 nm

Figure 4.7. Images of recombinant *P. pastoris* cells growing on methanol. (A) Representative graph showing the (%) of the cells, of the total counted cells, in which the vacuole is clearly engulfing the peroxisome. Samples of *P. pastoris* X-33 producing IP and *P. pastoris* GS115 producing HBsAg at 48 and 100 h* after methanol induction were analyzed. (B) Electron microscopy of *P. pastoris* X-33 at 48 h and at 96 h on methanol for production of secretory IP. At 48 hours the peroxisomes are still in cluster near to the vacuole and no pexophagy is observed. At 96 h pexophagy could be observed. (C) Electron microscopy of *P. pastoris* GS115 at 48 h and at 112 h on methanol for production of HBsAg. Pexophagy could be already observed at 48 h. The red arrow points to the vacuole engulfing the peroxisomes. P, peroxisome; V, vacuole. The (*) symbol means approximately 100 h, (i.e., 96 h in IP and 112 h in HBsAg cultivation).

In *Hansenula polymorpha*, the increase of ROS related to excess of methanol was linked with peroxisome degradation [146]. Pexophagy is considered a housekeeping mechanism where the peroxisomes are constantly degraded and regenerated in a vegetative growth condition (i.e., chemostat cultivation with the same carbon source) probably to prevent the accumulation of non-functional peroxisomal proteins [56]. However, the threshold to launch the peroxisome degradation is still unclear. The increase of ROS in the peroxisomes in an *atg1 H. polymorpha* mutant (*atg1* is required for autophagy) was linked to catalase activity reduction in some peroxisomes of the mutant cells [56]. The peroxisomal membrane proteins, such as Pex3, have been speculated to be the signal for the peroxisome turnover, suggesting that the signal for degradation comes from the inside of the organelle [146]. It is accepted that ROS induces autophagy in general, and H_2O_2 has been implicated as a signalling molecule in various signal transduction pathways, including autophagy [167]. Nevertheless, how this oxidative signal is transmitted is still a question to be solved.

In agreement with the previous chapter, the peroxisomes were degraded by micropexophagy mode (it can be observed in the close views of Figure 4.7 B at 100 h). In micropexophagy, the vacuole membrane invaginates and engulfs the peroxisomal cluster directly to degrade it. This vacuolar membrane re-arrangement is an energy demanding process and the choice of autophagy mode was assumed to be controlled according to the ATP availability in the cell [51]. To control the ROS accumulation in the peroxisomes may help to reduce the oxidative stress to the cell

and may delay the initiation of pexophagy and avoid the cell energy consumption deviation from the final product production.

4.3. Conclusions

The presented data revealed a general down-regulation of the proteins related to UPR and ERAD along the production phase of the secreted insulin precursor. It suggests that the production of insulin precursor does not provoke any significant stress to the cell. The physical feature of the insulin precursor, such as its small size and low number of disulfide bonds, may facilitate a correct protein folding and consequently leads to a successful secretion of the recombinant protein. Additionally, the environmental condition, such as relative high temperature and high osmolarity during the growth phase of the cultivation, may trigger the induction of proteins related to UPR which could benefit and increase the folding competence of the cells facilitating the secretion of insulin precursor to the medium.

So far, most of the studies focus on the induction of unfolded protein response in order to discover new bottlenecks of this pathway or the application of these proteins to increase the final production and secretion of the recombinant protein [89, 96, 136]. Protein secretion in eukaryotic cells is a complex process involving many interacting participants. The successful high level secretion of recombinant protein may be limited not only at a number of different steps, such as folding, disulfide bridge formation, glycosylation, transport within the cell, and release from the cell but also it is intimately related to the protein physical properties as demonstrated in this work.

Autophagic responses to nutrient conditions during the cultivation were also observed. At the end of the growth phase, just before induction with methanol, the cells were subjected to a short carbon starvation condition. At this transition period, the cells have to find a source of energy and degrade its own organelles. According to the results, apparent degradation of ribosome, called ribophagy, was observed. Ribophagy is most reported in *S. cerevisiae* under nitrogen starvation. Here, ribophagy in *P. pastoris* as a response to the cell under carbon starvation condition

can be strongly suggested. During the induction phase, the degradation of the peroxisomes, named as pexophagy was observed. Differently from the HBsAg production strain, where the degradation of peroxisome was observed in the beginning of the production phase, in the IP cultivation the pexophagy process started later. This is probably due to the lower ROS generated as consequence of the lower methanol consumption rate during the IP production. Pexophagy seems to have an important role in cell maintenance during growth on methanol, making it essential to better understand the mechanism, the stimulus behind it and the influence of pexophagic process on the final protein production. This knowledge may help to improve final recombinant protein yields.

4.4. Methods

4.4.1. Yeast strains

The construction of the *P. pastoris* host strain X-33 carrying insulin precursor gene under the control of the *aox1* promoter and harbouring a Mut^+ phenotype used for this study was described previously [156]. A synthetic codon-optimized gene encoding the IP was inserted into the polylinker of this vector, in-frame with the *S. cerevisiae* α-factor secretion signal sequence to create the expression plasmid pPICZα-IP, which was then integrated into the genome of *P. pastoris* strain X-33. Transformation of *P. pastoris*, selection and screening of transformants to identify clones harboring the IP inserts, the isolation of putative multicopy clones using the zeocin screening protocol, and the identification of the methanol utilization (*mut*) phenotype were described previously [156]. The clone GS115-Den2-EDIII-HBsAg (GS115 cells harbouring 4 copies of HBsAg gene and 1 copy of chimeric protein possessing envelope domain III of dengue virus serotype 2 fused with HBsAg) used as a control is from a collaboration project (ICGEB, India). The *P. pastoris* X-33 and GS115 host strains, used as a control are from Invitrogen (Invitrogen, Carlsbad, CA).

4.4.2. Growth conditions

Shake flask cultivation

In 500 mL baffled shake flasks, 100 mL basal medium (20 g L^{-1} glycerol, 13.4 g L^{-1} yeast nitrogen base without amino acids, 400 µg L^{-1} biotin in ddH_2O) were inoculated with 100 µL glycerol stock of the respective *P. pastoris* clones, X-33 host strain, X-33 insulin producer, GS115 host strain and GS115-EDIII-HBsAg. The cultures were grown for approximately 36 hours at 30°C and 250 rpm to gain an OD_{600} of 8 – 10. Next, 1 mL of this pre-inoculum was used to inoculate 100 mL fresh basal medium. After approximately 20 h, when the culture reached an OD_{600} of 3 – 5, 450 mL defined medium (as described below for the bioreactor cultivation) were inoculated with 50 mL of inoculum in a 2 L baffled shake flask. The culture was grown for 30 – 40 hours at 30°C and 150 rpm. Afterwards cells were washed with sterile PBS and resuspended in defined medium without glycerol to an OD_{600} of 100. To induce recombinant protein production, 0.5% of methanol (100%) was added, which was repeated every 12 hours. Samples at different time points were harvested by centrifugation at 13.000 rpm at 4°C. The pellet was immediately frozen in liquid nitrogen and stored at -80°C.

Bioreactor

High-cell density cultivations were carried out in a 15 L BIOSTAT-C (B. Braun Biotech International, Germany) bioreactor essentially as described previously [126]. A 1 L preculture was transferred to the bioreactor containing 7 L growth medium. The growth medium contained per liter: glycerol, 95.2 g; potassium di-hydrogen phosphate, 9.4 g; yeast trace metal (YTM) solution, 4.56 g; ammonium sulfate, 15.7 g; magnesium sulfate hepta-hydrate, 4.6 g; calcium chloride di-hydrate, 0.28 g; and biotin, 0.4 mg. The YTM solution contained: potassium iodide, 207.5 mg L^{-1}; manganese sulfate, 760.6 mg L^{-1}; di-sodium molybdate, 484 mg L^{-1}; boric acid, 46.3 mg L^{-1}; zinc sulfate hepta-hydrate, 5.032 g L^{-1}; ferric chloride hexa-hydrate, 12.0 g L^{-1}; and sulfuric acid, 9.2 g L^{-1}. Foaming was controlled by the addition of antifoam (Ucolub N115). Temperature was maintained at 30°C and pH at pH 5.5 with 12.5% (v/v) NH_4OH or 1 mol L^{-1} H_3PO_4. Aeration rate was maintained at 4 L min^{-1} throughout the process. The stirrer speed was controlled between 100 to 1370 rpm aiming at dissolved oxygen

(DO) concentration of 20% air saturation. After consumption of glycerol, indicated by an increase of the DO concentration, production of recombinant IP was initiated by step-wise addition of a methanol solution [96.6% (w/w) methanol and 4.4% (w/w) YTM] to a final methanol concentration of 2 g L^{-1}, which was maintained constant throughout the remainder of the induction period based on on-line measured methanol concentrations determined from the methanol vapor in the off-gas using a flame ionization detector (Ratfish Instruments, Germany). Based on the gas liquid phase equilibrium methanol concentrations were determined in the off-gas using two point calibrations directly before and after induction. The concentrations of oxygen and carbon dioxide in the exhaust gas were determined by paramagnetic and infrared exhaust gas analysis systems, respectively (Maihak, Hamburg, Germany) [156]. Cells were harvested by centrifugation and washed with phosphate buffered saline to remove extracellular proteins and other contaminants. The pellet was stored at -80°C immediately.

Methanol consumption rate

Methanol consumption rate (g L^{-1} h^{-1}) during the methanol phase, was determined by dividing the total methanol consumed (g) by the cultivation time (h) and volume of the culture (L). The volume of the culture was assumed to be constant 10 L.

4.4.2.1. Osmolarity analysis of the culture supernatant

The osmolarity of the culture supernatant samples was measured by freezing-point depression with an Osmomat 030 (Gonotec, GmbH, Berlin, Germany).

4.4.3. Two-dimensional gel electrophoresis

The detailed protocol of 2D gel electrophoresis is described in Appendix IV.

4.4.3.1. Sample preparation

Cell pellets were washed with ice-cold 1× PBS, resuspended in 1 mL cell lysis buffer (7 mol L^{-1} urea, 2 mol L^{-1} thiourea, 30 mmol L^{-1} Tris, 4% (w/v) Triton, pH 8.5), OD_{600} adjusted to a final 50 and combined with 500 µL of glass beads (0.5 mm, Sartorius, Germany). For cell disruption, samples were treated in a Thermo Savant Fastprep FP120 (homogenizer) twice (speed 6.00 m/s for 30 s; cooling

interval of 30 s between treatments). Afterwards, cellular debris was pelleted by centrifugation at 13000 rpm at 4°C for 5 min, the supernatant was removed and protein was precipitated using chloroform and methanol. Finally the protein pellets were air-dried and dissolved in 500 µL of resolubilization solution (9 mol L^{-1} urea, 2 mol L^{-1} thiourea, 4% CHAPS, 2 mg mL^{-1} Tris, 0.2% SDS, 0.002% bromophenol blue, containing IPG commercial buffer). The solubilized protein was stored at -80 ºC until further analysis by two-dimentional gel electrophoresis.

4.4.3.2. Isoelectric focusing and SDS-PAGE

The first-dimensional of isoelectric focussing (IEF) was run with the IPGphor™ Isoelectric Focussing System (Amersham Biosciences, UK) at 20°C with a current of 30 µA per strip. 400 µg of each protein sample were loaded onto Immobiline DryStrip gels of pH 3–10 NL (IPG strips, Amersham Biosciences, UK) by in-gel rehydration. IEF was performed with the following setting: 0 V × 35h, 50 V × 4 h, gradient from 100 V to 300 V within 4h, gradient from 300 V to 1000 V within 3h, gradient from 1000 V to 3500 V within 4h, gradient from 3500 V to 5000V within 3h, 5000 V × 3h, gradient 5000 V to 8000 v within 3h, then 8000 V × 10h. Before the second-dimension (SDS-PAGE), the IPG strips were equilibrated and then transferred onto 12% SDS-PAGE gel. The second-dimension was carried out using the vertical separation unit Hoefer™ System (Amersham Biosciences) at 10°C in constant working voltage mode as follows: 40 V for 2 h and then 100 V overnight. Subsequently, gels were stained using colloidal Coomassie Blue G-250 according to the "Blue silver" protocol [15]. The gels were then scanned (Epson Perfection V750 Pro, Epson, Germany) at 300 dpi resolution to acquire the gel images.

4.4.4. In-gel trypsin digestion and peptide extraction

The detailed protocol of in-gel trypsin digestion is described in Appendix IV.

Protein spots were excised manually from the stained gels, washed several times with 200 µL water, dehydrated in 200 µl acetonitrile, and dried in a vacuum concentrator (Eppendorf ® Vacufuge Concentrator 5301, Eppendorf AG, Hamburg). The gel pieces were treated with 100 mmol L^{-1} ammonium bicarbonate, containing 20 mmol L^{-1} DTT at 56°C for 30 min and then with 100 mmol L^{-1} ammonium bicarbonate containing 55 mmol L^{-1} iodoacetamide in the dark at room

temperature for 30 min. Acetonitrile was added in between the treatments to dehydrate the gel pieces. Finally, the gel pieces were washed twice with 100 mmol L^{-1} ammonium bicarbonate, dehydrated with acetonitrile and dried in the vacuum concentrator. In-gel digestion was carried out by incubation with 2 ng μL^{-1} trypsin (sequencing grade modified, Promega Corp.) in 50 mmol L^{-1} ammonium bicarbonate at 37°C overnight. Obtained peptides were extracted, washed with a buffer for desalting (10 mmol L^{-1} ammonium phosphate, monobasic in 0.1% TFA) and then loaded to PAC (Prespotted Anchor Chip, Bruker Daltonics GmbH, Germany) targed for MALDI-TOF analysis. The molecular masses of the tryptic peptides were determined on a Bruker Ultraflex time-of-flight mass spectrometer (Bruker Daltonics GmbH, Germany).

4.4.5. Database searching and identification of proteins

Peptide mass fingerprints obtained by the MALDI-TOF MS were processed using FlexAnalysis 2.0 (Bruker Daltonics GmbH, Germany) and used to search NCBInr database by using Mascot 2.10 software (http://www.matrixscience.com). The parameters used for the search were as follows: taxonomy: other Fungi, tryptic digestion, modifications were allowed for carbamidomethylation of cysteine (fixed modification) and methionine oxidation (variable modification), one missed cleavage site was allowed, all peptides monoisotopic, peptide tolerance at 100 ppm. Mascot scores (probability based MOWSE scores) and expect values were generated from the Mascot search program. All proteins with a Mowse score greater than 71 were regarded as significant ($p < 0.05$). For most peptide mass fingerprints, a single significant ($P<0.05$) hit with probability-based Mowse score >71 was obtained. In rare cases the Mowse score was <71, which indicates that the protein was not identified with reliability above the level of significance. These protein spots was excluded from the results unless the identification was confirmed by MS/MS. Image analysis from the scanned gels, namely protein spot detection, matching and quantification were performed using Proteomweaver™ 3.0 (Definiens AG, Germany). For each sample, 2D gels were made in triplicate. And the best two gels were analyzed. The spot volumes were computed and normalized for each spot on each gel in relation to the total volume spot on each 2D gel. To obtain comparable data, spot intensities were normalized, using the log2 ratio of induced samples *versus* uninduced samples. Log2 fold changes above 0.6

(equivalent to a 1.5 fold change) were considered significant. The gene name used is this study is according to *Pichia pastoris* strain GS115 (http://www.uniprot.org/). If no gene name is given for this strain the gene name is according to *Pichia pastoris* (strain ATCC 76273 / CBS 7435 / CECT 11047 / NRRL Y-11430 / Wegner 21-1) or *Pichia pastoris* (yeast) in case of 100% sequence identity (http://www.uniprot.org/).

4.4.6. SDS-PAGE and Western Blot

The crude extract of the samples from the shake flask cultivation, described in 4.3.2, was analyzed by SDS-PAGE 12%. Sample at 0 h i.e., at the end of the growth phase directly before induction with methanol and at 72 h and 96 h after induction with methanol were harvested. Samples corresponding to 100 OD units (1 mL) were transferred and pelleted by centrifugation at 13,000 rpm for 15 min. Cell pellets were resuspended in cell lysis buffer (25 mmol L^{-1} phosphate buffer, 5 mmol L^{-1} EDTA, 0.5 mol L^{-1} NaCl, 8% glycerol, 1 µg/mL pepstatin A, 1 mmol L^{-1} PMSF, pH 8.0) and adjusted to a final OD_{600} 30 and a final 700 mL was combined with 500 µL of glass beads (0.5 mm, Sartorius). For cell disruption, samples were treated in a Thermo Savant Fastprep FP120 (homogenizer) seven times (speed 6.00 m/s for 30 s; cooling interval of 30 s between treatments).

For the Western blot analysis, the intracellular proteins were separated on 12% SDS-PAGE and electrobloted onto a PVDF membrane (Bio-Rad, Hercules, USA) at 12 volts for 45 min. The membrane was blocked with 5% skimmed milk (Difco, France) in PBS (phosphate buffer saline) containing 0.5% Tween 20 (PBS-T buffer) for 2 h. After washing the membrane with PBS-T buffer, the mouse anti-HDEL (2E7) (sc-53472; Santa Cruz Biotechnology), diluted to 1:1000 in PBS-T containing 2.5% skimmed milk, was added and the membrane incubated for 1 h at room temperature. After washing with PBS-T buffer, the secondary antibody, anti-mouse (Calbiochem, Germany) diluted to 1:5000 was added and incubated for 1 h. Protein bands of Western blots were visualized using TMB (3,3´,5,5´ tetramethylbenzidine, Sigma, Germany) as substrate.

4.4.7. Quantification of insulin precursor production by reverse phase high performance liquid chromatography

A HPLC system equipped with a system controller, intelligent pump L-6200A (Merck-Hitachi), auto sampler, column temperature control compartment and an UV-Vis detector IS-3702 Sama was used. The analyses were carried out on reversed phase ZORBAX Poroshell 300SB C8 column (Agilent Technology) (75 × 2.1 mm, with a pore size of 300 Å). Seeing that IP doesn`t contain any tryptophan residue, the main contributor for absorbance at 280 nm, the detector was set at 214 nm. Mobile phase A consisted of 0.1% (v/v) trifluoroacetic acid (TFA) (Sigma-Aldrich, Germany) in water and mobile phase B consisted of 0.1% (v/v) TFA in acetonitrile (Carl Roth GmbH, Germany). The analyses were performed at a column temperature of 30°C and flow rate of 1.0 mL min^{-1}. Elution was done with a linear gradient of increasing acetonitrile concentration (0.5% up to 29%) over 22 min. The injection volume was 50 µL for both standard and samples. Samples were taken at 120 h after induction and cells were lysed with glass beads as described previously. Pure IP was used as control for the retention time. Sample before induction and GS115 host strain were used as a negative control to check if none of natural proteins has the same retention time.

4.4.8. Electron microscopy and image analysis

Electron microscopic studies were carried out essentially as described previously [125]. For the vacuole morphology analysis a total of 628 cells were randomly chosen (100 cells at the end of the growth phase, 223 cells after 48 h and 305 cells after 96 h of methanol induction).

5. Final conclusions and outlook

The methylotrophic yeast *Pichia pastoris* is one of the most important expression systems and has been extensively used for the production of recombinant proteins. However, this yeast is still not adequately characterized at the physiological and proteomic level, especially in relation to its physiological responses to the stressful environment in a bioreactor.

In this work, a comprehensive analysis of the *P. pastoris* cell response when forced to produce recombinant proteins under methanol induction in a relevant bioprocess condition was done at proteomic and morphological level. The response to the overproduction of the hydrophobic hepatitis B virus surface antigen (HBsAg) in strain GS115 and the secreted insulin precursor (IP) in strain X-33 was evaluated using 2D gel electrophoresis combined with MALDI-TOF. In parallel, morphological studies using transmission electron microscopy (TEM) were also performed to investigate autophagic processes, the auto-degradation of cellular components, during the cultivation as a response to nutrient conditions.

In both cultivations, basically the same strategy was used. The cells were first grown in defined medium with high amounts of glycerol as carbon source. After depletion of glycerol, the production phase was initiated by adding a defined amount of methanol. For HBsAg, methanol was maintained at 6 g L^{-1}, and for IP the final concentration was maintained at 2 g L^{-1}. The most significant change in the intracellular proteome after methanol induction compared to the profile before induction was detected in the proteins from the carbon metabolism. The majority of methanol was metabolized via the energy generating dissimilation pathway leading to a corresponding increase in mitochondrial size and numbers. Although the energy generation is one of the roles of the dissimilation pathway during growth on methanol, the detoxification of formaldehyde, which is a by-product of methanol metabolism, is considered its main task [25, 168]. Regarding the methanol metabolism, the assimilation pathway is a potential target to enhance the assimilation of methanol into biomass and recombinant protein. Moreover, the presence of alcohol dehydrogenases (ADHs) in the cells during the methanol-fed batch phase, in both cultivations, indicates that ADHs may play an important role in formaldehyde detoxification in *P. pastoris.*

Due to the methanol induction, cells were subjected to oxidative stress. In addition to formaldehyde, the reactive hydrogen peroxide (H_2O_2) is also generated in the first step of the methanol oxidation and the up-regulation of anti-oxidant enzymes and degradation of peroxisomes were detected in both cultivations. The accumulation of the reactive oxygen species (ROS), as well as the decrease of the activity of some peroxisomal enzymes, has been linked to peroxisome degradation, also named pexophagy [56]. It was observed that the initiation of the pexophagy started earlier in the cells from HBsAg cultivation compared to the IP cultivation. This is probably a result of the higher methanol consumption rate during HBsAg production, which may generate and accumulate more ROS in the peroxisomes. However, in both cultivations, pexophagy was observed throughout the production phase. A housekeeping mechanism can be suggested for *P. pastoris* cells growing on methanol as was suggested for the yeast *H. polymorpha* [146]. Such mechanism may prevent the accumulation of non-functional peroxisomal proteins by degrading the old and regenerating new peroxisomes. Despite of its significance, several aspects regarding pexophagy still remain to be solved. The origin of membrane material for the autophagosome, the signaling for pexophagy regulation or the physiological roles for micro- or macropexophagy is still unclear. Moreover, to investigate if pexophagy has some influence on the final recombinant proteins yield could be an interesting point to be elucidated.

Autophagic response was observed not only during production phase but also at the end of the growth phase as a consequence of nutrient limitation, as analysed in the IP cultivation. Before methanol induction, the cells were subjected to a short carbon starvation period and as a response the cells started to degrade its own components. Autophagic bodies were observed inside the vacuole during this transition period from glycerol to methanol. Structures with appearance of ribosomes were detected inside the autophagic bodies and also entering into the vacuole. Ribophagy, the degradation of ribosomes, has been reported on *S. cerevisiae* under nitrogen starvation [47]. Here, ribophagy in *P. pastoris* cells as a response to carbon starvation condition can be strongly suggested.

The stress related to protein overproduction was also analyzed. Regarding this point, two different cell responses were observed depending on the protein which was produced. The production of HBsAg caused stress to the cells, showed by the

up-regulation of some proteins related to ERAD (endoplasmic reticulum associated degradation) and UPR (unfolded protein response). During the methanol production phase, high-level of HBsAg was produced and translocated into the ER but not further processed in the secretory pathway. The accumulation of HBsAg in the ER triggered the expansion of the ER which bulged into cloud-shaped irregular formations [125]. HBsAg contains 14 cysteines per 226 amino acid monomer, providing opportunity for numerous different disulfide bonds formation [169]. The folding stress might be provoked not only because of the physical feature of the recombinant protein, such as hydrophobicity, size and number of disulfide bonds, but also due to the high copy number of the HBsAg gene inserted into the yeast genome.

On the other hand, the production of the small IP does not provoke any relevant unfolded protein stress response to the cells. During the production phase, the down-regulation of proteins related to UPR and ERAD were detected. The IP physical nature, such as its small size and low number of disulfide bonds, may facilitate protein folding and consequently the secretion to the extracellular space. Additionally, an elevated amount of proteins from the UPR and ERAD during the glycerol growth phase was observed. This is probably due to the cultivation conditions used, such as the high temperature and the high osmolarity. This prior induction of chaperones and foldases might condition the cells for a better folding performance and seemed to positively affect the IP folding and secretion. Further studies should be done to better understand the regulation of the ERAD and UPR related proteins during the growth phase of *P. pastoris* facing different environmental conditions, such as osmotic stress, and its influence on insulin precursor secretion level.

When the folding machinery gets overloaded, the folding is slow compared to the disulfide bond formation and the unfolded protein may go through many futile redox cycles, required to fix incorrect disulfide bonds, producing excess of ROS [81]. For a successful production of the recombinant protein, the transcription rate should be as high as possible without overloading the ER folding capacity and sending the cell into an oxidative stressed state [81]. But this optimal condition will be different for different proteins. As described in this work, different cell response regarding unfolding protein stress was observed in *P. pastoris* producing HBsAg

and IP. Such differences might be caused because of the properties of each protein. To reach a balance, either the protein folding rate must be increased by expression of chaperones for instance [98], or the oxidation rate must be decreased by limiting the oxidation of ERO1, as suggested by Tyo *et al*. [81].

Improvements in the production titer of heterologous protein have been achieved from milligrams to grams per liter based on optimization of the fermentation process and strain engineering in the past decade. However, the strategies sometimes are useful only for a specific protein and the same engineered strain could not be used as a general cell factory platform for the production of a range of different recombinant proteins. The protein properties as well as the gene copy number inserted in the strain play an important role on the production efficiency. An increased molecular understanding of the secretory pathway of the individual processes can be used to guide general models for protein secretion and used for engineering design of new cell factories.

6. References

1. Martinez JL, Liu L, Petranovic D, Nielsen J: **Pharmaceutical protein production by yeast: towards production of human blood proteins by microbial fermentation**. *Curr Opin Biotechnol* 2012, **23**(6):965-971.

2. Huang CJ, Lin H, Yang X: **Industrial production of recombinant therapeutics in *Escherichia coli* and its recent advancements**. *J Ind Microbiol Biotechnol* 2012, **39**(3):383-399.

3. Walsh G: **Biopharmaceutical benchmarks 2010**. *Nat Biotechnol* 2010, **28**(9):917-924.

4. Cregg JM, Barringer KJ, Hessler AY, Madden KR: ***Pichia pastoris* as a host system for transformations**. *Mol Cell Biol* 1985, **5**(12):3376-3385.

5. Wriessnegger T, Sunga AJ, Cregg JM, Daum G: **Identification of phosphatidylserine decarboxylases 1 and 2 from *Pichia pastoris***. *FEMS Yeast Res* 2009, **9**(6):911-922.

6. Bollok M, Resina D, Valero F, Ferrer P: **Recent patents on the *Pichia pastoris* expression system: expanding the toolbox for recombinant protein production**. *Recent Pat Biotechnol* 2009, **3**(3):192-201.

7. Siegel RS, Brierley RA: **Methylotrophic yeast *Pichia pastoris* produced in high-cell-density fermentations with high cell yields as vehicle for recombinant protein-production**. *Biotech Bioeng* 1989, **34**(3):403-404.

8. Cregg JM, Cereghino JL, Shi JY, Higgins DR: **Recombinant protein expression in *Pichia pastoris***. *Mol Biotechnol* 2000, **16**(1):23-52.

9. Cregg JM, Vedvick TS, Raschke WC: **Recent advances in the expression of foreign genes in P*ichia pastoris***. *Biotechn* 1993, **11**(8):905-910.

10. Cereghino GPL, Cereghino JL, Ilgen C, Cregg JM: **Production of recombinant proteins in fermenter cultures of the yeast *Pichia pastoris***. *Curr Opin Biotechnol* 2002, **13**(4):329-332.

11. Li P, Anumanthan A, Gao XG, Ilangovan K, Suzara VV, Duzgunes N, Renugopalakrishnan V: **Expression of recombinant proteins in *Pichia pastoris***. *Appl Biochem Biotechnol* 2007, **142**(2):105-124.

12. Romanos MA, Scorer CA, Clare JJ: **Foreign gene-expression in yeast - a Review**. *Yeast* 1992, **8**(6):423-488.

13. Sunga AJ, Tolstorukov I, Cregg JM: **Posttransformational vector amplification in the yeast *Pichia pastoris***. *FEMS Yeast Res* 2008, **8**(6):870-876.

14. Werten MW, van den Bosch TJ, Wind RD, Mooibroek H, de Wolf FA: **High-yield secretion of recombinant gelatins by *Pichia pastoris***. *Yeast* 1999, **15**(11):1087-1096.

15. Durocher Y, Butler M: **Expression systems for therapeutic glycoprotein production**. *Curr Opin Biotechnol* 2009, **20**(6):700-707.

16. Li H, d'Anjou M: **Pharmacological significance of glycosylation in therapeutic proteins**. *Curr Opin Biotechnol* 2009, **20**(6):678-684.

17. Chung BKS, Selvarasu S, Andrea C, Ryu J, Lee H, Ahn J, Lee H, Lee DY: **Genome-scale metabolic reconstruction and in silico analysis of methylotrophic yeast *Pichia pastoris* for strain improvement**. *Microb Cell Fact* 2010, **9**(1):50.

18. Hamilton SR, Gerngross TU: **Glycosylation engineering in yeast: the advent of fully humanized yeast**. *Curr Opin Biotechnol* 2007, **18**(5):387-392.

19. Kurtzman CP: **Biotechnological strains of *Komagataella (Pichia) pastoris* are *Komagataella phaffii* as determined from multigene sequence analysis**. *J Ind Microbiol Biotechnol* 2009, **36**(11):1435-1438.

20. Gellissen G: **Heterologous protein production in methylotrophic yeasts**. *Appl Microbiol Biotechnol* 2000, **54**(6):741-750.

21. Cereghino JL, Cregg JM: **Heterologous protein expression in the methylotrophic yeast *Pichia pastoris***. *FEMS Microbiol Rev* 2000, **24**(1):45-66.

22. Macauley-Patrick S, Fazenda ML, McNeil B, Harvey LM: **Heterologous protein production using the *Pichia pastoris* expression system**. *Yeast* 2005, **22**(4):249-270.

23. Yurimoto H, Oku M, Sakai Y: **Yeast methylotrophy: metabolism, gene regulation and peroxisome homeostasis**. *Int J Microbiol* 2011, **2011**:101298.

24. Yurimoto H, Kato N, Sakai Y: **Assimilation, dissimilation, and detoxification of formaldehyde, a central metabolic intermediate of methylotrophic metabolism**. *Chem Rec* 2005, **5**(6):367-375.

25. Hartner FS, Glieder A: **Regulation of methanol utilisation pathway genes in yeasts**. *Microb Cell Fact* 2006, **5**:39.

26. Yurimoto H, Lee B, Yasuda F, Sakai Y, Kato N: **Alcohol dehydrogenases that catalyse methyl formate synthesis participate in formaldehyde detoxification in the methylotrophic yeast *Candida boidinii***. *Yeast* 2004, **21**(4):341-350.

27. Vijay Kumar N, Rangarajan PN: **The zinc finger proteins Mxr1p and ROP have the same DNA binding specificity but regulate methanol metabolism antagonistically in *Pichia pastoris***. *J Biol Chem* 2012.

28. Krainer FW, Dietzsch C, Hajek T, Herwig C, Spadiut O, Glieder A: **Recombinant protein expression in *Pichia pastoris* strains with an engineered methanol utilization pathway**. *Microb Cell Fact* 2012, **11**:22.

29. Schroer K, Luef KP, Hartner FS, Glieder A, Pscheidt B: **Engineering the *Pichia pastoris* methanol oxidation pathway for improved NADH regeneration during whole-cell biotransformation**. *Metab Eng* 2010, **12**(1):8-17.

30. Aksam EB, de Vries B, van der Klei IJ, Kiel JA: **Preserving organelle vitality: peroxisomal quality control mechanisms in yeast**. *FEMS Yeast Res* 2009, **9**(6):808-820.

31. Li Q, Harvey LM, McNeil B: **Oxidative stress in industrial fungi**. *Crit Rev Biotechnol* 2009, **29**(3):199-213.

32. Bener Aksam E, de Vries B, van der Klei IJ, Kiel JA: **Preserving organelle vitality: peroxisomal quality control mechanisms in yeast**. *FEMS Yeast Res* 2009, **9**(6):808-820.

33. Purdue PE, Lazarow PB: **Peroxisome biogenesis**. *Annu Rev Cell Dev Biol* 2001, **17**:701-752.

34. van der Klei IJ, Yurimoto H, Sakai Y, Veenhuis M: **The significance of peroxisomes in methanol metabolism in methylotrophic yeast**. *Biochim Biophys Acta* 2006, **1763**(12):1453-1462.

35. Kraft C, Reggiori F, Peter M: **Selective types of autophagy in yeast**. *Biochim Biophys Acta* 2009, **1793**(9):1404-1412.

36. Dunn WA, Jr., Cregg JM, Kiel JA, van der Klei IJ, Oku M, Sakai Y, Sibirny AA, Stasyk OV, Veenhuis M: **Pexophagy: the selective autophagy of peroxisomes**. *Autophagy* 2005, **1**(2):75-83.

37. Pollack JK, Harris SD, Marten MR: **Autophagy in filamentous fungi**. *Fungal Genet Biol* 2009, **46**(1):1-8.

38. Klionsky DJ, Emr SD: **Cell biology - Autophagy as a regulated pathway of cellular degradation**. *Science* 2000, **290**(5497):1717-1721.

39. Kiel JAKW: **Autophagy in unicellular eukaryotes**. *Philos Trans R Soc Lond B Biol Sci* 2010, **365**(1541):819-830.

40. Manjithaya R, Nazarko TY, Farre JC, Subramani S: **Molecular mechanism and physiological role of pexophagy**. *FEBS Lett* 2010, **584**(7):1367-1373.

41. Kissova I, Salin B, Schaeffer J, Bhatia S, Manon S, Camougrand N: **Selective and non-selective autophagic degradation of mitochondria in yeast**. *Autophagy* 2007, **3**(4):329-336.

42. Bernales S, McDonald KL, Walter P: **Autophagy counterbalances endoplasmic reticulum expansion during the unfolded protein response**. *PLoS Biol* 2006, **4**(12):e423.

43. Takeshige K, Baba M, Tsuboi S, Noda T, Ohsumi Y: **Autophagy in yeast demonstrated with proteinase-deficient mutants and conditions for its induction**. *J Cell Biol* 1992, **119**(2):301-311.

44. Eskelinen EL, Reggiori F, Baba M, Kovacs AL, Seglen PO: **Seeing is believing: The impact of electron microscopy on autophagy research**. *Autophagy* 2011, **7**(9):935-956.

45. Hamasaki M, Noda T, Baba M, Ohsumi Y: **Starvation triggers the delivery of the endoplasmic reticulum to the vacuole via autophagy in yeast**. *Traffic* 2005, **6**(1):56-65.

46. Cebollero E, Reggiori F, Kraft C: **Reticulophagy and ribophagy: regulated degradation of protein production factories**. *Int J Cell Biol* 2012, **2012**.

47. Kraft C, Deplazes A, Sohrmann M, Peter M: **Mature ribosomes are selectively degraded upon starvation by an autophagy pathway requiring the Ubp3p/Bre5p ubiquitin protease**. *Nat Cell Biol* 2008, **10**(5):602-610.

48. Oku M, Sakai Y: **Peroxisomes as dynamic organelles: autophagic degradation**. *Febs Journal* 2010, **277**(16):3289-3294.

49. Farre JC, Subramani S: **Peroxisome turnover by micropexophagy: an autophagy-related process**. *Trends Cell Biol* 2004, **14**(9):515-523.

50. Sakai Y, Oku M, van der Klei IJ, Kiel JAKW: **Pexophagy: Autophagic degradation of peroxisomes**. *Biochim Biophys Acta* 2006, **1763**(12):1767-1775.

51. Ano Y, Hattori T, Kato N, Sakai Y: **Intracellular ATP correlates with mode of pexophagy in *Pichia pastoris***. *Biosci Biotechnol Biochem* 2005, **69**(8):1527-1533.

52. Farre JC, Manjithaya R, Mathewson RD, Subramani S: **PpAtg30 tags peroxisomes for turnover by selective autophagy**. *Dev Cell* 2008, **14**(3):365-376.

53. Stasyk OV, Stasyk OG, Mathewson RD, Farre JC, Nazarko VY, Krasovska OS, Subramani S, Cregg JM, Sibirny AA: **Atg28, a novel coiled-coil protein involved in autophagic degradation of peroxisomes in the methylotrophic yeast *Pichia pastoris***. *Autophagy* 2006, **2**(1):30-38.

54. Oku M, Warnecke D, Noda T, Muller F, Heinz E, Mukaiyama H, Kato N, Sakai Y: **Peroxisome degradation requires catalytically active sterol glucosyltransferase with a GRAM domain**. *EMBO J* 2003, **22**(13):3231-3241.

55. Nazarko VY, Nazarko TY, Farre JC, Stasyk OV, Warnecke D, Ulaszewski S, Cregg JM, Sibirny AA, Subramani S: **Atg35, a micropexophagy-specific protein that regulates micropexophagic apparatus formation in *Pichia pastoris***. *Autophagy* 2011, **7**(4):375-385.

56. Bener Aksam E, Koek A, Kiel JA, Jourdan S, Veenhuis M, van der Klei IJ: **A peroxisomal lon protease and peroxisome degradation by autophagy play key roles in vitality of *Hansenula polymorpha* cells**. *Autophagy* 2007, **3**(2):96-105.

57. Polupanov AS, Nazarko VY, Sibirny AA: **Gss1 protein of the methylotrophic yeast *Pichia pastoris* is involved in glucose sensing, pexophagy and catabolite repression**. *Int J Biochem Cell Biol* 2012, **44**(11):1906-1918.

58. Tuttle DL, Dunn WA, Jr.: **Divergent modes of autophagy in the methylotrophic yeast *Pichia pastoris***. *J Cell Sci* 1995, **108 (Pt 1)**:25-35.

59. Mattanovich D, Gasser B, Hohenblum H, Sauer M: **Stress in recombinant protein producing yeasts**. *J Biotechnol* 2004, **113**(1-3):121-135.

60. Li Q, Bai Z, O'Donnell A, Harvey LM, Hoskisson PA, McNeil B: **Oxidative stress in fungal fermentation processes: the roles of alternative respiration**. *Biotechnol Lett* 2011, **33**(3):457-467.

61. Anelli T, Sitia R: **Protein quality control in the early secretory pathway**. *Embo J* 2008, **27**(2):315-327.

62. van Anken E, Braakman I: **Versatility of the endoplasmic reticulum protein folding factory**. *Crit Rev in Biochem Mol Biol* 2005, **40**(4):191-228.

63. Idiris A, Tohda H, Kumagai H, Takegawa K: **Engineering of protein secretion in yeast: strategies and impact on protein production**. *Appl Microbiol Biotechnol* 2010, **86**(2):403-417.

64. Pfeffer M, Maurer M, Stadlmann J, Grass J, Delic M, Altmann F, Mattanovich D: **Intracellular interactome of secreted antibody Fab fragment in *Pichia pastoris* reveals its routes of secretion and degradation**. *Appl Microbiol Biotechnol* 2012, **93**(6):2503-2512.

65. Haynes CM, Titus EA, Cooper AA: **Degradation of misfolded proteins prevents ER-derived oxidative stress and cell death**. *Mol Cell Biol* 2004, **15**(5):767-776.

66. Hou J, Tyo KE, Liu Z, Petranovic D, Nielsen J: **Metabolic engineering of recombinant protein secretion by *Saccharomyces cerevisiae***. *FEMS Yeast Res* 2012, **12**(5):491-510.

67. Patil C, Walter P: **Intracellular signaling from the endoplasmic reticulum to the nucleus: the unfolded protein response in yeast and mammals**. *Curr Opin Cell Biol* 2001, **13**(3):349-356.

68. Xu P, Robinson AS: **Decreased secretion and unfolded protein response up-regulation are correlated with intracellular retention for single-chain antibody variants produced in yeast**. *Biotechnol Bioeng* 2009, **104**(1):20-29.

69. Kimata Y, Kimata YL, Shimizu Y, Abe H, Farcasanu RC, Takeuchi M, Rose MD, Kohno K: **Genetic evidence for a role of BiP/Kar2 that regulates Ire1 in response to accumulation of unfolded proteins**. *Mol Biol Cell* 2003, **14**(6):2559-2569.

70. Bukau B, Horwich AL: **The Hsp70 and Hsp60 chaperone machines**. *Cell* 1998, **92**(3):351-366.

71. Kimata Y, Ishiwata-Kimata Y, Yamada S, Kohno K: **Yeast unfolded protein response pathway regulates expression of genes for anti-oxidative stress and for cell surface proteins**. *Genes Cells* 2006, **11**(1):59-69.

72. Ruegsegger U, Leber JH, Walter P: **Block of HAC1 mRNA translation by long-range base pairing is released by cytoplasmic splicing upon induction of the unfolded protein response**. *Cell* 2001, **107**(1):103-114.

73. Guerfal M, Ryckaert S, Jacobs PP, Ameloot P, Van Craenenbroeck K, Derycke R, Callewaert N: **The HAC1 gene from *Pichia pastoris*: characterization and effect of its overexpression on the production of secreted, surface displayed and membrane proteins**. *Microb Cell Fact* 2010, **9**:49.

74. Xu X, Kanbara K, Azakami H, Kato A: **Expression and characterization of *Saccharomyces cerevisiae* Cne1p, a calnexin homologue**. *J Biochem* 2004, **135**(5):615-618.

75. Kleizen B, Braakman I: **Protein folding and quality control in the endoplasmic reticulum**. *Curr Opin Cell Biol* 2004, **16**(4):343-349.

76. Tu BP, Weissman JS: **Oxidative protein folding in eukaryotes: mechanisms and consequences**. *J Cell Biol* 2004, **164**(3):341-346.

77. Nishikawa S, Brodsky JL, Nakatsukasa K: **Roles of molecular chaperones in endoplasmic reticulum (ER) quality control and ER-associated degradation (ERAD)**. *J Biochem* 2005, **137**(5):551-555.

78. Gasser B, Saloheimo M, Rinas U, Dragosits M, Rodriguez-Carmona E, Baumann K, Giuliani M, Parrilli E, Branduardi P, Lang C *et al*: **Protein folding and conformational stress in microbial cells producing recombinant proteins: a host comparative overview**. *Microb Cell Fact* 2008, **7**:11.

79. Stolz A, Wolf DH: **Endoplasmic reticulum associated protein degradation: A chaperone assisted journey to hell**. *Biochim Biophys Acta* 2010, **1803**(6):694-705.

80. Sevier CS, Kaiser CA: **Formation and transfer of disulphide bonds in living cells**. *Nat Rev Mol Cell Biol* 2002, **3**(11):836-847.

81. Tyo KE, Liu Z, Petranovic D, Nielsen J: **Imbalance of heterologous protein folding and disulfide bond formation rates yields runaway oxidative stress**. *BMC Biol* 2012, **10**:16.

82. Schulman BA, Harper JW: **Ubiquitin-like protein activation by E1 enzymes: the apex for downstream signalling pathways**. *Nat Rev Mol Cell Biol* 2009, **10**(5):319-331.

83. Rabinovich E, Kerem A, Frohlich KU, Diamant N, Bar-Nun S: **AAA-ATPase p97/Cdc48p, a cytosolic chaperone required for endoplasmic reticulum-associated protein degradation**. *Mol Cell Biol* 2002, **22**(2):626-634.

84. Gillece P, Luz JM, Lennarz WJ, de La Cruz FJ, Romisch K: **Export of a cysteine-free misfolded secretory protein from the endoplasmic reticulum for degradation requires interaction with protein disulfide isomerase**. *J Cell Biol* 1999, **147**(7):1443-1456.

85. Nishikawa SI, Fewell SW, Kato Y, Brodsky JL, Endo T: **Molecular chaperones in the yeast endoplasmic reticulum maintain the solubility of proteins for retrotranslocation and degradation**. *J Cell Biol* 2001, **153**(5):1061-1070.

86. Zhang YM, Nijbroek G, Sullivan ML, McCracken AA, Watkins SC, Michaelis S, Brodsky JL: **Hsp70 molecular chaperone facilitates endoplasmic reticulum-associated protein degradation of cystic fibrosis transmembrane conductance regulator in yeast**. *Mol Biol Cell* 2001, **12**(5):1303-1314.

87. Buck TM, Wright CM, Brodsky JL: **The activities and function of molecular chaperones in the endoplasmic reticulum**. *Semin Cell Dev Biol* 2007, **18**(6):751-761.

88. Dragosits M, Stadlmann J, Albiol J, Baumann K, Maurer M, Gasser B, Sauer M, Altmann F, Ferrer P, Mattanovich D: **The effect of temperature on the proteome of recombinant *Pichia pastoris***. *J Proteome Res* 2009, **8**(3):1380-1392.

89. Baumann K, Carnicer M, Dragosits M, Graf AB, Stadlmann J, Jouhten P, Maaheimo H, Gasser B, Albiol J, Mattanovich D *et al*: **A multi-level study of recombinant *Pichia pastoris* in different oxygen conditions**. *BMC Syst Biol* 2010, **4**:141.

90. Baumann K, Maurer M, Dragosits M, Cos O, Ferrer P, Mattanovich D: **Hypoxic fed-batch cultivation of *Pichia pastoris* increases specific and volumetric productivity of recombinant proteins**. *Biotechnol Bioeng* 2008, **100**(1):177-183.

91. Kim Y, Nandakumar MP, Marten MR: **Proteome map of *Aspergillus nidulans* during osmoadaptation**. *Fungal Genet Biol* 2007, **44**(9):886-895.

92. Blomberg A: **Global changes in protein synthesis during adaptation of the yeast *Saccharomyces cerevisiae* to 0.7 M NaCl**. *J Bacteriol* 1995, **177**(12):3563-3572.

93. Lahav R, Nejidat A, Abeliovich A: **Alterations in protein synthesis and levels of heat shock 70 proteins in response to salt stress of the halotolerant yeast *Rhodotorula mucilaginosa***. *Antonie Van Leeuwenhoek* 2004, **85**(4):259-269.

94. Dragosits M, Stadlmann J, Graf A, Gasser B, Maurer M, Sauer M, Kreil DP, Altmann F, Mattanovich D: **The response to unfolded protein is involved in osmotolerance of *Pichia pastoris***. *Bmc Genomics* 2010, **11**.

95. Shi X, Karkut T, Chamankhah M, Alting-Mees M, Hemmingsen SM, Hegedus D: **Optimal conditions for the expression of a single-chain antibody (scFv) gene in *Pichia pastoris***. *Protein Expr Purif* 2003, **28**(2):321-330.

96. Gasser B, Maurer M, Gach J, Kunert R, Mattanovich D: **Engineering of *Pichia pastoris* for improved production of antibody fragments**. *Biotechnol Bioeng* 2006, **94**(2):353-361.

97. Vad R, Nafstad E, Dahl LA, Gabrielsen OS: **Engineering of a *Pichia pastoris* expression system for secretion of high amounts of intact human parathyroid hormone**. *J Biotechnol* 2005, **116**(3):251-260.

98. Kim MD, Han KC, Kang HA, Rhee SK, Seo JH: **Coexpression of BiP increased antithrombotic hirudin production in recombinant *Sacchdromyces cerevisiae***. *J Biotechnol* 2003, **101**(1):81-87.

99. Robinson AS, Hines V, Wittrup KD: **Protein disulfide-isomerase overexpression increases secretion of foreign proteins in *Saccharomyces cerevisiae***. *Bioechnology* 1994, **12**(4):381-384.

100. Shen Q, Wu M, Wang HB, Naranmandura H, Chen SQ: **The effect of gene copy number and co-expression of chaperone on production of albumin fusion proteins in *Pichia pastoris***. *Appl Microbiol Biotechnol* 2012, **96**(3):763-772.

101. Butz JA, Niebauer RT, Robinson AS: **Co-expression of molecular chaperones does not improve the heterologous expression of mammalian G-protein coupled receptor expression in yeast**. *Biotechnol Bioeng* 2003, **84**(3):292-304.

102. Sauer M, Branduardi P, Gasser B, Valli M, Maurer M, Porro D, Mattanovich D: **Differential gene expression in recombinant *Pichia pastoris* analysed by heterologous DNA microarray hybridisation**. *Microb Cell Fact* 2004, **3**(1):17.

103. Austin RJ, Kuestner RE, Chang DK, Madden KR, Martin DB: **SILAC compatible strain of *Pichia pastoris* for expression of isotopically labeled protein standards and quantitative proteomics**. *J Proteome Res* 2011, **10**(11):5251-5259.

104. Szopinska A, Morsomme P: **Quantitative proteomic approaches and their application in the study of yeast stress responses**. *Omics* 2010, **14**(6):639-649.

105. Katayama H, Nagasu T, Oda Y: **Improvement of in-gel digestion protocol for peptide mass fingerprinting by matrix-assisted laser desorption/ionization time-of-flight mass spectrometry**. *Rapid Commun Mass Spectrom* 2001, **15**(16):1416-1421.

106. Wilkins MR, Sanchez JC, Gooley AA, Appel RD, HumpherySmith I, Hochstrasser DF, Williams KL: **Progress with proteome projects: Why all proteins expressed by a genome should be identified and how to do it**. *Biotechnol Genet Eng Rev* 1996, **13**:19-50.

107. Griffin TJ, Gygi SP, Ideker T, Rist B, Eng J, Hood L, Aebersold R: **Complementary profiling of gene expression at the transcriptome and proteome levels in *Saccharomyces cerevisiae***. *Mol Cell Proteomics* 2002, **1**(4):323-333.

108. de Groot MJ, Daran-Lapujade P, van Breukelen B, Knijnenburg TA, de Hulster EA, Reinders MJ, Pronk JT, Heck AJ, Slijper M: **Quantitative proteomics and transcriptomics of anaerobic and aerobic yeast cultures reveals post-transcriptional regulation of key cellular processes**. *Microbiology* 2007, **153**(Pt 11):3864-3878.

109. Pradet-Balade B, Boulme F, Beug H, Mullner EW, Garcia-Sanz JA: **Translation control: bridging the gap between genomics and proteomics?** *Trends Biochem Sci* 2001, **26**(4):225-229.

110. De Schutter K, Lin YC, Tiels P, Van Hecke A, Glinka S, Weber-Lehmann J, Rouze P, de Peer YV, Callewaert N: **Genome sequence of the recombinant protein production host *Pichia pastoris***. *Nat Biotechnol* 2009, **27**(6):561-U104.

111. Mattanovich D, Graf A, Stadlmann J, Dragosits M, Redl A, Maurer M, Kleinheinz M, Sauer M, Altmann F, Gasser B: **Genome, secretome and glucose transport highlight unique features of the protein production host *Pichia pastoris***. *Microb Cell Fact* 2009, **8**.

112. Damasceno LM, Huang CJ, Batt CA: **Protein secretion in *Pichia pastoris* and advances in protein production**. *Appl Microbiol Biotechnol* 2012, **93**(1):31-39.

113. Vanz AL, Lunsdorf H, Adnan A, Nimtz M, Gurramkonda C, Khanna N, Rinas U: **Physiological response of *Pichia pastoris* GS115 to methanol-induced high level production of the Hepatitis B surface antigen: catabolic adaptation, stress responses, and autophagic processes**. *Microb Cell Fact* 2012, **11**(1):103.

114. Mattanovich D, Branduardi P, Dato L, Gasser B, Sauer M, Porro D: **Recombinant protein production in yeasts**. *Methods Mol Biol* 2012, **824**:329-358.

115. Cregg JM, Madden KR, Barringer KJ, Thill GP, Stillman CA: **Functional characterization of the two alcohol oxidase genes from the yeast *Pichia pastoris***. *Mol Cell Biol* 1989, **9**(3):1316-1323.

116. Vassileva A, Chugh DA, Swaminathan S, Khanna N: **Effect of copy number on the expression levels of hepatitis B surface antigen in the methylotrophic yeast *Pichia pastoris***. *Protein Expr Purif* 2001, **21**(1):71-80.

117. Zhu T, Guo M, Tang Z, Zhang M, Zhuang Y, Chu J, Zhang S: **Efficient generation of multi-copy strains for optimizing secretory expression of porcine insulin precursor in yeast *Pichia pastoris***. *J Appl Microbiol* 2009, **107**(3):954-963.

118. Clare JJ, Romanos MA, Rayment FB, Rowedder JE, Smith MA, Payne MM, Sreekrishna K, Henwood CA: **Production of mouse epidermal growth factor in yeast: high-level secretion using *Pichia pastoris* strains containing multiple gene copies**. *Gene* 1991, **105**(2):205-212.

119. Mansur M, Cabello C, Hernandez L, Pais J, Varas L, Valdes J, Terrero Y, Hidalgo A, Plana L, Besada V *et al*: **Multiple gene copy number enhances insulin precursor secretion in the yeast *Pichia pastoris***. *Biotechnol Lett* 2005, **27**(5):339-345.

120. Zhu TC, Guo MJ, Zhuang YP, Chu J, Zhang SL: **Understanding the effect of foreign gene dosage on the physiology of *Pichia pastoris* by transcriptional analysis of key genes**. *Appl Microbiol Biotechnol* 2011, **89**(4):1127-1135.

121. Hohenblum H, Gasser B, Maurer M, Borth N, Mattanovich D: **Effects of gene dosage, promoters, and substrates on unfolded protein stress of recombinant *Pichia pastoris***. *Biotechnol Bioeng* 2004, **85**(4):367-375.

122. Cos O, Serrano A, Montesinos JL, Ferrer P, Cregg JM, Valero F: **Combined effect of the methanol utilization (Mut) phenotype and gene dosage on recombinant protein production in *Pichia pastoris* fed-batch cultures**. *J Biotechnol* 2005, **116**(4):321-335.

123. Whyteside G, Alcocer MJ, Kumita JR, Dobson CM, Lazarou M, Pleass RJ, Archer DB: **Native-state stability determines the extent of degradation relative to secretion of protein variants from *Pichia pastoris***. *PLoS One* 2011, **6**(7):e22692.

124. Gasser B, Maurer M, Rautio J, Sauer M, Bhattacharyya A, Saloheimo M, Penttila M, Mattanovich D: **Monitoring of transcriptional regulation in *Pichia pastoris* under protein production conditions**. *BMC Genomics* 2007, **8**:179.

125. Lunsdorf H, Gurramkonda C, Adnan A, Khanna N, Rinas U: **Virus-like particle production with yeast: ultrastructural and immunocytochemical insights into *Pichia pastoris* producing high levels of the Hepatitis B surface antigen**. *Microb Cell Fact* 2011, **10**:48.

126. Gurramkonda C, Adnan A, Gabel T, Lunsdorf H, Ross A, Nemani SK, Swaminathan S, Khanna N, Rinas U: **Simple high-cell density fed-batch technique for high-level recombinant protein production with *Pichia pastoris*: Application to intracellular production of Hepatitis B surface antigen**. *Microb Cell Fact* 2009, **8**:13.

127. Lu X, Sun JB, Nimtz M, Wissing J, Zeng AP, Rinas U: **The intra- and extracellular proteome of *Aspergillus niger* growing on defined medium with xylose or maltose as carbon substrate**. *Microb Cell Fact* 2010, **9**:23.

128. Inan M, Meagher MM: **The effect of ethanol and acetate on protein expression in *Pichia pastoris***. *J Biosci Bioeng* 2001, **92**(4):337-341.

129. Chiruvolu V, Eskridge K, Cregg J, Meagher M: **Effects of glycerol concentration and pH on growth of recombinant *Pichia pastoris* yeast**. *Appl Biochem Biotechnol* 1998, **75**(2-3):163-173.

130. Horiguchi H, Yurimoto H, Goh T, Nakagawa T, Kato N, Sakai Y: **Peroxisomal catalase in the methylotrophic yeast *Candida boidinii*: transport efficiency and metabolic significance**. *J Bacteriol* 2001, **183**(21):6372-6383.

131. Horiguchi H, Yurimoto H, Kato N, Sakai Y: **Antioxidant system within yeast peroxisome - Biochemical and physiological characterization of CbPmp20 in the methylotrophic yeast *Candida boidinii***. *J Biol Chem* 2001, **276**(17):14279-14288.

132. Yano T, Takigami E, Yurimoto H, Sakai Y: **Yap1-regulated glutathione redox system curtails accumulation of formaldehyde and reactive oxygen species in methanol metabolism of *Pichia pastoris***. *Eukaryot Cell* 2009, **8**(4):540-549.

133. Bener Aksam E, Jungwirth H, Kohlwein SD, Ring J, Madeo F, Veenhuis M, van der Klei IJ: **Absence of the peroxiredoxin Pmp20 causes peroxisomal protein leakage and necrotic cell death**. *Free Radic Biol Med* 2008, **45**(8):1115-1124.

134. Kim IS, Yun HS, Park IS, Sohn HY, Iwahashi H, Jin IN: **A knockout strain of CPR1 induced during fermentation of *Saccharomyces cerevisiae* KNU5377 is susceptible to various types of stress**. *J Biosci Bioeng* 2006, **102**(4):288-296.

135. Zhao Q, Wang Y, Freed D, Fu TM, Gimenez JA, Sitrin RD, Washabaugh MW: **Maturation of recombinant hepatitis B virus surface antigen particles**. *Hum Vaccin* 2006, **2**(4):174-180.

136. Graf A, Gasser B, Dragosits M, Sauer M, Leparc GG, Tuchler T, Kreil DP, Mattanovich D: **Novel insights into the unfolded protein response using *Pichia pastoris* specific DNA microarrays**. *Bmc Genomics* 2008, **9**:390.

137. Taxis C, Hitt R, Park SH, Deak PM, Kostova Z, Wolf DH: **Use of modular substrates demonstrates mechanistic diversity and reveals differences in chaperone requirement of ERAD**. *J Biol Chem* 2003, **278**(38):35903-35913.

138. Hoseki J, Ushioda R, Nagata K: **Mechanism and components of endoplasmic reticulum-associated degradation**. *J Biochem* 2010, **147**(1):19-25.

139. Zolkiewski M, Zhang T, Nagy M: **Aggregate reactivation mediated by the Hsp100 chaperones**. *Arch Biochem Biophys* 2012, **520**(1):1-6.

140. Glover JR, Lindquist S: **Hsp104, Hsp70, and Hsp40: a novel chaperone system that rescues previously aggregated proteins**. *Cell* 1998, **94**(1):73-82.

141. Stolz A, Hilt W, Buchberger A, Wolf DH: **Cdc48: a power machine in protein degradation**. *Trends Biochem Sci* 2011, **36**(10):515-523.

142. Wolf DH, Stolz A: **The Cdc48 machine in endoplasmic reticulum associated protein degradation**. *Biochim Biophys Acta* 2012, **1823**(1):117-124.

143. Baba M, Takeshige K, Baba N, Ohsumi Y: **Ultrastructural analysis of the autophagic process in yeast: detection of autophagosomes and their characterization**. *J Cell Biol* 1994, **124**(6):903-913.

144. Sakai Y, Koller A, Rangell LK, Keller GA, Subramani S: **Peroxisome degradation by microautophagy in *Pichia pastoris*: identification of specific steps and morphological intermediates**. *J Cell Biol* 1998, **141**(3):625-636.

145. Ogata M, Hino S, Saito A, Morikawa K, Kondo S, Kanemoto S, Murakami T, Taniguchi M, Tanii I, Yoshinaga K *et al*: **Autophagy is activated for cell survival after endoplasmic reticulum stress**. *Mol Cell Biol* 2006, **26**(24):9220-9231.

146. van Zutphen T, Veenhuis M, van der Klei IJ: **Damaged peroxisomes are subject to rapid autophagic degradation in the yeast Hansenula polymorpha**. *Autophagy* 2011, **7**(8):863-872.

147. Kimura S, Maruyama J, Kikuma T, Arioka M, Kitamoto K: **Autophagy delivers misfolded secretory proteins accumulated in endoplasmic reticulum to vacuoles in the filamentous fungus *Aspergillus oryzae***. *Biochem Biophys Res Commun* 2011, **406**(3):464-470.

148. Candiano G, Bruschi M, Musante L, Santucci L, Ghiggeri GM, Carnemolla B, Orecchia P, Zardi L, Righetti PG: **Blue silver: A very sensitive colloidal Coomassie G-250 staining for proteome analysis**. *Electrophoresis* 2004, **25**(9):1327-1333.

149. Schmidt FR: **Recombinant expression systems in the pharmaceutical industry**. *Appl Microbiol Biotechnol* 2004, **65**(4):363-372.

150. Sreekrishna K, Brankamp RG, Kropp KE, Blankenship DT, Tsay JT, Smith PL, Wierschke JD, Subramaniam A, Birkenberger LA: **Strategies for optimal synthesis and secretion of heterologous proteins in the methylotrophic yeast *Pichia pastoris***. *Gene* 1997, **190**(1):55-62.

151. Kjeldsen T, Pettersson AF, Hach M: **Secretory expression and characterization of insulin in *Pichia pastoris***. *Biotechnol Appl Biochem* 1999, **29 (Pt 1)**:79-86.

152. Porro D, Sauer M, Branduardi P, Mattanovich D: **Recombinant protein production in yeasts**. *Mol Biotechnol* 2005, **31**(3):245-259.

153. Whyteside G, Nor RM, Alcocer MJC, Archer DB: **Activation of the unfolded protein response in *Pichia pastoris* requires splicing of a HAC1 mRNA intron and retention of the C-terminal tail of Hac1p**. *Febs Letters* 2011, **585**(7):1037-1041.

154. Papanikou E, Glick BS: **The yeast Golgi apparatus: insights and mysteries**. *FEBS Lett* 2009, **583**(23):3746-3751.

155. Vajo Z, Fawcett J, Duckworth WC: **Recombinant DNA technology in the treatment of diabetes: insulin analogs**. *Endocr Rev* 2001, **22**(5):706-717.

156. Gurramkonda C, Polez S, Skoko N, Adnan A, Gabel T, Chugh D, Swaminathan S, Khanna N, Tisminetzky S, Rinas U: **Application of simple fed-batch technique to high-level secretory production of insulin precursor using *Pichia pastoris* with subsequent purification and conversion to human insulin**. *Microb Cell Fact* 2010, **9**:31.

157. Kjeldsen T: **Yeast secretory expression of insulin precursors**. *Appl Microbiol Biotechnol* 2000, **54**(3):277-286.

158. Walsh G: **Therapeutic insulins and their large-scale manufacture**. *Appl Microbiol Biotechnol* 2005, **67**(2):151-159.

159. Dudek J, Benedix J, Cappel S, Greiner M, Jalal C, Muller L, Zimmermann R: **Functions and pathologies of BiP and its interaction partners**. *Cell Mol Life Sci* 2009, **66**(9):1556-1569.

160. Lewis MJ, Sweet DJ, Pelham HR: **The ERD2 gene determines the specificity of the luminal ER protein retention system**. *Cell* 1990, **61**(7):1359-1363.

161. Delic M, Rebnegger C, Wanka F, Puxbaum V, Haberhauer-Troyer C, Hann S, Kollensperger G, Mattanovich D, Gasser B: **Oxidative protein folding and unfolded protein response elicit differing redox regulation in endoplasmic reticulum and cytosol of yeast**. *Free Radic Biol Med* 2012, **52**(9):2000-2012.

162. Smith JD, Robinson AS: **Overexpression of an archaeal protein in yeast: Secretion bottleneck at the ER**. *Biotechnol Bioeng* 2002, **79**(7):713-723.

163. Parekh R, Forrester K, Wittrup D: **Multicopy overexpression of bovine pancreatic trypsin inhibitor saturates the protein folding and secretory capacity of *Saccharomyces cerevisiae***. *Protein Expr Purif* 1995, **6**(4):537-545.

164. Mulhern ML, Madson CJ, Danford A, Ikesugi K, Kador PF, Shinohara T: **The unfolded protein response in lens epithelial cells from galactosemic rat lenses**. *Invest Ophthalmol Vis Sci* 2006, **47**(9):3951-3959.

165. Baba M, Osumi M, Ohsumi Y: **Analysis of the membrane structures involved in autophagy in yeast by freeze-replica method**. *Cell Struct Funct* 1995, **20**(6):465-471.

166. Mijaljica D, Prescott M, Devenish RJ: **The intriguing life of autophagosomes**. *Int J Mol Sci* 2012, **13**(3):3618-3635.

167. Scherz-Shouval R, Elazar Z: **Regulation of autophagy by ROS: physiology and pathology**. *Trends Biochem Sci* 2011, **36**(1):30-38.

168. Sakai Y, Murdanoto AP, Konishi T, Iwamatsu A, Kato N: **Regulation of the formate dehydrogenase gene, *FDH1*, in the methylotrophic yeast *Candida boidinii* and growth characteristics of an *FDH1*-disrupted strain on methanol, methylamine, and choline**. *J Bacteriol* 1997, **179**(14):4480-4485.

169. Wampler DE, Lehman ED, Boger J, Mcaleer WJ, Scolnick EM: **Multiple chemical forms of Hepatitis-B surface antigen produced in yeast**. *Proc Natl Acad Sci USA* 1985, **82**(20):6830-6834.

7. Appendix I

7.1. All identified intracellular proteins

The complete list of all identified proteins classified into functional categories, a representative 2D gel image indicating the spots of all identified proteins and their log2 changes in response to methanol-induced high-level production of the HBsAg are given.

The complete list of all identified proteins classified into functional categories.

NCBI Accession-No [1]	Locus ID [1]	Gene name [2]	Protein name[2]	MM (kDa) [3]	p*I* [3]	Mascot Score	Spot No [4]
Functional category [1]							
1. Metabolism							
1.1 Carbohydrate metabolism							
Methanol metabolism							
XP_002494271	PAS_chr4_0821	*AOX1*	Alcohol oxidase	74.5	6.0	109	123*, 83*
XP_002492075	PAS_chr2-2_0131	*CTA1*	Catalase A	58.1	6.6	193	92*, 93*
XP_002493065	PAS_chr3_0832	*DAS1*	Transketolase (Dihydroxyacetone synthase), similar to Tkl2p	79.1	6.1	137	94*, 95*, 96*, 101*, 102*
XP_002493270	PAS_chr3_1028	*FLD1*	S-(hydroxymethyl) glutathione dehydrogenase	41.4	6.1	110	27*, 31*
XP_002493100	PAS_chr3_0867	*FGH1*	Non-essential intracellular esterase that can function as an S-formylglutathione hydrolase	33.4	6.3	222	5*
XP_002493171	PAS_chr3_0932	*FDH1*	NAD(+)-dependent formate dehydrogenase	40.4	6.6	191	2*, 3*, 4*, 29*, 30*, 85*, 103*
Glycolysis							
XP_002494063	PAS_chr4_0624	*EMI2*	Hexokinase	52.5	6.1	237	22*
XP_002491345	PAS_chr2-1_0437	*TDH1*	Glyceraldehyde-3-phosphate dehydrogenase, isozyme 3	35.7	6.2	154	114*, 117*

NCBI Accession-No [1]	Locus ID [1]	Gene name [2]	Protein name[2]	MM (kDa) [3]	p*I* [3]	Mascot Score	Spot No [4]
Functional category [1]							
XP_002489713	PAS_chr1-1_0072	*FBA1*	Fructose 1,6-bisphosphate aldolase	39.9	6.0	108	33*
XP_002490411	PAS_chr1-4_0292	*PGK1*	3-Phosphoglycerate kinase	44.1	7.8	263	52*
XP_002493191	PAS_chr3_0951	*TPI1*	Triose phosphate isomerase	27.1	5.7	160	50*
XP_002493059	PAS_chr3_0826	*GMP1*	Tetrameric phosphoglycerate mutase	28.0	6.0	131	51*
XP_002492293	PAS_chr3_0082	*ENO2*	Enolase I	46.5	5.4	181	39*, 120*
Ethanol metabolism							
CAY67035	PAS_c034_0018	*ADH*	Alcohol dehydrogenase	38.1	6.3	195	78*
XP_002491382	PAS_chr2-1_0472	*ADH3*	Mitochondrial alcohol dehydrogenase isozyme III	37.3	5.8	140	35*
Citrate cycle (TCA cycle)							
XP_002489444	PAS_chr1-3_0104	*ACO1*	Aconitase	85.0	5.7	237	15*, 16*
XP_002491004	PAS_chr2-1_0120	*IDH2*	Subunit of mitochondrial NAD(+)-dependent isocitrate dehydrogenase	40.3	8.1	96	115*
XP_002492874	PAS_chr3_0647	*FUM1*	Fumarase	52.8	6.4	82	24*
XP_002491128	PAS_chr2-1_0238	*MDH1*	Mitochondrial malate dehydrogenase	36.5	5.3	230	34*, 46*
Pentose phosphate pathway							
XP_002492495	PAS_chr3_0277	*6PGD [GND]*	6-Phosphogluconate dehydrogenase (decarboxylating)	54.2	5.9	209	21*
XP_002493617	PAS_chr4_0212	*RKI1*	Ribose-5-phosphate ketol-isomerase	23.6	6.0	226	69*
Sugar metabolism and others							
XP_002490557	PAS_chr1-4_0426	*BGL2*	Endo-beta-1,3-glucanase	34.2	4.1	108	136*

NCBI Accession-No [1]	Locus ID [1]	Gene name [2]	Protein name[2]	MM (kDa) [3]	p*I* [3]	Mascot Score	Spot No [4]
Functional category [1]							
Pyruvate metabolism							
XP_002494290	PAS_chr4_0842	*GLO1*	Monomeric glyoxalase I	36.9	5.6	76	40*
XP_002491701	PAS_chr2-1_0767	*acsB [ACS1]*	Acetyl-coA synthetase isoform	74.1	5.7	88	18*, 19*
1.2 Energy Metabolism							
Oxidative phosphorylation							
XP_002489364	PAS_chr1-3_0028	*IPP1*	Cytoplasmic inorganic pyrophosphatase (PPase)	32.3	5.3	214	65*, 134*
XP_002493409	PAS_c131_0021	*[VMA2]*	Vacuolar ATP synthase subunit B	55.4	5.3	169	14*
XP_002494179	PAS_chr4_0737	*MCR1*	Mitochondrial NADH-cytochrome b5 reductase	33.6	8.8	183	54*, 105*
1.3 Nucleotide metabolism							
XP_002492473	PAS_chr3_0257	*ADK1*	Adenylate kinase	28.2	7.0	122	106*
XP_002492154	PAS_chr2-2_0059	*YNK1*	Nucleoside diphosphate kinase	17.0	6.2	111	89*
1.4 Amino acid metabolism							
XP_002489848	PAS_chr1-1_0200	*AAT1*	Cytosolic aspartate aminotransferase	47.9	6.7	200	28*, 25*
XP_002492036	PAS_chr2-2_0168	*[LYS12]*	Homo-isocitrate dehydrogenase	40.1	6.0	121	41*
XP_002490090	PAS_chr1-1_0432	*ILV5*	Acetohydroxyacid reductoisomerase	44.4	7.7	94	43*
XP_002491046	PAS_chr2-1_0160	*metE [MET6]*	Cobalamin-independent methionine synthase	85.9	5.9	228	17*, 118*
XP_002492638	PAS_chr3_0410	*CAR2*	L-Ornithine transaminase	47.5	5.9	100	26*
XP_002493966	PAS_chr4_0974	*[AAT2]*	Aspartate aminotransferase	42.5	7.2	174	133*
XP_002492166	PAS_chr2-2_0048	*[LPD1]*	Dihydrolipoamide dehydrogenase	52.6	6.3	110	119*

NCBI Accession-No [1]	Locus ID [1]	Gene name [2]	Protein name[2]	MM (kDa) [3]	p*I* [3]	Mascot Score	Spot No [4]
Functional category [1]							
1.5 Metabolism of cofactors and vitamins							
XP_002493470	PAS_chr4_0065	*THI5*	Protein involved in synthesis of the thiamine precursor hydroxymethylpyrimidine (HMP)	38.7	6.3	140	116*
XP_002493989	PAS_chr4_0550	-	Pyridoxine 4-dehydrogenase	36.3	5.6	192	42*
XP_002492582	PAS_chr3_0361	*[PNC1]*	Nicotinamidase	24.7	5.3	126	70*
2. Genetic information processing							
2.1 Transcription and translation							
XP_002489515	PAS_chr1-3_0172	*EGD1*	Subunit beta1 of the nascent polypeptide-associated complex (NAC)	17.9	4.8	76	72*
XP_002489404	PAS_chr1-3_0068	*RPP0*	Conserved ribosomal protein P0 similar to rat P0, human P0, and E. coli L10e	33.7	4.6	110	63*
XP_002493616	PAS_chr4_0211	*[RPS7B]*	Protein component of the small (40S) ribosomal subunit. nearly identical to Rps7Bp	21.3	9.2	90	112*
XP_002491009	PAS_chr2-1_0812	*EFT1*	Elongation factor 2	93.9	6.3	83	100*
XP_002492789	PAS_chr3_0562	*TUF1*	Mitochondrial translation elongation factor Tu	47.0	5.6	103	44*
XP_002493313	PAS_chr3_1071	*CAM1*	Translation elongation factor EF-1 gamma	24.3	6.4	111	107*, 132*
2.2 Sorting and degradation							
XP_002492588	PAS_chr3_0365	*SSC1*	Mitochondrial matrix ATPase	69.7	5.4	98	99*
XP_002490239	PAS_chr1-4_0130	-	Heat shock protein Hsp90	80.9	4.8	100	122*
XP_002490142	PAS_chr1-4_0027	*COF1*	Cofilin	18.2	6.1	97	71*
XP_002493333	PAS_chr3_1087	*APR1 [PEP4]*	Vacuolar aspartyl protease (proteinase A)	44.5	4.6	134	86*
XP_002490155	PAS_chr1-4_0043	*SBA1*	Co-chaperone that binds to and regulates Hsp90 family chaperones	22.5	4.3	77	113*
XP_002489443	PAS_chr1-3_0102	*clpB [HSP104]*	Heat shock protein that cooperates with Ydj1p (Hsp40) and Ssa1p (Hsp70)	100.6	5.3	160	84*
XP_002494360.1	PAS_FragD_0026	*[CDC48]*	ATPase in ER, nuclear membrane and cytosol with homology to mammalian p97	91.4	4.8	216	1*

NCBI Accession-No [1]	Locus ID [1]	Gene name [2]	Protein name[2]	MM (kDa) [3]	p*I* [3]	Mascot Score	Spot No [4]
Functional category [1]							
XP_002492868	PAS_chr3_0640	*TFS1*	Carboxypeptidase Y inhibitor	29.8	7.8	155	6*, 7*
2.3 Folding catalysts							
CAC33587	PAS_chr4_0844	*PDI*	Protein disulfide isomerase	58.1	4.6	160	11*
XP_002493562	PAS_chr4_0158	*CPNA [HSP60]*	Tetradecameric mitochondrial chaperonin	60.5	5.1	180	12*
XP_002489608	PAS_chr1-3_0264	*[CPR1]*	Cytoplasmic peptidyl-prolyl cis-trans isomerase (cyclophilin)	18.1	6.1	103	56*
XP_002490274	PAS_chr1-4_0163	*[HSP10]*	10 kDa chaperonin	11.1	9.0	82	82*
3. Cellular processes							
3.1 Transport and catabolism							
XP_002490181	PAS_chr1-4_0071	*SOD2*	Mitochondrial superoxide dismutase	25.2	7.9	111	76*
3.2 Cell growth and death							
XP_002493242	PAS_chr3_1001	*TUP1*	General repressor of transcription, forms complex with Cyc8p	66.3	6.0	135	20*
XP_002490416	PAS_chr1-4_0297	*[STM1]*	Suppressor protein STM1	29.7	9.7	102	87*
4. Others							
4.1 Stress response							
XP_002493863	PAS_chr4_0433	-	NADPH-dependent alpha-keto amide reductase	33.7	5.6	113	73*
XP_002490683	PAS_chr1-4_0547	*PMP20*	Peroxiredoxin	18.4	9.5	178	9*
XP_002493699	PAS_chr4_0284	*TRX2*	Cytoplasmic thioredoxin isoenzyme of the thioredoxin system	11.4	4.9	110	80*
XP_002492079	PAS_chr2-2_0127	*CCP1*	Mitochondrial cytochrome-c peroxidase	42.0	6.6	197	66*
XP_002491803	PAS_chr2-2_0382	*GPX1 [HYR1]*	Thiol peroxidase (Glutathione peroxidase)	18.4	6.2	164	8*
XP_002493423	PAS_chr4_0018	*CYC1*	Cytochrome c, isoform 1	12.2	9.6	94	81*

NCBI Accession-No [1]	Locus ID [1]	Gene name [2]	Protein name[2]	MM (kDa) [3]	p*I* [3]	Mascot Score	Spot No [4]
Functional category [1]							
BAH80186	PAS_chr2-2_0480	*TRR1*	Thioredoxin reductase 1	35.3	5.5	141	67*
5. Unclassified							
XP_002491489	PAS_chr2-1_0573	-	Putative xylose and arabinose reductase	32.2	6.1	167	75*
XP_002491564	PAS_chr2-1_0640	-	Putative protein of unknown function	21.7	6.3	119	129*
XP_002491418	PAS_chr2-1_0853	-	Hypothetical protein	57.0	6.0	119	121*
XP_002489760	PAS_chr1-1_0118	-	Hypothetical protein	46.3	7.0	77	127*
XP_002490519	PAS_chr1-4_0675	-	Hypothetical protein	53.8	6.7	96	23*
XP_002491208	PAS_chr2-1_0313	-	Bifunctional enzyme with alcohol dehydrogenase and glutathione-dependent formaldehyde dehydrogenase	39.1	5.8	177	37*
XP_002491071	PAS_chr2-1_0183	-	Acyl-protein thioesterase responsible for depalmitoylation of Gpa1p	24.3	6.3	102	130*
XP_002491989	PAS_chr2-2_0208	-	Hypothetical protein	18.6	6.5	85	10*
XP_002491901	PAS_chr2-2_0289	-	Hypothetical protein	28.3	4.8	125	64*
XP_002492584	PAS_chr3_0362	-	Mitochondrial peculiar membrane protein 1	32.7	5.7	92	68*
XP_002493742	PAS_chr4_0320	*MYH4*	Myosin-4	92.6	4.9	152	59*

1 Accession numbers and locus IDs are according to the NCBI Reference Sequence database (http://www.ncbi.nlm.nih.gov/RefSeq/). Functional classifications are mostly according to KEGG PATHWAY database (http://www.genome.jp/kegg/metabolism.html).

2 Gene/protein names are according to the sequenced genome of *P. pastoris* GS115 (http://www.uniprot.org/). If no name was found for *P. pastoris* GS115, a Blast search of the respective *P. pastoris* GS115 gene/protein against different *P. pastoris* strains was carried out in the following order: search against ATCC 76273 / CBS 7435 / CECT 11047 / NRRL Y-11430 / Wegner 21-1 and *P. pastoris* (yeast). Gene/protein names from other *P. pastoris* strains were only adopted in case of 100% sequence identity (http://www.uniprot.org/). Gene names in brackets are from *S. cerevisiae* if the names differ for both yeasts (http://www.uniprot.org/).

3 Theoretical molecular mass (MM) and isoelectric point (p*I*) not considering potential posttranslational modifications.

4 "Spot-No" indicates the serial number of all identified protein spots of the intracellular proteome of *P. pastoris* GS115. Proteins appearing in multiple spots indicate the existence of isoforms which probably derive from posttranslational modification events such as phosphorylation, glycosylation or limited proteolysis. A representative 2D gel of the intracellular proteome from a cell sample taken after 114 hours of growth on methanol with the respective spot numbers is shown below. Spot numbers in this table and the following gel are marked by an asterix (*) for simplified searchability

A representative 2D gel of the intracellular proteome of *P. pastoris* GS115 producing HBsAg.

The sample was taken after 114 h of growth on methanol. Spot numbers correspond to numbers in the table above and are marked by an asterix (*) for simplified searchability.

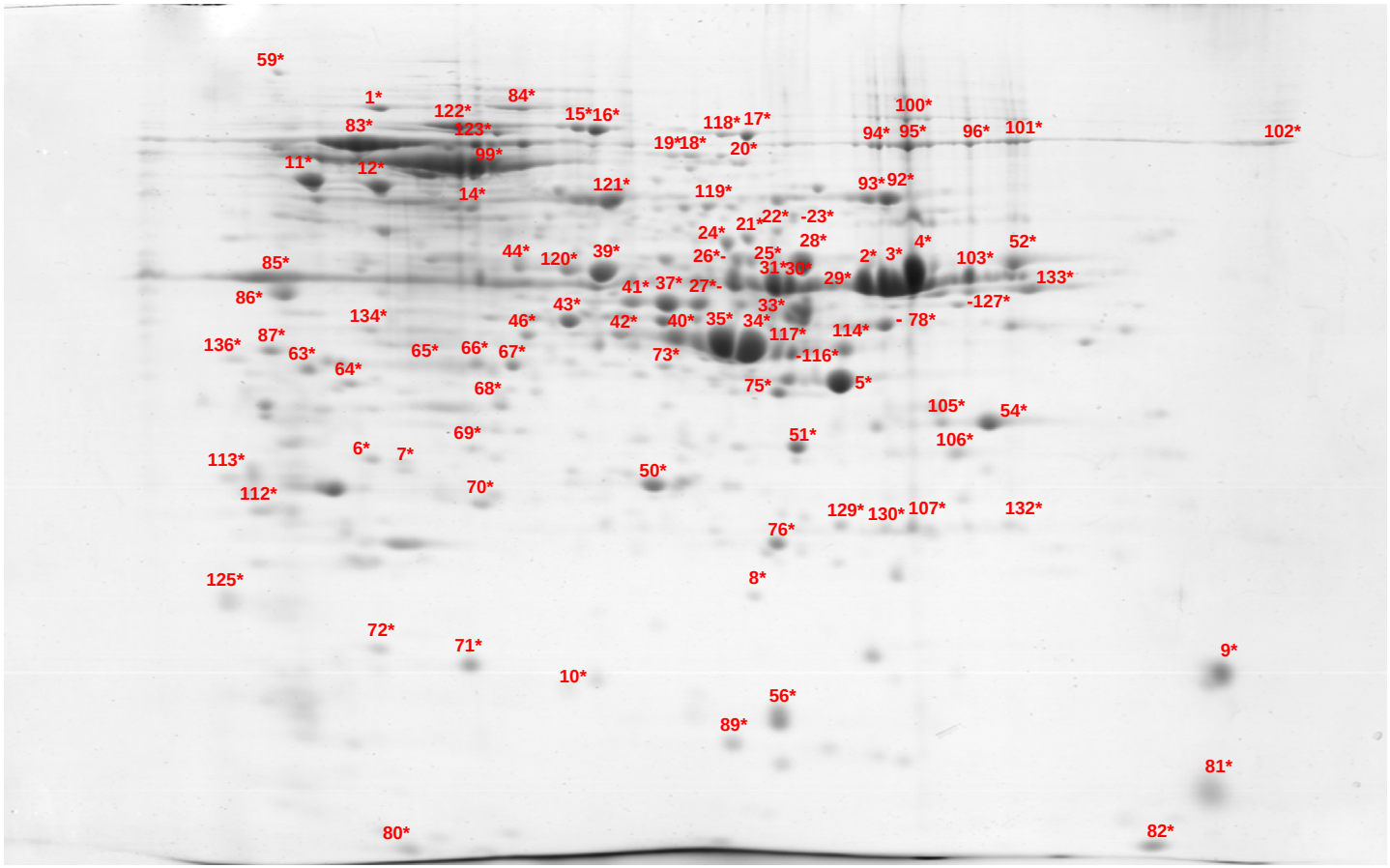

Change of the intracellular proteome in response to high-level methanol-induced production of HBsAg.

Samples before methanol addition at the end of the glycerol batch phase and 4, 16, 72 and 114 hours after the onset of methanol feeding were analyzed and the protein changes in response to methanol-induced HBsAg production are shown (numbers. log2 changes; n.a. not analyzable, color code: light orange to red, increase, light green to dark green: decrease, yellow: no significant change).

Functional category	Gene name [1]	Gene ID	0h [2]	4h	16h	72h	114h
Carbohydrate metabolism							
Methanol metabolism	*AOX1*	PAS_chr4_0821	0.0	10.8	11.6	10.8	12.0
	CTA1	PAS_chr2-2_0131	0.0	0.6	1.0	1.0	1.5
	DAS1	PAS_chr3_0832	0.0	0.5	3.8	3.2	3.1
	FLD1	PAS_chr3_1028	0.0	9.1	10.0	9.0	10.7
	FGH1	PAS_chr3_0867	0.0	2.0	3.8	4.5	4.2
	FDH1	PAS_chr3_0932	0.0	10.6	12.7	13.4	13.5
Glycolysis	*EMI2*	PAS_chr4_0624	0.0	-0.7	-1.8	-3.8	-1.8
	TDH1	PAS_chr2-1_0437	0.0	-0.2	0.4	-0.7	0.0
	FBA1	PAS_chr1-1_0072	0.0	0.1	-0.4	-0.5	-0.8
	PGK1	PAS_chr1-4_0292	0.0	0.1	-0.9	-0.7	-0.7
	TPI1	PAS_chr3_0951	0.0	-0.1	-1.3	-2.0	-1.7
	GMP1	PAS_chr3_0826	0.0	0.0	-0.2	0.1	-0.8
	ENO2	PAS_chr3_0082	0.0	-0.4	-0.5	-0.2	-0.7
Ethanol metabolism	*ADH*	PAS_c034_0018	0.0	0.8	0.2	0.8	0.7
	ADH3	PAS_chr2-1_0472	0.0	0.5	0.7	1.0	0.6
Citrate cycle (TCA)	*ACO1*	PAS_chr1-3_0104	0.0	-0.3	-0.6	0.6	0.3
	IDH2	PAS_chr2-1_0120	0.0	0.3	-0.8	-0.4	-0.6
	FUM1	PAS_chr3_0647	0.0	-0.1	-0.7	-0.1	-0.7
	MDH1	PAS_chr2-1_0238	0.0	0.8	1.1	1.7	1.0
Pentose phosphate pathway	*6PGD [GND]*	PAS_chr3_0277	0.0	0.0	n.a	n.a	-1.0
	RKI1	PAS_chr4_0212	0.0	-0.2	1.0	1.2	0.2
Sugar metabolism	*BGL2*	PAS_chr1-4_0426	0.0	-1.2	-1.4	-0.8	-1.3

Functional category	Gene name [1]	Gene ID	0h [2]	4h	16h	72h	114h
Pyruvate metabolism	*GLO1*	PAS_chr4_0842	0.0	0.5	0.3	1.3	1.2
	acsB [ACS1]	PAS_chr2-1_0767	0.0	0.0	-1.8	-1.6	-0.9
Energy metabolism							
Oxidative phosphorylation	*IPP1*	PAS_chr1-3_0028	0.0	1.1	2.9	0.4	0.0
	[VMA2]	PAS_c131_0021	0.0	0.0	0.0	0.4	-0.4
	MCR1	PAS_chr4_0737	0.0	0.1	-0.4	0.9	0.4
Nucleotide metabolism							
	ADK1	PAS_chr3_0257	0.0	0.0	-1.1	0.0	-0.2
	YNK1	PAS_chr2-2_0059	0.0	-0.1	-1.2	-0.3	-1.2
Amino acid metabolism							
	AAT1	PAS_chr1-1_0200	0.0	0.3	0.9	1.3	1.1
	[LYS12]	PAS_chr2-2_0168	0.0	-0.3	-0.6	1.0	-0.4
	ILV5	PAS_chr1-1_0432	0.0	0.0	-0.4	0.1	-0.5
	metE [MET6]	PAS_chr2-1_0160	0.0	0.2	-4.2	-5.2	-1.8
	CAR2	PAS_chr3_0410	0.0	0.0	0.2	-0.1	n.a
	[AAT2]	PAS_chr4_0974	0.0	1.0	0.6	0.9	1.2
	[LPD1]	PAS_chr2-2_0048	0.0	0.5	-1.1	-0.1	-0.5
Metabolism of cofactors and vitamins							
	THI5	PAS_chr4_0065	0.0	1.1	1.0	-1.0	-0.3
	-	PAS_chr4_0550	0.0	-0.2	-0.2	-0.1	-0.7
	[PNC1]	PAS_chr3_0361	0.0	-1.3	-1.2	-0.2	-0.7
Genetic information processing							
Transcription and translation	*EGD1*	PAS_chr1-3_0172	0.0	0.5	0.4	0.5	-0.5
	RPP0	PAS_chr1-3_0068	0.0	7.9	6.9	7.6	7.0
	[RPS7B]	PAS_chr4_0211	0.0	-0.3	-0.3	-0.5	n.a
	EFT1	PAS_chr2-1_0812	0.0	n.a	-3.4	n.a	-0.8
	TUF1	PAS_chr3_0562	0.0	0.0	-0.4	-0.1	-1.9
	CAM1	PAS_chr3_1071	0.0	-1.4	-1.3	0.7	0.8

Functional category	Gene name [1]	Gene ID	0h [2]	4h	16h	72h	114h
Sorting and degradation	*SSC1*	PAS_chr3_0365	0.0	0.3	1.0	1.0	-0.3
	-	PAS_chr1-4_0130	0.0	0.7	0.4	1.0	1.2
	COF1	PAS_chr1-4_0027	0.0	0.0	-0.3	0.3	-0.5
	APR1 [PEP4]	PAS_chr3_1087	0.0	-0.1	2.5	3.4	3.2
	SBA1	PAS_chr1-4_0043	0.0	-0.8	-0.3	-0.1	-1.0
	clpB [HSP104]	PAS_chr1-3_0102	0.0	8.2	5.7	n.a	7.1
	[CDC48]	PAS_FragD_0026	0.0	1.4	1.3	1.0	0.8
	TFS1	PAS_chr3_0640	0.0	0.1	-0.6	-0.1	-1.3
Folding catalysts	*PDI*	PAS_chr4_0844	0.0	0.7	1.3	1.8	1.7
	CPNA [HSP60]	PAS_chr4_0158	0.0	0.1	0.4	0.8	0.1
	[CPR1]	PAS_chr1-3_0264	0.0	1.3	1.2	1.3	0.3
	[HSP10]	PAS_chr1-4_0163	0.0	0.1	0.5	0.7	0.8
Cellular processes							
Transport and catabolism	*SOD2*	PAS_chr1-4_0071	0.0	0.5	-0.1	0.2	0.2
Cell growth and death	*TUP1*	PAS_chr3_1001	0.0	0.3	-1.2	-1.5	-1.9
	[STM1]	PAS_chr1-4_0297	0.0	0.3	-0.3	0.4	-0.6
Others							
Stress response	-	PAS_chr4_0433	0.0	-0.5	-1.5	-2.0	-1.9
	PMP20	PAS_chr1-4_0547	0.0	8.9	10.1	10.0	9.7
	TRX2	PAS_chr4_0284	0.0	0.3	0.0	0.3	-0.9
	CCP1	PAS_chr2-2_0127	0.0	0.7	0.1	0.4	-1.1
	GPX1 [HYR1]	PAS_chr2-2_0382	0.0	0.6	0.3	0.6	-0.5
	CYC1	PAS_chr4_0018	0.0	0.3	-0.1	0.6	0.8
	TRR1	PAS_chr2-2_0480	0.0	0.2	-0.3	-0.4	-1.3

Functional category	Gene name [1]	Gene ID	0h [2]	4h	16h	72h	114h
Unclassified	-	PAS_chr2-1_0573	0.0	0.0	0.4	1.1	0.7
	-	PAS_chr2-1_0640	0.0	-0.1	-0.7	-0.5	-1.8
	-	PAS_chr2-1_0853	0.0	1.0	1.0	-0.2	2.6
	-	PAS_chr1-1_0118	0.0	-1.6	-1.0	-0.2	-1.3
	-	PAS_chr1-4_0675	0.0	-0.4	-1.7	-2.5	-1.1
	-	PAS_chr2-1_0313	0.0	-0.1	-0.5	-0.4	0.3
	-	PAS_chr2-1_0183	0.0	0.4	1.8	1.9	2.0
	-	PAS_chr2-2_0208	0.0	1.8	2.5	1.0	1.1
	-	PAS_chr2-2_0289	0.0	-0.2	-1.6	0.2	-1.2
	-	PAS_chr3_0362	0.0	-1.1	-0.8	0.6	-0.1
	MYH4	PAS_chr4_0320	0.0	-0.3	-2.0	-0.1	-1.5

1. Gene names in brackets are from *S. cerevisiae* if the names differ for both yeasts (http://www.uniprot.org/).
2. When no protein spot was detectable at the end of the glycerol batch phase (methanol metabolism), a virtual number of 0.001 was taken for the spot intensity to allow the calculation of log2 values (spot intensities were normalized using the log2 ratio of induced samples *versus* uninduced sample).

8. Appendix II

8.1. Identification of AOX1 in *P. pastoris* GS115 with a "Mut^s phenotype"

8.1.1. Results and discussion

The HBsAg producing strain was originally identified as a Mut^s (**m**ethanol **u**tilization **s**low) strain devoid of the *aox1* gene [1]. Thus, the identification of AOX1 in the intracellular proteome of *P. pastoris* GS115 after methanol-induced production of HBsAg by MALDI-TOF MS was unexpected (Figure 8.1). To confirm the presence of AOX1 and exclude a misidentification of AOX2, peptides which sequence differences in AOX1 and AOX2 were selected for sequencing by MS/MS. These results confirmed the correct identification of AOX1 (Figure 8.1). Finally, the presence of the entire *aox1* gene in the genome was confirmed by PCR analysis (Figure 8.2). The first attempt to verify the presence of the entire *aox1* gene by PCR with external primers using the Taq DNA polymerase failed; only the multicopy *HBsAg* gene was amplified under the applied conditions (Figure 8.2 A, lane 1). However, the presence of *aox1* or at least parts of the *aox1* gene was confirmed by using internal primers (Figure 8.2 A, lane 2). Finally, the presence of the entire *aox1* gene in the genome was confirmed by PCR analysis using a high performance DNA polymerase and a modified PCR protocol (see Materials and Methods for details).

Our results clearly show that a Mut^s phenotype, namely slow growth on methanol, does not necessarily prove the absence of a functional *aox1* gene. For example, slow growth on methanol was also observed with of an *aox1*$^+$ strain carrying multiple copies of a gene encoding a porcine insulin precursor [2]. Thus, high level expression of foreign genes can result in a metabolic burden and cellular stress response which may lead to impaired growth on methanol despite the presence of functional *aox1*.

Moreover, the absence of a visible *aox1* PCR product using external *aox1* primers does not necessarily proof the absence of *aox1*. It is advised to use internal *aox1* primers to allow selective *aox1* amplification this way preventing interference

through selective amplification of multiple copies of shorter foreign DNA fragments. Alternatively, PCR protocols can be optimized to allow simultaneous amplification of *aox1* and the foreign DNA fragment.

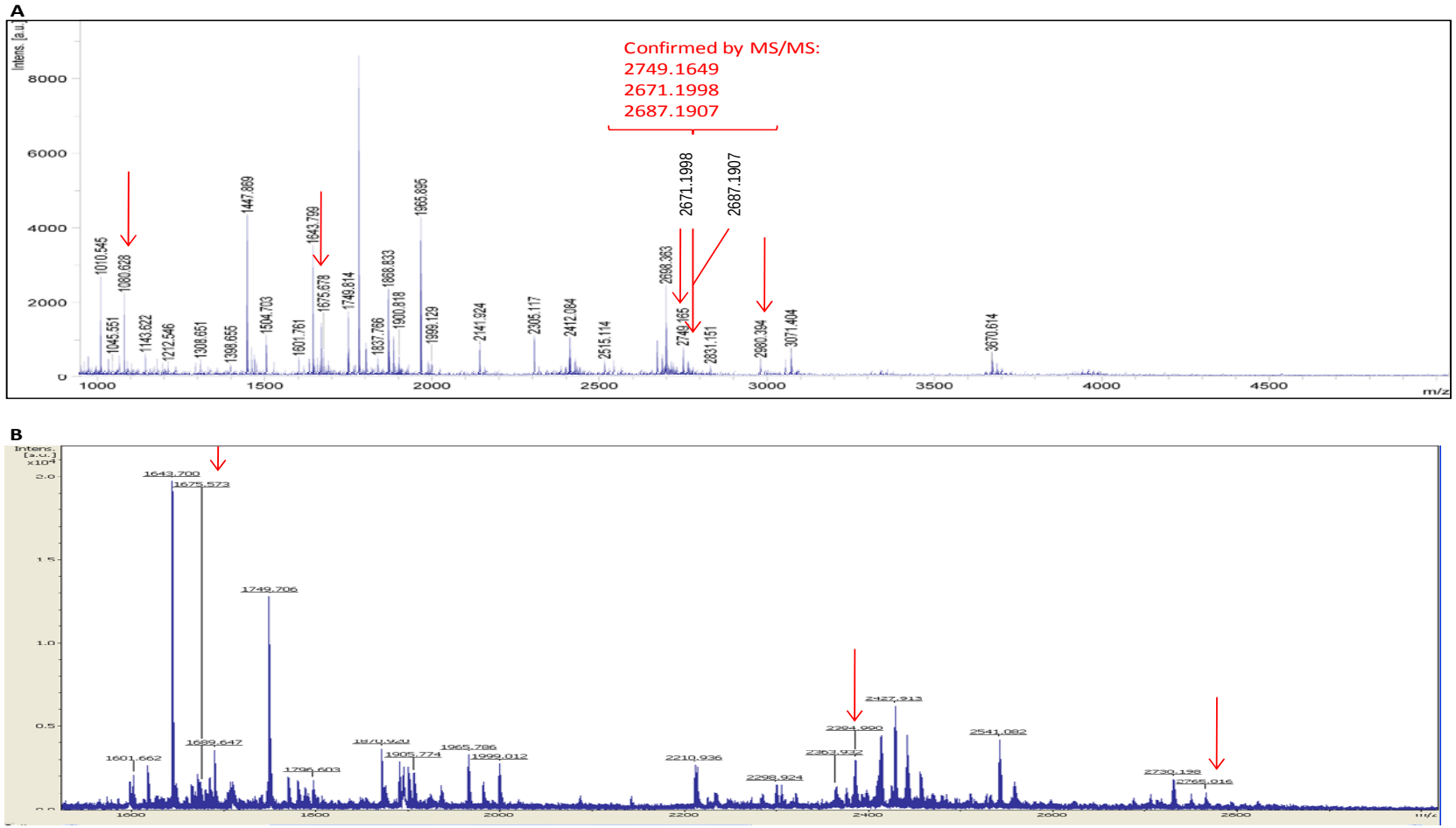

Figure 8.1. MALDI-TOF MS spectra obtained from an AOX1 protein spot. The red arrows indicate peptide peaks which are only present in AOX1 and not in AOX2. Three of these peptides (indicated in spectra A) were additionaly submitted to MS/MS for sequence analysis.

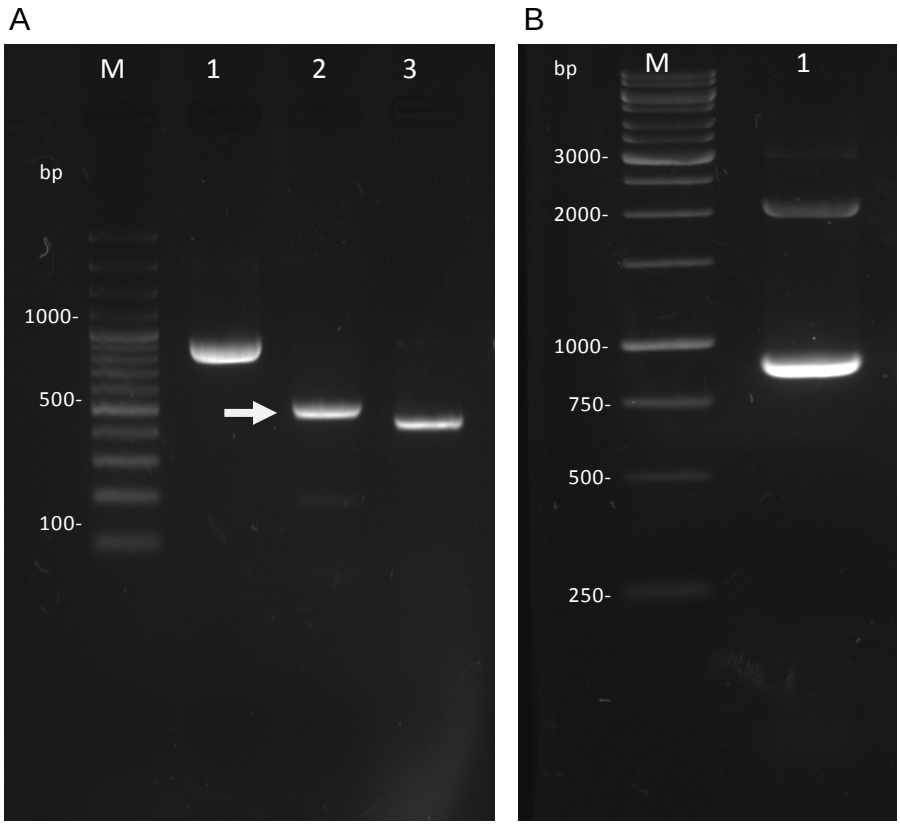

Figure 8.2. Agarose gel electrophoresis of PCR amplified *aox1* and *HBsAg* using *aox1* external and internal primers and *HBsAg* internal primer. (A) Represents the results for the first PCR experiment with Taq DNA polymerase and (B) the results of the second PCR experiment using the high performance polymerase, longer elongation time and higher annealing temperature. **Gel A:** M, 100bp DNA ladder (Fermentas); lane 1, *aox1* external primer (only *HBsAg* visible~900 bp), lane 2, *aox1* internal primer (*aox1* internal sequence 507 bp) and lane 3, *HBsAg* internal primer (*HBsAg* internal sequence 447pb). The band indicated by the arrow was subjected to sequencing and verified as *aox1*. **Gel B:** M, 1Kb DNA ladder (Fermentas); lane 1, with *aox1* external primer now 2 bands visible corresponding to *aox1* 2105 bp and *HBsAg* ~900bp.

```
Query 1   MAIPEEFDILVLGGGSSGSCIAGRLANLDHSLKVGLIEAGENNLNNPWVYLPGIYPRNMK 60
          MAIPEEFDILVLGGGSSGSCIAGRLANLDHSLKVGLIEAGENNLNNPWVYLPGIYPRNMK
Sbjct 1   MAIPEEFDILVLGGGSSGSCIAGRLANLDHSLKVGLIEAGENNLNNPWVYLPGIYPRNMK 60

Query  61 LDSKTASFYTSNPSPHLNGRRAIVPCANVLGGGSSINFMMYTRGSASDYDDFQAEGWKTK 120
          LDSKTASFYTSNPSPHLNGRRAIVPCAN+LGGGSSINFMMYTRGSASDYDDF+AEGWKTK
Sbjct  61 LDSKTASFYTSNPSPHLNGRRAIVPCANILGGGSSINFMMYTRGSASDYDDFEAEGWKTK 120

Query 121 DLLPLMKKTETYQRACNNPDIHGFEGPIKVSFGNYTYPVCQDFLRASESQGIPYVDDLED 180
          DLLPLMKKTETYQRACNNP+IHGFEGPIKVSFGNYTYPVCQDFLRA+ESQGIPYVDDLED
Sbjct 121 DLLPLMKKTETYQRACNNPEIHGFEGPIKVSFGNYTYPVCQDFLRATESQGIPYVDDLED 180

Query 181 LVTAHGAEHWLKWINRDTGRRSDSAHAFVHSTMRNHDNLYLICNTKVDKIIVEDGRAAAV 240
          LVTAHGAEHWLKWINRDTGRRSDSAHAFVHSTMRNHDNLYLICNTKVDKIIVEDGRAAAV
Sbjct 181 LVTAHGAEHWLKWINRDTGRRSDSAHAFVHSTMRNHDNLYLICNTKVDKIIVEDGRAAAV 240

Query 241 RTVPSKPLNPKKPSHKIYRARKQIVLSCGTISSPLVLQRSGFGDPIKLRAAGVKPLVNLP 300
          RTVPSKPLN KKP+HK+YRAR QIVLSCGTISSPLVLQRSGFGDPIKLRAAGVKPLVNLP
Sbjct 241 RTVPSKPLNAKKPTHKVYRARTQIVLSCGTISSPLVLQRSGFGDPIKLRAAGVKPLVNLP 300

Query 301 GVGRNFQDHYCFFSPYRIKPQYESFDDFVRGDAEIQKRVFDQWYANGTGPLATNGIEAGV 360
          GVGRNFQDHYCFFSPYRIKPQYESFDDFVRGDA IQK+VFDQWYANGTGPLATNGIEAGV
Sbjct 301 GVGRNFQDHYCFFSPYRIKPQYESFDDFVRGDANIQKKVFDQWYANGTGPLATNGIEAGV 360

Query 361 KIRPTPEELSQMDESFQEGYREYFEDKPDKPVMHYSIIAGFFGDHTKIPPGKYMTMFHFL 420
          KIRPTPEELSQMDESFQEGYREYFEDKPDKPVMHYSIIAGFFGDHTKIPPGKYMTMFHFL
Sbjct 361 KIRPTPEELSQMDESFQEGYREYFEDKPDKPVMHYSIIAGFFGDHTKIPPGKYMTMFHFL 420

Query 421 EYPFSRGSIHITSPDPYAAPDFDPGFMNDERDMAPMVWAYKKSRETARRMDHFAGEVTSH 480
          EYPFSRGSIHITSPDPYA PDFDPGFMNDERDMAPMVW+YKKSRETAR+MDHFAGEVTSH
Sbjct 421 EYPFSRGSIHITSPDPYATPDFDPGFMNDERDMAPMVWSYKKSRETARKMDHFAGEVTSH 480

Query 481 HPLFPYSSEARALEMDLETSNAYGGPLNLSAGLAHGSWTQPLKKPTAKNEGHVTSNQVEL 540
          HPLFPYSSEARA EMDLETSNAYGGPLNL+AGLAHGSWTQPLKKP  +NEGHVTSNQVEL
Sbjct 481 HPLFPYSSEARAYEMDLETSNAYGGPLNLTAGLAHGSWTQPLKKPAGRNEGHVTSNQVEL 540

Query 541 HPDIEYDEEDDKAIENYIREHTETTWHCLGTCSIGPREGSKIVKWGGVLDHRSNVYGVKG 600
          HPDIEYDEEDDKAIENYIREHTETTWHCLGTCSIGPREGSKIVKWGGVLDHRSNVYGVKG
Sbjct 541 HPDIEYDEEDDKAIENYIREHTETTWHCLGTCSIGPREGSKIVKWGGVLDHRSNVYGVKG 600

Query 601 LKVGDLSVCPDNVGCNTYTTALLIGEKTATLVGEDLGYSGEALDMTVPQFKLGTYEKTGL 660
          LKVGDLSVCPDNVGCNTYTTALLIGEKTATLVGEDLGY+GEALDMTVPQFKLGTYEKTGL
Sbjct 601 LKVGDLSVCPDNVGCNTYTTALLIGEKTATLVGEDLGYTGEALDMTVPQFKLGTYEKTGL 660

Query 661  ARF  663
          ARF
Sbjct 661  ARF  663
```

Identities = 644/663 (98%), positives = 656/663 (99%), gaps = 0/663 (0%) Query 1= AOX1 Sbjct 1= AOX2

Figure 8.3. Sequence differences between AOX1 and AOX2. Amino acid sequences of AOX1 and AOX2 are from the Uniprot database (accession number Q9URI8 and Q9URI7, respectively). Protein homologies were determined using NCBI BLAST program via NCBI web-server. Amino acids with green background represent the differences between AOX1 and AOX2.

8.1.2. Material and methods

8.1.2.1. MALDI-TOF MS and MS/MS analysis

MALDI-TOF MS and MS/MS analysis and sample preparation were carried out as described in the main manuscript. AOX1 was identified from several gels with samples from different cultivations (shake flask and bioreactor) using the same transformant [1, 3, 4]. Three peptides, which reveal sequence differences in AOX1 and AOX2, were sequenced by MS/MS (Figure 8.1). The theoretical mass of AOX1 and AOX2 and corresponding peptides were predicted using [http://web.expasy.org/peptide_mass/]. The amino acid sequence of AOX1 and AOX2 are given in Figure 8.3.

8.1.2.2. PCR analysis and DNA sequencing

Cells were lysed in TRIzol reagent (Invitrogen, Carlsbad, CA) and the DNA isolated for PCR analysis according to the manufacturer´s instruction (www.invitrogen.com). The following primers were employed for PCR: AOX1 external primer, AOX1 internal primer and HBsAg internal primer (sequence given below). Two PCR protocols were used: the first PCR was carried out using the Taq DNA polymerase (Takara™, Japan) and the following conditions: initial denaturation at 95°C for 30 sec; annealing at 55°C for 30 sec and extension at 72°C for 30 sec with 35 cycles of amplification. The second PCR was carried out using a high performance polymerase (Ex Taq DNA polymerase, Takara™, Japan) and the following conditions: initial denaturation at 95°C for 30 sec; annealing at 57°C for 30 sec and extension at 72°C for 1 min with 35 circles of amplification. The second protocol allowed the simultaneous amplification of the shorter *HBsAg* and the longer *aox1* sequence. The PCR products were separated by agarose electrophoresis, the DNA extracted and subjected to sequence analysis. The identity of *aox1* was confirmed by sequencing (Eurofins MWG GmbH) (data not shown).

DNA sequence of *aox1* from *P. pastoris* strain GS115 with 5' promoter and 3' terminator

AGATCTAACATCCAAAGACGAAAGGTTGAATGAAACCTTTTTGCCATCCGACATCCACAGGTCCATTCTCACA
CATAAGTGCCAAACGCAACAGGAGGGGATACACTAGCAGCAGACCGTTGCAAACGCAGGACCTCCACTCCTC
TTCTCCTCAACACCCACTTTTGCCATCGAAAAACCAGCCCAGTTATTGGGCTTGATTGGAGCTCGCTCATTCCA
ATTCCTTCTATTAGGCTACTAACACCATGACTTTATTAGCCTGTCTATCCTGGCCCCCCTGGCGAGGTTCATGTT
TGTTTATTTCCGAATGCAACAAGCTCCGCATTACACCCGAACATCACTCCAGATGAGGGCTTTCTGAGTGTGGG
GTCAAATAGTTTCATGTTCCCCAAATGGCCCAAAACTGACAGTTTAAACGCTGTCTTGGAACCTAATATGACAA
AAGCGTGATCTCATCCAAGATGAACTAAGTTTGGTTCGTTGAAATGCTAACGGCCAGTTGGTCAAAAAGAAAC
TTCCAAAAGTCGGCATACCGTTTGTCTTGTTTGGTATTGATTGACGAATGCTCAAAAATAATCTCATTAATGCT
TAGCGCAGTCTCTCTATCGCTTCTGAACCCCGGTGCACCTGTGCCGAAACGCAAATGGGGAAACACCCGCTTTT
TGGATGATTATGCATTGTCTCCACATTGTATGCTTCCAAGATTCTGGTGGGAATACTGCTGATAGCCTAACGTT
CATGATCAAAATTTAACTGTTCTAACCCCTACTTGACAGCAATATATAAACAGAAGGAAGCTGCCCTGTCTTAA
ACCTTTTTTTTTATCATCATTATTAGCTTACTTTCATAATTGCGACTGGTTCCAATTGACAAGCTTTTGATTTTAA
CGACTTTTAACGACAACTTGAGAAGATCAAAAAACAACTAATTATTCGAAACGATGGCTATCCCCGAAGAGTT
TGATATCCTAGTTCTAGGTGGTGGATCCAGTGGATCCTGTATTGCCGGAAGATTGGCAAACTTGGACCACTCCT
TGAAAGTTGGTCTTATCGAAGCAGGTGAGAACAACCTCAACAACCCATGGGTCTACCTTCCAGGTATTTACCC
AAGAAACATGAAGTTGGACTCCAAGACTGCTTCCTTCTACACTTCTAACCCATCTCCTCACTTGAATGGTAGAA
GAGCCATTGTTCCATGTGCTAACGTCTTGGGTGGTGGTTCTTCTATCAACTTCATGATGTACACCAGAGGTTCT
GCTTCTGATTACGATGACTTCCAAGCCGAGGGCTGGAAAACCAAGGACTTGCTTCCATTGATGAAAAAGACTG
AGACCTACCAAAGAGCTTGCAACAACCCTGACATTCACGGTTTCGAAGGTCCAATCAAGGTTTCTTTCGGTAA
CTACACCTACCCAGTTTGCCAGGACTTCTTGAGGGCTTCTGAGTCCCAAGGTATTCCATACGTTGACGACTTGG
AAGACTTGGTTACTGCTCACGGTGCTGAACACTGGTTGAAGTGGATCAACAGAGACACTGGTCGTCGTTCCGA
CTCTGCTCATGCATTTGTCCACTCTACTATGAGAAACCACGACAACTTGTACTTGATCTGTAACACGAAGGTCG
ACAAAATTATTGTCGAAGACGGAAGAGCTGCTGCTGTTAGAACCGTTCCAAGCAAGCCTTTGAACCCAAAGAA
GCCAAGTCACAAGATCTACCGTGCTAGAAAGCAAATCGTTTTGTCTTGTGGTACCATCTCCTCTCCATTGGTTT
TGCAAAGATCCGGTTTTGGTGACCCAATCAAGTTGAGAGCCGCTGGTGTTAAGCCTTTGGTCAACTTGCCAGGT
GTCGGAAGAAACTTCCAAGACCACTACTGTTTCTTCAGTCCTTACAGAATCAAGCCTCAGTACGAGTCTTTCGA
TGACTTCGTCCGTGGTGATGCTGAGATTCAAAAGAGAGTCTTTGACCAATGGTACGCCAATGGTACTGGTCCTC
TTGCCACTAACGGTATCGAAGCTGGTGTCAAGATCAGACCAACACCAGAAGAACTCTCTCAAATGGACGAATC
CTTCCAGGAGGGTTACAGAGAATACTTCGAAGACAAGCCAGACAAGCCAGTTATGCACTACTCCATCATTGCT
GGTTTCTTCGGTGACCACACCAAGATTCCTCCTGGAAAGTACATGACTATGTTCCACTTCTTGGAATACCCATT
CTCCAGAGGTTCCATTCACATTACCTCCCCAGACCCATACGCAGCTCCAGACTTCGACCCAGGTTTCATGAACG
ATGAAAGAGACATGGCTCCTATGGTTTGGGCTTACAAGAAGTCTAGAGAAACCGCTAGAAGAATGGACCACTT
TGCCGGTGAGGTCACTTCTCACCACCCTCTGTTCCCATACTCATCCGAGGCCAGAGCCTTGGAAATGGATTTGG
AGACCTCTAATGCCTACGGTGGACCTTTGAACTTGTCTGCTGGTCTTGCTCACGGTTCTTGGACTCAACCTTTGA
AGAAGCCAACTGCAAAGAACGAAGGCCACGTTACTTCGAACCAGGTCGAGCTTCATCCAGACATCGAGTACG
ATGAGGAGGATGACAAGGCCATTGAGAACTACATTCGTGAGCACACTGAGACCACATGGCACTGTCTGGGAA
CCTGTTCCATCGGTCCAAGAGAAGGTTCCAAGATCGTCAAATGGGGTGGTGTTTTGGACCACAGATCCAACGT
TTACGGAGTCAAGGGCTTGAAGGTTGGTGACTTGTCCGTGTGCCCAGACAATGTTGGTTGTAACACCTACACC
ACCGCTCTTTTGATCGGTGAAAAGACTGCCACTTTGGTTGGAGAAGATTTAGGATACTCTGGTGAGGCCTTAGA
CATGACTGTTCCTCAGTTCAAGTTGGGCACTTACGAGAAGACCGGTCTTGCTAGATTCTAATCAAGAGGATGTC
AGAATGCCATTTGCCTGAGAGATGCAGGCTTCATTTTTGATTACTTTTTTATTTGTAACCTATATAGTATAGGAT
TTTTTTTGTCATTTTGTTTCTTCTCGTACGAGCTTGCTCCTGATCAGCCTATCTCGCAGCTGATGAATATCTTGTG
GTAGGGGTTTGGGAAAATCATTCGAGTTTGATGTTTTTCTTGGTATTTCCCACTCCTCTTCAGAGTACAGAAGA
TTAAGTGAGACGTTCGTTTGTGC

Color code:

Red underlined – 5’ promoter, 940 bp (1-940 bp)
Black – *aox1* gene, 1992bp (941- 2932 bp)
Purple underlined – 3’ terminator, 338 bp (2865 – 3193 bp)
Green background – External primer binding sites, 2105 bp between primers (855-875, 2939-2959)
Primers used for PCR
f *aox1* external – 5′ GACTGGTTCCAATTGACAAGC 3′
r *aox1* external – 5′ GCAAATGGCATTCTGACATCC 3′
Blue background – Internal primer binding sites, 507bp between primers (996-1015, 1483-1502)
Primers used for PCR
f aox 1 internal – 5′ CCTGTATTGCCGGAAGATTG 3′
r *aox*1 internal – 5′ CAGCACCGTGAGCAGTAACC 3′
Yellow background – sequence difference of *aox1* and *aox2* within the two internal primers

HBsAg sequence

ATG GAG AAC ATC ACA TCA GGA TTC CTA GGA CCC CTG CTC GTG TTA CAG GCG GGG TTT TTC TTG TTG ACA AGA ATC CTC ACA ATA CCG CAG AGT CTA GAC TCG TGG TGG GCT TCT CTC AAT TTT CTA GGG GGA TCA CCC GTG TGT CTT GGC CAA AAT TCG CAG TCC CCA ACC TCC AAT CAC TCA CCA ACC TCC TGT CCT CCA ATT TGT CCT GGT TAT CGC TGG ATG TGT CTG CGG CGT TTT ATC ATA TTC CTC TTC ATC CTG CTG CTA TGC CTC ATC TTC TTA TTG GTT CTT CTG GAT TAT CAA GGT ATG TTG CCC GTT TGT TCT CTA ATT CCA GGA TCA ACA ACA ACC AGT ACG GGA CCA TGC AAA ACC TGC ACG ACT CCT GCT CAA GGC AAC TCT ATG TTT CCC TCA TGT TGC TGT ACA AAA CCT ACG GAT GGA AAT TGC ACC TGT ATT CCC ATC CCA TCG TCC TGG GCT TTC GCA AAA TAC CTA TGG GAG TGG GCC TCA GTC CGT TTC TCT TGG CTC AGT TTA CTA GTG CCA TTT GTT CAG TGG TTC GTA GGG CTT TCC CCC ACT GTT TGG CTT TCA GCT ATA TGG ATG ATG TGG TAT TGG GGG CCA AGT CTG TAC AGC ATC GTG AGT CCC TTT ATA CCG CTG TTA CCA ATT TTC TTT TGT CTC TGG GTA TAC ATT TAA

Color code:

Blue underlined – start codon
Black – *HBsA*g gene
Red underlined – stop codon
Green background – *HBsAg* internal primer binding sites, 447bp between primers (162-183, 588-608)
Primers used for PCR
f *HBsAg* internal – 5′ GTCCCCAACCTCCAATCACTCA 3′
r *HBsAg* internal – 5′ GGCCCCCAATACCACATCATC 3′

8.1.3. References

1. Vassileva A, Chugh DA, Swaminathan S, Khanna N: **Effect of copy number on the expression levels of hepatitis B surface antigen in the methylotrophic yeast *Pichia pastoris*.** *Protein Expr Purif* 2001, 21: 71-80.

2. Zhu T, Guo M, Tang Z, Zhang M, Zhuang Y, Chu J et al.: **Efficient generation of multi-copy strains for optimizing secretory expression of porcine insulin precursor in yeast *Pichia pastoris***. *J Appl Microbiol* 2009, 107: 954-963.

3. Gurramkonda C, Adnan A, Gäbel T, Lünsdorf H, Ross A, Nemani SK et al.: **Simple high-cell density fed-batch technique for high-level recombinant protein production with *Pichia pastoris*: Application to intracellular production of Hepatitis B surface antigen**. *Microb Cell Fact* 2009, 8: 13.

4. Lünsdorf H, Gurramkonda C, Adnan A, Khanna N, Rinas U: **Virus-like particle production with yeast: ultrastructural and immunocytochemical insights into *Pichia pastoris* producing high levels of the Hepatitis B surface antigen.** *Microb Cell Fact* 2011, 10: 48.

9. Appendix III

9.1. All identified intracellular proteins of *P. pastoris* X-33

The complete list of all identified proteins classified into functional categories, two representative 2D gels indicating the spots of all identified proteins and their log2 changes in response to methanol-induced high-level production of the IP are given.

The complete list of all identified proteins classified into functional categories.

NCBI Accession-No[1]	Locus ID[1]	Gene name[2]	Protein name[2]	MW (KDa)[3]	pI[3]	Mascot Score	Spot No[4]
Functional category[1]							
1. Metabolism							
1.1 Carbohydrate metabolism							
Methanol metabolism							
XP_002494271	PAS_chr4_0821	*AOX1*	Alcohol oxidase	74.5	6.0	124	14*,15*,148*, 156* (74.5 kDa), 163* (~25 kDa)
XP_002492075	PAS_chr2-2_0131	*CTA1*	Catalase A	58.1	6.6	183	18*
XP_002493065	PAS_chr3_0832	*DAS1*	Transketolase (Dihydroxyacetone synthase), similar to Tkl2p	79.1	6.0	174	153*, 223*,16*
XP_002493071	PAS_chr3_0841	*DAK*	Dihydroxyacetone kinase	65.4	5.4	114	57*, 58*
XP_002493270	PAS_chr3_1028	*FLD1*	S-(hydroxymethyl) glutathione dehydrogenase	41.4	6.1	81[5]	24*, 25*, 28*
XP_002493100	PAS_chr3_0867	*FGH1*	Non-essential intracellular esterase that can function as an S-formylglutathione hydrolase	33.4	6.3	131	49*, 54*
XP_002493171	PAS_chr3_0932	*FDH1*	NAD(+)-dependent formate dehydrogenase	40.4	6.6	119	29*, 30*, 31*, 32*, 33* (40 kDa), 61* (~10 kDa), 80*, 81* (~17 kDa), 87*, 89* (~30 kDa)
Glycolysis							
XP_002494228	PAS_chr4_0783	*GUT1*	Glycerol kinase	68.8	5.3	104	145*

NCBI Accession-No[1]	Locus ID[1]	Gene name[2]	Protein name[2]	MW (KDa)[3]	p*I*[3]	Mascot Score	Spot No[4]
Functional category[1]							
XP_002493103	PAS_chr3_0868	*FBP1*	Fructose-1,6-bisphosphatase	38.4	6.1	118	41*
XP_002491345	PAS_chr2-1_0437	*TDH1*	Glyceraldehyde-3-phosphate dehydrogenase, isozyme 3	35.7	6.2	106	45*, 48*, 95*,118*
XP_002489713	PAS_chr1-1_0072	*FBA1*	Fructose 1,6-bisphosphate aldolase	39.9	6.0	186	115*
XP_002490411	PAS_chr1-4_0292	*PGK1*	3-Phosphoglycerate kinase	44.1	7.8	152	210*, 211*
XP_002493191	PAS_chr3_0951	*TPI1*	Triose phosphate isomerase	27.1	5.7	244	112*
XP_002493059	PAS_chr3_0826	*GMP1*	Tetrameric phosphoglycerate mutase	28.0	6.0	165	65*
XP_002492293	PAS_chr3_0082	*ENO2*	Enolase I	46.5	5.4	102	22*, 59*, 150*
Ethanol metabolism							
CAY67035	PAS_c034_0018	*ADH*	Alcohol dehydrogenase	38.1	6.3	195	78*
XP_002491382	PAS_chr2-1_0472	*ADH3*	Mitochondrial alcohol dehydrogenase isozyme III	37.3	5.8	145	42*, 44*, 55*, 93*, 96*
Citrate cycle (TCA cycle)							
XP_002489764	PAS_chr1-1_0475	*CIT1*	Citrate synthase	51.9	7.8	102	27*
XP_002489444	PAS_chr1-3_0104	*ACO1*	Aconitase	85.0	5.7	77	129*
XP_002491128	PAS_chr2-1_0238	*MDH1*	Mitochondrial malate dehydrogenase	36.5	5.3	129	43*, 47*, 53*, 56*, 103*, 141*
Pentose phosphate pathway							
XP_002492495	PAS_chr3_0277	*6PGD [GND]*	6-Phosphogluconate dehydrogenase (decarboxylating)	54.2	5.9	116	23*
XP_002491849	PAS_chr2-2_0337	*TAL1*	Transaldolase	35.7	5.1	111	109*
Sugar metabolism and others							
XP_002490557	PAS_chr1-4_0426	*BGL2*	Endo-beta-1,3-glucanase	34.2	4.1	109	158*
XP_002493105	PAS_chr3_0870	*VIG9 [PSA1]*	GDP-mannose pyrophosphorylase (mannose-1-phosphate guanyltransferase)	40.1	6.0	95	215*

NCBI Accession-No[1]	Locus ID[1]	Gene name[2]	Protein name[2]	MW (KDa)[3]	pI[3]	Mascot Score	Spot No[4]
Functional category[1]							
Pyruvate metabolism							
XP_002492397	PAS_chr3_0188	*PDC1*	Major of three pyruvate decarboxylase isozymes	61.5	5.6	118	11*, 12*
XP_002491703	PAS_chr2-1_0769	*PYK2*	Pyruvate kinase	55.9	6.1	190	161*
1.2 Energy Metabolism							
Oxidative phosphorylation							
XP_002493409	PAS_c131_0021	*[VMA2]*	Vacuolar ATP synthase subunit B	55.4	5.3	159	167*
XP_002492803	PAS_chr3_0576	*atpA*	Alpha subunit of the F1 sector of mitochondrial F1F0 ATP synthase	59.0	9.1	76	52*, 66*, 125*
XP_002492039	PAS_chr2-2_0165	*atpD*	Beta subunit of the F1 sector of mitochondrial F1F0 ATP synthase	54.0	5.2	83	6*, 35*, 68*
XP_002494179	PAS_chr4_0737	*MCR1*	Mitochondrial NADH-cytochrome b5 reductase	33.6	8.8	151	67*
1.3 Nucleotide metabolism							
XP_002492154	PAS_chr2-2_0059	*YNK1*	Nucleoside diphosphate kinase	17.0	6.2	83	121*
1.4 Amino acid metabolism							
XP_002490090	PAS_chr1-1_0432	*ILV5*	Acetohydroxyacid reductoisomerase	44.4	7.7	92	37*
XP_002491046	PAS_chr2-1_0160	*metE [MET6]*	Cobalamin-independent methionine synthase	85.9	5.9	193	107*, 128*
XP_002492638	PAS_chr3_0410	*CAR2*	L-Ornithine transaminase	47.5	5.9	249	200*
XP_002490747	PAS_chr1-4_0608	*ARO8*	Aromatic aminotransferase I	54.2	5.4	172	165*
XP_002492166	PAS_chr2-2_0048		Dihydrolipoamide dehydrogenase	52.6	6.3	113	13*
XP_002493126	PAS_chr3_0890	*SAHH*	S-adenosyl-L-homocysteine hydrolase	49.2	5.4	147	151*
XP_002493112	PAS_chr3_0876	*SAM2*	S-adenosylmethionine synthetase	42.6	6.1	96	205*

NCBI Accession-No[1]	Locus ID[1]	Gene name[2]	Protein name[2]	MW (KDa)[3]	pI[3]	Mascot Score	Spot No[4]
Functional category[1]							
1.5 Metabolism of cofactors and vitamins							
XP_002493470	PAS_chr4_0065	*THI5*	Protein involved in synthesis of the thiamine precursor hydroxymethylpyrimidine (HMP)	38.7	6.3	94	46*
XP_002493989	PAS_chr4_0550	-	Pyridoxine 4-dehydrogenase	36.3	5.6	97	138*
XP_002492875	PAS_chr3_0648	*THI4*	Thiazole synthase	37.3	6.2	92	113*
2. Genetic information processing							
2.1 Transcription and translation							
XP_002491688	PAS_chr2-1_0755	*EGD2*	Alpha subunit of the heteromeric nascent polypeptide-associated complex (NAC)	21.6	4.6	78[5]	73*
XP_002489404	PAS_chr1-3_0068	*RPP0*	Conserved ribosomal protein P0 similar to rat P0, human P0, and E. coli L10e	33.7	4.6	128	72*
XP_002491277	PAS_chr2-1_0376	*EFB1*	Putative GTPase, member of the Obg family	23.2	4.3	122	108*
XP_002490107	PAS_chr1-1_0449	*PST2*	Protein with similarity to members of a family of flavodoxin-like proteins	20.9	6.4	73	86*
XP_002493447	PAS_chr4_0041	-	Protein component of the large (60S) ribosomal subunit	15.1	5.8	86	94*
XP_002489653	PAS_chr1-1_0019	*SUB2*	Component of the TREX complex required for nuclear mRNA export	49.6	5.4	91	166*
XP_002490604	PAS_chr1-4_0471	*RPS0*	Protein component of the small (40S) ribosomal subunit, nearly identical to Rps0Bp	29.3	4.6	72	71*
XP_002493313	PAS_chr3_1071	*CAM1*	Translation elongation factor EF-1 gamma	24.3	6.4	104	78*, 137*
XP_002493749	PAS_chr4_0327	*GCN1*	Positive regulator of the Gcn2p kinase activity, forms a complex with Gcn20p	30.4	5.6	79	101*
2.2 Sorting and degradation							
XP_002492588	PAS_chr3_0365	*SSC1*	Mitochondrial matrix ATPase	69.7	5.4	152	106*
XP_002490239	PAS_chr1-4_0130	*HSP90*	Heat shock protein Hsp90	80.9	4.8	81	1*, 2*
XP_002489443	PAS_chr1-3_0102	*clpB [HSP104]*	Heat shock protein that cooperates with Ydj1p (Hsp40) and Ssa1p (Hsp70)	100.6	5.3	140	315*

NCBI Accession-No[1]	Locus ID[1]	Gene name[2]	Protein name[2]	MW (KDa)[3]	pI[3]	Mascot Score	Spot No[4]
Functional category[1]							
XP002494360.1	PAS_FragD_0026	*[CDC48]*	ATPase in ER, nuclear membrane and cytosol with homology to mammalian p97	91.4	4.8	108	146*
CCA38590	PP7435Chr2-0908	*AAP1*	Aminopeptidase N	23.0	4.7	142	316*
XP_002493087	PAS_chr3_0856	*UBA1*	Ubiquitin activating enzyme (E1)	115.6	5.0	142	325*
2.3 Folding catalysts							
CAC33587	PAS_chr4_0844	*PDI*	Protein disulfide isomerase	58.1	4.6	161	134*
XP_002493562	PAS_chr4_0158	*CPNA [HSP60]*	Tetradecameric mitochondrial chaperonin	60.5	5.1	115	4*
XP_002489608	PAS_chr1-3_0264	*[CPR1]*	Cytoplasmic peptidyl-prolyl cis-trans isomerase (cyclophilin)	18.1	6.1	99	92*
XP_002493991	PAS_chr4_0552	*HSP70-HSA1 [SSA1]*	ATPase involved in protein folding and nuclear localization signal (NLS)-directed	69.7	4.1	89	207*
XP_002492959	PAS_chr3_0731	*HSP70 [SSB]*	Cytoplasmic ATPase that is a ribosome-associated molecular chaperone	66.6	5.1	100	209*
XP_002491027	PAS_chr2-1_0140	*KAR2*	ATPase involved in protein import into the ER	74.2	4.8	146	133*
XP_002492443	PAS_chr3_0230	*HSP70 [SSA3]*	ATPase involved in protein folding and the response to stress	70.9	5.1	102	76* (70.9 KDa) 105* (~25 KDa)
3. Cellular processes							
3.1 Transport and catabolism							
XP_002490181	PAS_chr1-4_0071	*SOD2*	Mitochondrial superoxide dismutase	25.2	7.9	85	216*
XP_002493819	PAS_chr4_0391	*[TOM40]*	Component of the TOM (translocase of outer membrane) complex	42.8	5.6	78	36*
XP_002492446	PAS_chr3_1169	*ACT1*	Actin	41.9	5.3	148	21*
3.2 Cell growth and death							
XP_002490987	PAS_chr2-1_0809	*BMH1*	14-3-3 protein homolog	29.1	4.8	85	75*
XP_002492031	PAS_chr2-2_0172	*NAP1*	Protein that interacts with mitotic cyclin Clb2p	49.0	4.3	115	135*

NCBI Accession-No[1]	Locus ID[1]	Gene name[2]	Protein name[2]	MW (KDa)[3]	pI[3]	Mascot Score	Spot No[4]
Functional category[1]							
4. Other							
4.1 Stress response							
XP_002491977	PAS_chr2-2_0220	*TSA1*	Thioredoxin peroxidase	21.5	4.9	125	77*
XP_002490091	PAS_chr1-1_0433	*PRX1*	Mitochondrial peroxiredoxin (1-Cys Prx) with thioredoxin peroxidase activity	25.1	5.7	142	82*, 111*
BAH80186	PAS_chr2-2_0480	*TRR1*	Thioredoxin reductase 1	35.3	5.5	93	225*
XP_002491413	PAS_chr2-1_0502	-	Thiol-specific peroxiredoxin	19.3	8.6	106	120*
5. Unclassified							
XP_002491418	PAS_chr2-1_0853	-	Hypothetical protein	57.0	6.0	84	7*, 8*, 91*
XP_002489760	PAS_chr1-1_0118	-	Laminin subunit gamma-1	46.3	7.0	73	142*, 157*
XP_002491208	PAS_chr2-1_0313	-	Bifunctional enzyme with alcohol dehydrogenase and glutathione-dependent formaldehyde dehydrogenase	39.1	5.8	92	38*, 39*, 40*
XP_002490174	PAS_chr1-4_0063	-	G-protein beta subunit and guanine nucleotide dissociation inhibitor for Gpa2p	35.0	6.3	104	116*
XM_002490789	PAS_FragB_0024	-	Inositol 2-dehydrogenase	38.0	5.7	79	139*

1 Accession numbers and locus IDs are according to the NCBI Reference Sequence database (http://www.ncbi.nlm.nih.gov/RefSeq/). Functional classifications are mostly according to KEGG PATHWAY database (http://www.genome.jp/kegg/metabolism.html). The datas are according to databases on 01.10.12.

2 Gene/protein names are according to the sequenced genome of *P. pastoris* GS115 (http://www.uniprot.org/). If no name was found for *P. pastoris* GS115, a Blast search of the respective *P. pastoris* GS115 gene/protein against different *P. pastoris* strains was carried out in the following order: search against ATCC 76273 / CBS 7435 / CECT 11047 / NRRL Y-11430 / Wegner 21-1 and *P. pastoris* (yeast). Gene/protein names from other *P. pastoris* strains were only adopted in case of 100% sequence identity (http://www.uniprot.org/). Gene names in brackets are from *S. cerevisiae* if the names differ for both yeasts (http://www.uniprot.org/). The datas are according to database on 01.10.12.

3 Theoretical molecular mass (MM) and isoelectric point (p*I*) not considering potential posttranslational modifications.

4 "Spot-No" indicates the serial number of all identified protein spots of the intracellular proteome of *P. pastoris* X-33. Proteins appearing in multiple spots indicate the existence of isoforms which probably derive from posttranslational modification events such as phosphorylation, glycosylation or limited proteolysis. Two representative 2D gels of the intracellular proteome from cell samples taken at the end of glycerol phase and after 48 hours of growth on methanol with the respective spot numbers are shown below. Spot numbers in this table and the following gel are marked by an asterix (*) for simplified searchability. Fragments of full-length proteins, AOX1, FDH1 and SSA3, were identified and the respective Spot No and MW are indicated.

5 Score obtained from MSMS analysis.

Two representative 2D gels of the intracellular proteome of *P. pastoris* X-33 producing IP.

The sample was taken at the end of the glycerol phase (A) and after 48 h of growth on methanol (B). Spot numbers correspond to numbers in the table above and are marked by an asterix (*) for simplified searchability.

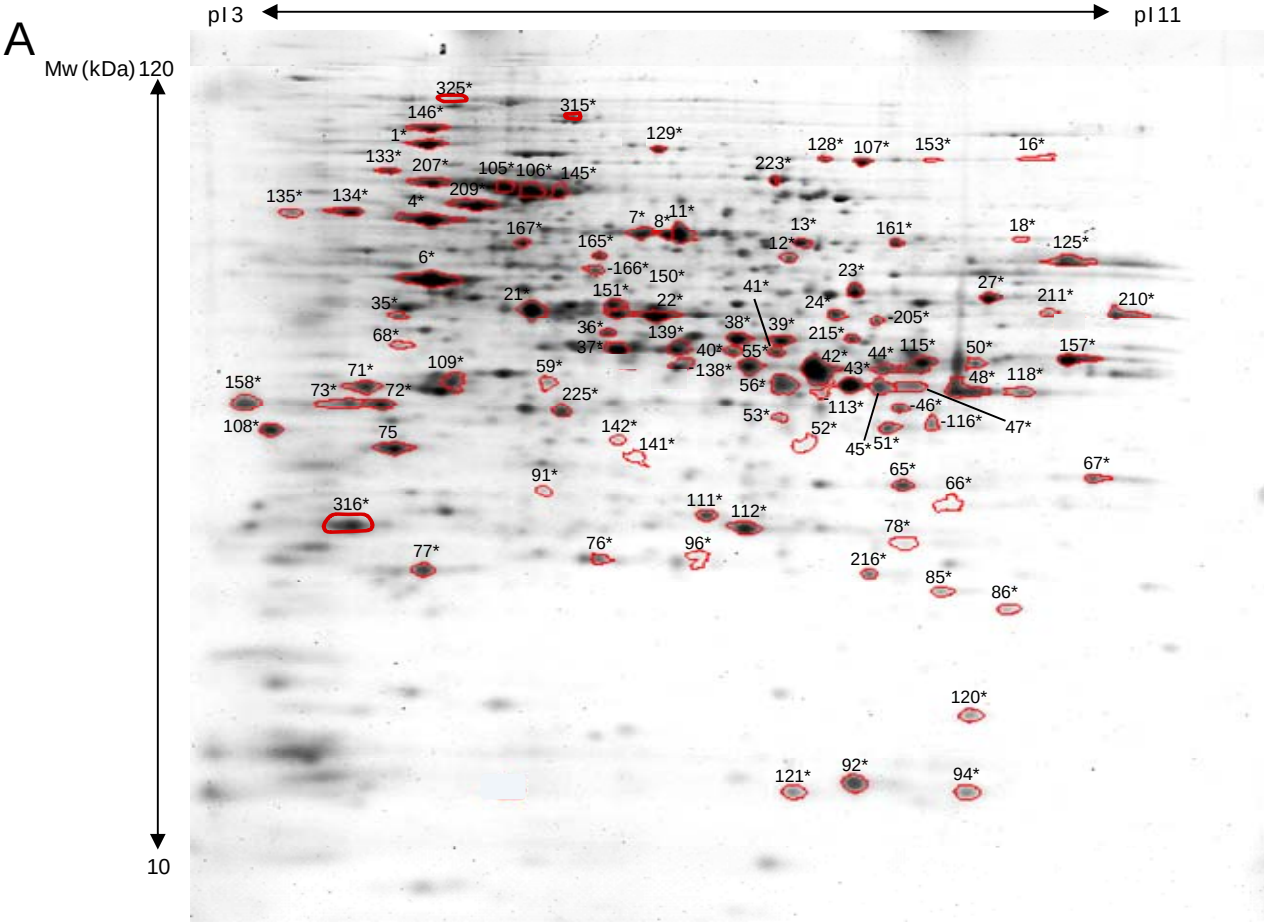

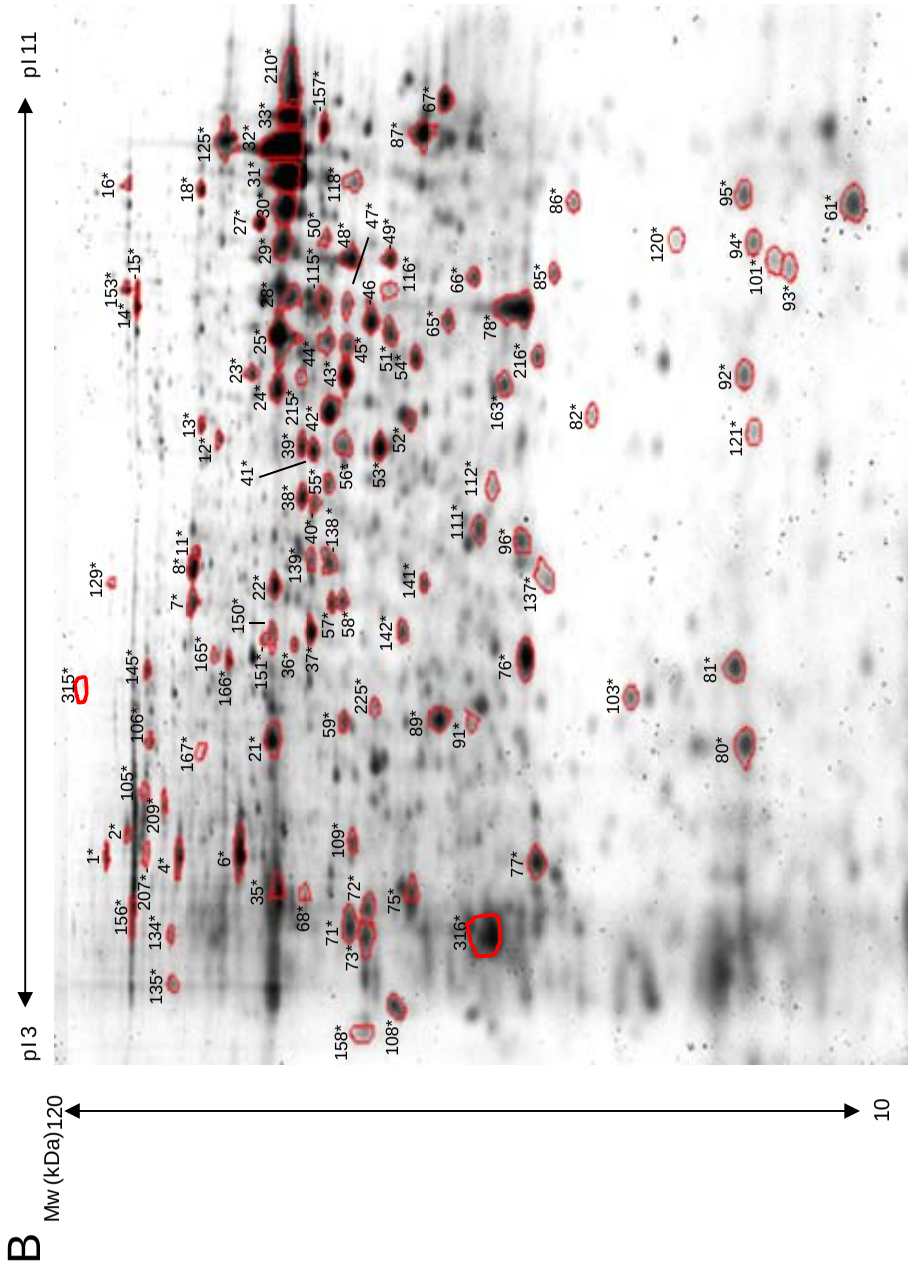
B
Mw (kDa) 120
pI 3
pI 11
10

Change of the intracellular proteome in response to IP production under methanol induction.

Samples before methanol addition at the end of the glycerol batch phase and 6, 18, 48 and 120 hours after the onset of methanol feeding were analyzed and the protein changes are shown (numbers. log2 changes; n.a. not analyzable, color code: light orange to red, increase, light green to dark green: decrease, yellow: no significant change).

Functional category	Gene name[1]	Gene ID	0h[2]	6h	18h	48h	120h
Carbohydrate metabolism							
Methanol metabolism	*AOX1*	PAS_chr4_0821	0.0	7.4	9.4	9.2	9.5
	AOX1 (~25 kDa)[3]		0.0	7.1	7.1	8.1	8.1
	CTA1	PAS_chr2-2_0131	0.0	1.7	2.0	1.5	2.3
	DAS1	PAS_chr3_0832	0.0	0.1	0.9	-0.1	-0.2
	DAK	PAS_chr3_0841	0.0	n.a	6.5	8.1	8.7
	FLD1	PAS_chr3_1028	0.0	9.4	9.9	10.7	10.8
	FGH1	PAS_chr3_0867	0.0	7.0	8.4	8.8	9.0
	FDH1	PAS_chr3_0932	0.0	10.7	11.6	12.3	12.3
	FDH1 (~30 kDa)[3]		0.0	6.2	8.3	10.1	10.5
	FDH1 (~17 kDa)[3]		0.0	0.0	8.1	9.6	10.5
	FDH1 (~10 kDa)[3]		0.0	0.0	7.1	9.3	9.4
Glycolysis	*GUT1*	PAS_chr4_0783	0.0	-0.4	0.1	-1.6	n.a
	FBP1	PAS_chr3_0868	0.0	0.1	0.6	0.6	0.6
	TDH1	PAS_chr2-1_0437	0.0	0.6	-0.3	-0.6	-1.1
	FBA1	PAS_chr1-1_0072	0.0	0.2	-0.6	-1.1	-1.0
	PGK1	PAS_chr1-4_0292	0.0	-1.0	n.a	1.1	0.4
	TPI1	PAS_chr3_0951	0.0	0.1	-0.4	-2.1	-2.2
	GMP1	PAS_chr3_0826	0.0	0.0	-0.2	-0.8	-1.1
	ENO2	PAS_chr3_0082	0.0	0.1	0.0	-1.1	-0.8
Ethanol metabolism	*ADH3*	PAS_chr2-1_0472	0.0	0.0	0.0	-0.7	-0.6

Functional category	Gene name[1]	Gene ID	0h[2]	6h	18h	48h	120h
Citrate cycle (TCA)	*CIT1*	PAS_chr1-1_0475	0.0	1.0	0.7	0.3	0.4
	ACO1	PAS_chr1-3_0104	0.0	0.5	0.1	-1.0	-0.4
	MDH1	PAS_chr2-1_0238	0.0	0.1	-0.2	-0.1	0.5
Pentose phosphate pathway	*6PGD [GND]*	PAS_chr3_0277	0.0	0.9	0.3	-0.5	-0.9
	TAL1	PAS_chr2-2_0337	0.0	1.1	0.4	-1.0	-0.4
Sugar metabolism	*BGL2*	PAS_chr1-4_0426	0.0	0.2	-0.1	-1.0	-0.9
	VIG9 [PSA1]	PAS_chr3_0870	0.0	0.4	-0.9	-0.9	n.a
Pyruvate metabolism	*PDC1*	PAS_chr3_0188	0.0	0.0	-0.5	-1.4	-2.0
	PYK2	PAS_chr2-1_0769	0.0	0.6	-0.5	-2.3	-1.9
Energy metabolism							
Oxidative phosphorylation	*[VMA2]*	PAS_c131_0021	0.0	-0.1	-1.0	-1.2	-1.6
	atpA	PAS_chr3_0576	0.0	0.8	0.3	0.4	1.1
	atpD	PAS_chr2-2_0165	0.0	-0.2	0.4	-0.7	0.1
	MCR1	PAS_chr4_0737	0.0	0.2	0.9	0.2	1.2
Nucleotide Metabolism							
	YNK1	PAS_chr2-2_0059	0.0	-0.2	-0.6	-1.0	-1.4
Amino Acid Metabolism							
	ILV5	PAS_chr1-1_0432	0.0	0.2	-0.1	-0.7	-0.1
	metE [MET6]	PAS_chr2-1_0160	0.0	0.8	-0.7	n.a	n.a
	CAR2	PAS_chr3_0410	0.0	0.1	-0.3	n.a	-0.3
	ARO8	PAS_chr1-4_0608	0.0	1.3	0.6	-0.1	0.5
	-	PAS_chr2-2_0048	0.0	0.6	-0.4	-0.7	-0.2
	SAHH	PAS_chr3_0890	0.0	0.0	-0.5	-1.6	-0.4
	SAM2	PAS_chr3_0876	0.0	0.9	-0.3	0.4	-0.1
Metabolism of cofactors and vitamins							
	-	PAS_chr4_0550	0.0	0.0	-0.7	-0.6	-1.2
	THI5	PAS_chr4_0065	0.0	1.5	2.3	1.0	-0.8
	THI4	PAS_chr3_0648	0.0	1.9	2.3	0.5	0.1

Functional category	Gene name[1]	Gene ID	0h[2]	6h	18h	48h	120h
Genetic information processing							
Transcription and translation	*EGD2*	PAS_chr2-1_0755	0.0	-0.3	-0.9	-0.3	-0.2
	RPP0	PAS_chr1-3_0068	0.0	0.7	-0.1	-0.4	-0.2
	EFB1	PAS_chr2-1_0376	0.0	-0.3	-0.4	-0.9	-1.0
	PST2	PAS_chr1-1_0449	0.0	0.3	0.3	-0.8	-0.5
	-	PAS_chr4_0041	0.0	0.1	-0.4	-0.1	-1.0
	SUB2	PAS_chr1-1_0019	0.0	0.6	0.0	0.1	1.2
	RPS0	PAS_chr1-4_0471	0.0	-0.3	-0.4	-0.2	-2.5
	CAM1	PAS_chr3_1071	0.0	0.8	2.2	3.5	2.5
	GCN1	PAS_chr4_0327	0.0	n.a	7.4	7.1	6.5
Sorting and Degradation	*SSC1*	PAS_chr3_0365	0.0	-0.3	-1.3	-2.6	-1.0
	Hps90	PAS_chr1-4_0130	0.0	-0.6	-1.6	-0.9	n.a
	clpB [HSP104]	PAS_chr1-3_0102	0.0	0.5	-1.2	-2.2	n.a
	[CDC48]	PAS_FragD_0026	0.0	-0.5	-1.4	-3.6	-3.4
	AAP1	PP7435_Chr2-0908	0.0	-0.5	-0.5	-0.8	-0.6
	UBA1	PAS_chr3_0856	0.0	-0.5	-1.5	n.a	n.a
Folding catalysts	*PDI*	PAS_chr4_0844	0.0	-0.2	-1.2	-2.7	-1.7
	CPNA [HSP60]	PAS_chr4_0158	0.0	0.0	-0.5	-1.5	-0.2
	[CPR1]	PAS_chr1-3_0264	0.0	-0.2	-0.7	-1.3	-1.4
	HSP70-HSA1 [SSA1]	PAS_chr4_0552	0.0	-0.7	-1.5	-2.9	-2.9
	HSP70 [SSB]	PAS_chr3_0731	0.0	0.1	-0.8	-2.5	-2.2
	KAR2	PAS_chr2-1_0140	0.0	0.1	-1.5	n.a	-1.4
	HSP70 [SSA3]	PAS_chr3_0230	0.0	-0.4	-1.0	-2.7	-2.2
	HSP70 [SSA3] (~ 25 KDa)[3]		0.0	0.3	1.4	1.8	2.4
Cellular processes							
Transport and catabolism	*SOD2*	PAS_chr1-4_0071	0.0	0.3	0.0	-0.1	0.2
	[TOM]	PAS_chr4_0391	0.0	0.4	-0.1	-1.0	1.1
	ACT1	PAS_chr3_1169	0.0	0.1	0.2	0.0	-0.2
Cell Growth and death	*BMH1*	PAS_chr2-1_0809	0.0	-0.1	0.0	-0.8	-0.9
	NAP1	PAS_chr2-2_0172	0.0	-0.7	-0.5	-0.4	-1.4

Functional category	Gene name[1]	Gene ID	0h[2]	6h	18h	48h	120h
Others							
Stress response	*TSA1*	PAS_chr2-2_0220	0.0	-0.2	0.4	-0.1	0.6
	PRX1	PAS_chr1-1_0433	0.0	0.0	0.3	-0.1	0.4
	TRR1	PAS_chr2-2_0480	0.0	0.3	-0.1	-1.8	-1.2
	-	PAS_chr2-1_0502	0.0	0.3	-0.4	-1.4	-1.3
Unclassified	-	PAS_chr2-1_0853	0.0	0.5	0.1	-0.1	0.6
	-	PAS_chr1-1_0118	0.0	0.5	-0.1	-0.7	-0.4
	-	PAS_chr2-1_0313	0.0	-0.1	-0.3	-0.7	-0.3
	-	PAS_chr1-4_0063	0.0	1.3	0.6	0.1	-0.4
	-	PAS_FragB_0024	0.0	0.2	-0.4	-1.4	-1.2

1. Gene names in brackets are from *S. cerevisiae* if the names differ for both yeasts (http://www.uniprot.org/).
2. When no protein spot was detectable at the end of the glycerol batch phase (methanol metabolism), a virtual number of 0.001 was taken for the spot intensity to allow the calculation of log2 values (spot intensities were normalized using the log2 ratio of induced samples *versus* uninduced sample).
3. Fragments of full-length proteins, AOX1, FDH1 and SSA3, were identified and the respective log2 fold changes are given.

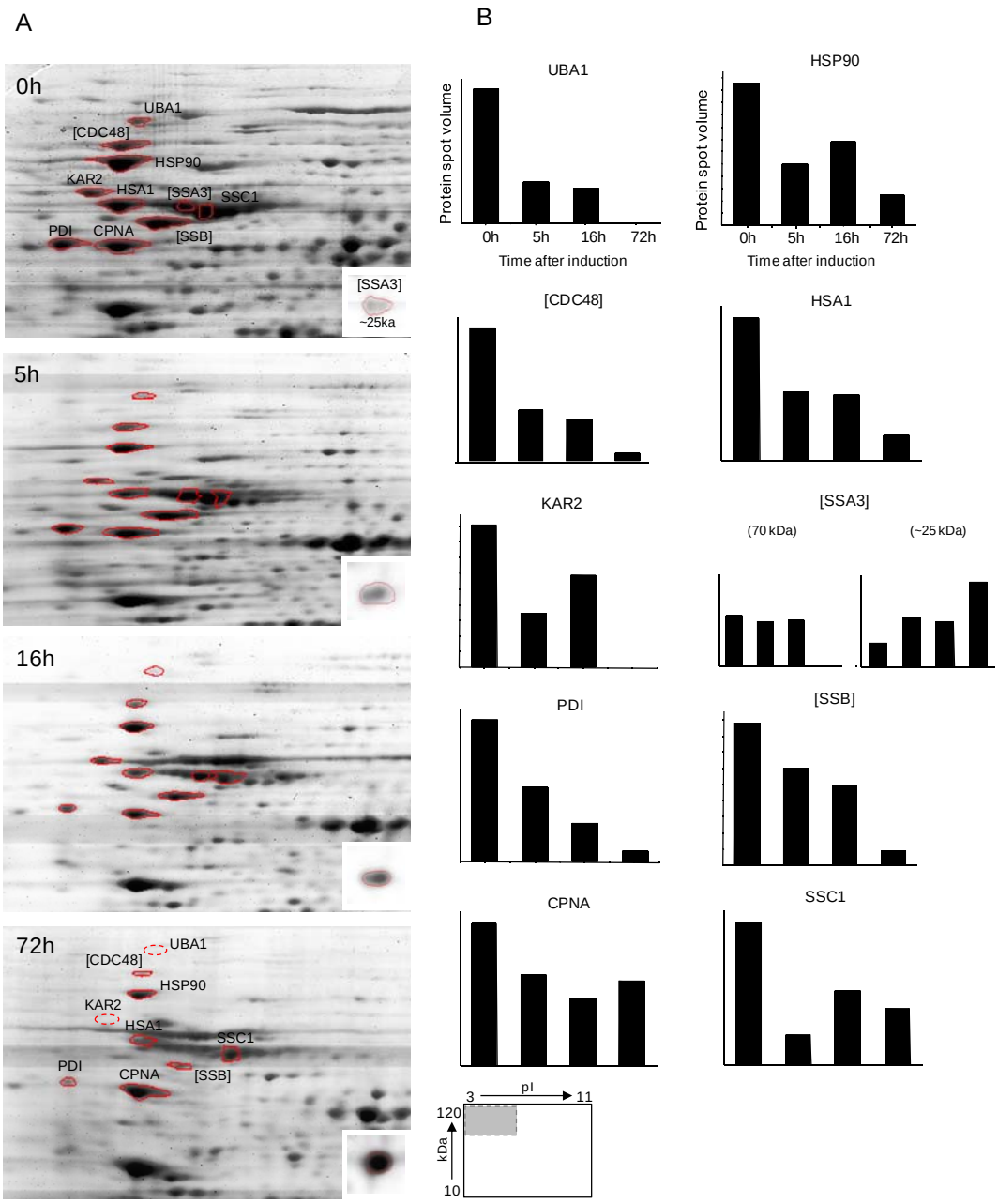

Figure 9.1. Changes of the intracellular proteome of *P. pastoris* X-33 in response to secretory insulin precursor production containing most of the identified ERAD and UPR related proteins. (A) Sections of 2D gels representing parts of the intracellular proteome and containing most of ERAD and UPR related proteins at 0, 5, 16 and 72h after induction with methanol. (B) Representative graphs of the abundance changes of each protein spot shown in A. The spot related to fragment SSA3 ~25 kDa is shown in the small. This cultivation was done in almost the same conditions as described in the Chapter 4, Methods 4.3.2. Only the induction with methanol was directly started with 2 g L^{-1}, instead to use the initiations pulses. The small map indicates the position of the 2D sections in the entire 2D gel.

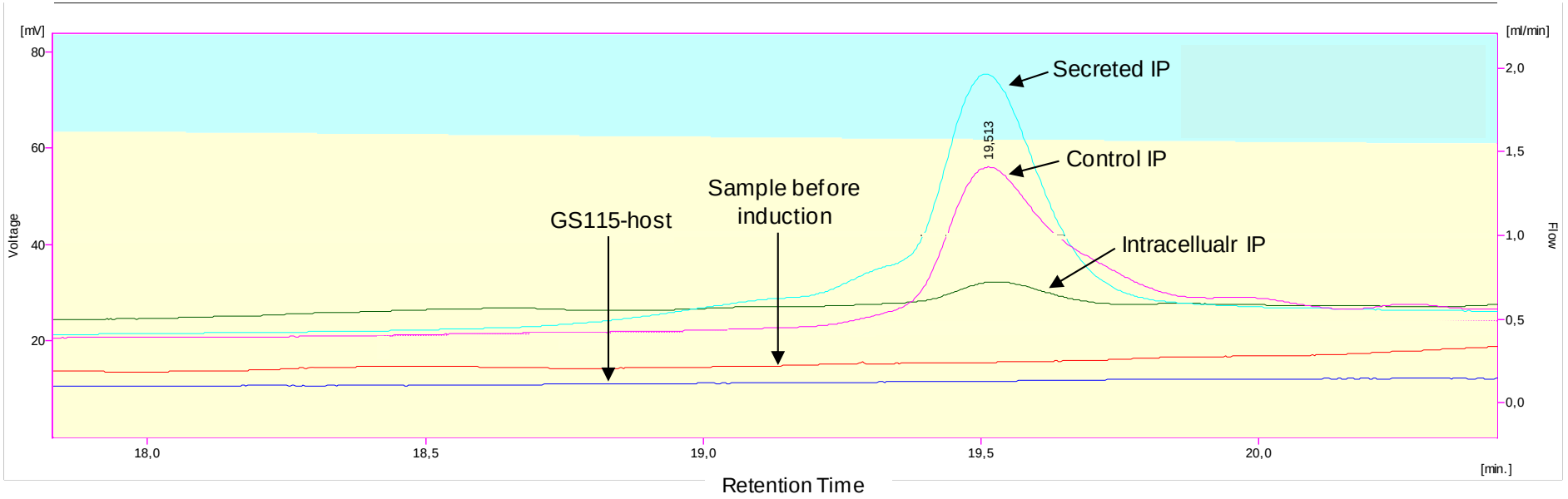

Figure 9.2. Chromatogram of intracellular and secreted insulin precursor. Quantification of intracellular and secreted insulin precursor was done by reverse phase high performance liquid chromatography (RP-HPLC). The injection volume was 50 µL for both standard and samples. Samples were taken at 120 h after induction. Pure IP (pink line-Control IP) was used as control for the retention time. Sample before induction (red line) and GS115 host strain (GS115-host) (blue line) were used as a negative control to check if none of natural proteins has the same retention time. The intracellular IP is represented by the green line and the secreted IP is represented by the turquoise line. The details of the analysis are described in the Chapter 4, Methods 4.3.2.

10. Appendix IV

10.1. Protocol for *P. pastoris* two-dimensional gel electrophoresis

This protocol is based on manufacturer's instruction (GE Healthcare, UK) and on the PhD thesis, Metabolic balance during protein production with recombinant *Escherichia coli*, Zhaopeng Li, 2012, Hannover University, with some modification for this study.

10.1.1. Sample preparation

10.1.1.1. Cell harvesting

Collect a certain volume of the cell culture to always bring the OD_{600} to 40. Centrifuge at 4°C, 13300 rpm for 3 min, discard the supernatant, freeze the final cell pellets in liquid nitrogen and store at -80°C.

10.1.1.2. Cell disruption

Wash the pellet with ice-cold 1× PBS, resuspend in 1 mL cell lysis buffer (7 mol L^{-1} urea, 2 mol L^{-1} thiourea, 30 mmol L^{-1} Tris, 4% (w/v) Triton X-100, pH 8.5) and adjust to OD_{600} ~50. Combine with 500 µL of glass beads (0.5 mm, Sartorius AG, Goettingen, Germany). For cell disruption, samples are treated in a Fastprep FP120 homogenizer (Thermo Savant, Holbrook, NY) twice (speed 6.00 m/s for 30 s; cooling interval of 30 s between treatments). Afterwards, cellular debris is pelleted by centrifugation at 13000 rpm at 4°C for 5 min.

10.1.1.3. Precipitation with chloroform/methanol

In order to separate the protein from the contaminating species, such as salts, nucleic acids, lipids, etc, the precipitation was done as described below. Prepare each sample in triplicate in order to run triplicate 2D gels. For each sample prepare one water control group, substituting the cell lysate for Milli-Q water.

1- Transfer 100 µL of lysate cells (or Milli-Q water for the control) into a 2 mL microcentrifuge tube.
2- Add 800 µL of methanol and vortex for 10 seconds.

3- Add 200 µL of chloroform and vortex for 10 seconds.
4- Add 600 µL of Milli-Q water and vortex for 10 seconds.
5- Centrifuge at 13300 rpm for 7 min at 4°C.
6- After centrifugation, a white pellet of protein should be visible. Use a pipette to remove the supernatant. Wash the surface of protein pellet using the upper layer of the control after the final centrifugation. Shake gently the tubes at 300 rpm for 1 min (do not vortex). Without disturbing the protein pellet, remove as much as possible of the supernatant using a pipette. Allow the pellet to air dry to let the residual methanol and chloroform evaporate till there no smell of methanol. This drying procedure should not last more than 10 min. Do not overdry the protein pellet.

10.1.1.4. Resuspension of pellet

After drying, resuspend the protein pellet in 500 µL of resolubilization solution (urea 9 mol L^{-1}, thiourea 2 mol L^{-1}, CHAPS 4%, Tris 2 mg/mL, SDS 0.2% and bromophenol blue 0.002%), 7.5 µL of IPG buffer and 7.5 µL of 1 mol L^{-1} DTT stock solution. To facilitate the resolubilization shake the sample at 1000 rpm for 3 h at 26^{o}C in an Eppendorf Thermomixer (Eppendorf, Germany). Freeze the final cell pellet in liquid nitrogen and store at -80^{o}C for later analysis.

10.1.2. First-dimension isoelectric focusing (IEF)

During the isoelectric focusing the proteins are separated according to their isoelectric points (p*I*).

The Ettan IPGphor strip holder (GE Healthcare, UK) should be clean and completely dry before use. For cleaning, wash with 10% SDS solution using a toothbrush, rinse well with Milli-Q water to remove the SDS and other residual contaminations and thoroughly air dry the strip holders.

1- Take out the samples from -80^{o}C and shake at 1000 rpm for 1.5 h at 28^{o}C in an Eppendorf Thermomixer. Make sure that urea and thiourea are completely dissolved. Add another 7.5 µL of 1 mol L^{-1} DTT stock solution to each sample to make the final DTT concentration to 30 mmol L^{-1}, shake for additional 10 min.

2- Centrifuge the sample at 13300 rpm for a 25 min at 25°C.

3- Transfer 420 µL of supernatant to a new microcentrifuge tube. Final resolubilization solution is urea 9 mol L^{-1}, thiourea 2 mol L^{-1}, CHAPS 4%, Tris 2 mg/mL, IPG buffer 1.5% (pH gradient 3-10), DTT 30 mmol L^{-1}, SDS 0.2% and bromophenol blue 0.002%.

4- Place two IEF sample application pieces (GE Healthcare, UK) in the lateral wells at both ends of the strip holder. Add 20 µL of rehydration solution (urea 9 mol L^{-1}, thiourea 2 mol L^{-1}, CHAPS 4%, Tris 2 mg/mL) onto each paper before the samples are loaded on to the strip holder.

5- Take note of the number of the IPG strip and which sample will be loaded onto this IPG strip. Do not write on the IPG strip.

6- Load 360 mL of sample into the center of a cleaned strip holder. The sample should be in between the two electrodes. Remove any larger bubble.

7- Remove the protective cover foil of the IPG strip with forceps starting at the acidic (+) end. Place the IPG strip with the gel side down. Do not generate bubbles. Put the (+) (conical side) and (–) (square side) side in the correct position.

8- Add 3 mL silicon oil on the plastic back of the IPG strip to minimize evaporation and, thus, prevent urea crystallization. Cover up the strip holder.

9- Start the IEF according the following protocol:

Procedure	Program Steps	Voltage (V)	Step duration (h)	Voltage gradient type	Theoretical voltage hours (Vhr)
Rehydration		0	35	Step-n-hold	0
Isoelectric Focusing	1	50	4 h	Step-n-hold	200
	2	100	4 h	Gradient	400
	3	300	3 h	Gradient	900
	4	1000	4 h	Gradient	2600
	5	3500	3 h	Gradient	6750
	6	5000	3 h	Gradient	12750
	7	5000	3 h	Step-n-hold	15000
	8	8000	3 h	Gradient	19500
End	9	8000	10 h	Step-n-hold	80000
Temperature: 20°C, Current limit for each strip: 30 µA (3-10 NL strip) or 35 µA (3-10 strip)					

10.1.3. Second dimension SDS-PAGE

During the second dimension SDS-PAGE the proteins are separated according to their molecular weights.

10.1.3.1. Preparing the electrophoresis tank

Around 2 hours before the start, prepare the buffer and fill the tank. Turn on the tank and set the temperature to 10°C at the cooling unit.

10.1.3.2. Equilibrating IPG strip

The equilibration step saturates the IPG strip with the SDS buffer necessary for the second-dimension separation and is always performed immediately prior to the second-dimension run.

1- With a pipette remove the silicon oil of the strip holder and use forceps to take out the IPG strips to a blotting paper to absorb the excess silicon oil. Make sure that the gel side is facing up to the air.
2- Place one strip, gel side up, in each channel of the plexiglass tray and fill the channel successively with the equilibration buffer. First, add 4 mL of SDS equilibration buffer with 1% DTT, previously prepared and incubate with gentle agitation for 15 min, then decant. This buffer reduces the disulfide bonds.
3- A second equilibration may be performed with iodoacetamide. Refill the channel with 4 mL of SDS equilibration buffer with 5% iodoacetamide, previously prepared and incubate again for 15 min with gentle shaking. This buffer alkylates the sulfhydryl groups. After equilibration pour out the SDS equilibration buffer with iodoacetamide to a special container. Do not discard iodoacetamide to the sink.

10.1.3.3. Transfer of IPG strips to the SDS-PAGE gel

1- During the IPG strip equilibration melt the agarose sealing solution in a microwave. Do not allow the solution to boil. The composition of the agarose sealing solution is: 1% agarose, 0.002% bromophenol blue, dissolved in SDS electrophoresis buffer.

2- Wash the SDS-PAGE slab gel cassettes with purified water; apply some SDS electrophoresis buffer to the loading space for the IPG strips to facilitate the transition procedure.
3- Place the IPG strip onto the long plate with the plastic backing against the plate. Do not damage the gel of the IPG strip. As convention, always put the pointed, acidic (+) end on the same end as the gel label. Make sure that the IPG strip is positioned directly on top of the second dimension gel and centered. Overlay the strip with molten 1% agarose sealing solution. Avoid bubbles when sealing with agarose, they can disturb protein migration. Wait 2 – 5 minutes to allow the agarose to solidify before proceeding.

10.1.3.4. Placement of cassettes into the DALT tank

Place the cassettes into the electrophoresis tank. The cassettes are correctly loaded in running orientation in the DALT tank (GE Healthcare, UK) slot with the IPG strips vertical along the left, or cathode (-), side and the rubber cassette hinge along the bottom. Do not drop the plates into the tank and onto the circulation flutes.

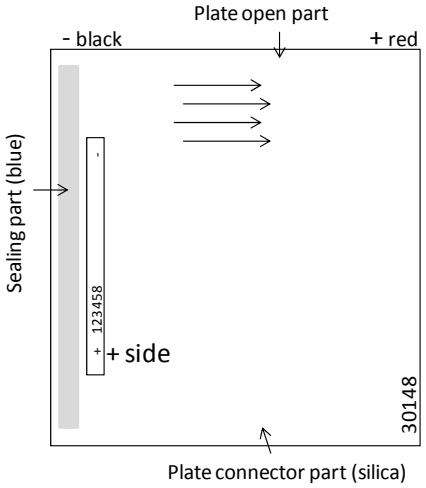

Adjust the buffer level after all the cassettes are placed and close the lid. Attach the electrical leads to make proper electrical contact with the power supply. Migration proceed toward the red (+), or right part of the chamber. Turn on the power supply to begin the separation. Set the power supply to 40 V constant voltage for the first 2 h and increase to 100 V for overnight run.

10.1.3.5. Ending second-dimension SDS-PAGE electrophoresis

Stop the running when bromophenol blue tracking dye reaches the edge of the polymerized acrylamide gel. Carefully take out of the tank and open the cassettes. Transfer the gels to a plastic box and incubate the gels in fixing solution for 1.5 h with gentle agitation. After 45 min, refresh the fixing solution and shake for another 45 min. After the fixation, remove all of the fixing solution and add some Colloidal Silver Coomassie G-250 staining solution and incubate overnight with gentle agitation. To destain the Coomassie stained gels use Milli-Q water. Refresh the water as often as necessary. After destaining, preserve the gel at 4°C with NaN_3 (Sodium Azide) (100 µL NaN_3 1% in 1000 mL H_20).

10.2. Protocol for MALDI analysis

10.2.1. Trypsin digestion

1. Excision of protein spot from polyacrylamide gels

1.1. Wash SDS-PAGE gel with Milli-Q water. Excise the gel spot of interest and put them into microcentrifuge tube. Do not touch the gel with fingers. Always wear gloves.

1.2. Wash the gel pieces 5 times with 1 mL Milli-Q water. For every washing step, very gently shake for 5 min. At the last washing step, use a small pipette tip to cut gel spots into small pieces. Withdraw water and be careful to not suck out and lose any piece of gel spots.

1.3. Dehydrate. Add 200 µL acetonitrile (ACN) for 10 min. Withdraw ACN completely.

2. Carbamidomethylation

2.1. Add 50 µL of DTT solution [20 mmol L^{-1} DTT (3.1 mg/mL) in 0.1 mol L^{-1} NH_4HCO_3] to each sample and incubate for 30 min at 56°C on a Eppendorf thermomixer (do not shake). This step is done to reduce the protein. Remove the DTT solution from each sample completely (be careful to not suck out any piece of gel spots).

2.2. Dehydrate with acetonitrile (see step 1.3 above).

2.3. Add 50 µL of iodacetamide solution [55 mmol L^{-1} iodacetamide (10.2 mg/mL) in 0.1 mol L^{-1} NH_4HCO_3] to each sample. Incubate for 30 min at room temperature in the dark. Withdraw iodacetamide solution completely.

2.4. Dehydrate with acetonitrile (see step 1.3 above).

3. Buffering

3.1. Add 200 µL of 0.1 mol L^{-1} NH_4HCO_3. Incubate for 15 min at room temperature. Withdraw NH_4HCO_3.

3.2. Dehydrate with acetonitrile (see step 1.3 above).

3.3. Dry the gel pieces in a vacuum centrifuge (about 10 min).

4. In gel trypsin digestion

4.1. Preparation of the trypsin solution. To one vial of 20 µg trypsin (Promega) add 100 µL of resuspension buffer (Promega) and incubate for 30 min at room temperature. Add 900 µL of 0.1 mol L^{-1} NH_4HCO_3. After mixing, aliquot 50 µL into 0.5 mL microcentrifuge tube and store at –20°C. Before using, thaw and add 450 µL Milli-Q water to make 500 mL of trypsin working solution.

4.2. Add about 30 µL of trypsin working solution to each gel spot. Incubate the sample overnight at 37°C.

10.2.2. Sample preparation for MALDI using ZipTips (C_{18})

5. Peptide extraction

5.1. Add 30 µL of acetonitrile (ACN) to the gel spot and mix on a Eppendorf thermomixer for 15 min at 37°C and 800 rpm.

5.2. Transfer supernatant of each sample into another Eppendorf tube.

5.3. Add 30 µL of 5% formic acid to each gel spot and mix on an Eppendorf thermomixer for 15 min at 37°C and 800 rpm.

5.4. Add 30 µL of ACN to each gel spot and mix for 15 min at 37°C and 800 rpm.

5.5. After 15 min, combine the supernatant with supernatant in the tube from step 5.2.

5.6. Use Speedvac to dry samples (the sample combined with the supernatant from step 5.2 and 5.5) about 1 hour.

5.7. After drying, add 20 µL 2% methanol, 0.5% formic acid and put samples into a sonication bath to sonicate for 5 min.

6. Desalting with ZipTips (C_{18})

6.1. Clean ZipTip 3 times with 10 µL elution solution (65% methanol, 0.5% formic acid).

6.2. Equilibrate ZipTip 3 times with 10 µL washing solution (2% methanol, 0.5% formic acid).

6.3. Pipette sample up and down for 10 to 15 times very slow.

6.4. Wash ZipTip 3 times with 10 µL washing solution.

6.5. Elution for MALDI. Add 5 µL elution solution into a 0.5 mL microcentrifuge tube. Using the ZipTip containing sample from step 6.4, pipette the 5 µL elution solution up and down 3 times to elute sample from ZipTip to elution solution.

7. Loading for MALDI mass spectroscopy analysis

Mix 1 µL of sample in elution solution from step 6.5 with 1 µL of MALDI loading solution (10 mg of α-cyano-4-hydroxycinnamic acid, 400 µL acetonitrile (ACN) and 600 µL 0.1% trifluoroacetic acid (TFA) and transfer 2 µL of this mixture onto a clean MALDI sample target. The mass spectroscopy analysis is preformed after the solution is completely evaporated.

10.2.3. Sample preparation for MALDI using Prespotted AnchorChip target

5. Peptide-Extraction

5.1. Add 30 µL of acetonitrile (ACN) to the gel spot and mix on an Eppendorf thermomixer for 15 min at 37°C and 800 rpm.

5.2. Transfer supernatant of each sample into another Eppendorf tube.

5.3. Add 30 µL of 5% formic acid to each gel spot and mix on an Eppendorf thermomixer for 15 min at 37°C and 800 rpm.

5.4. Add 30 µL of ACN to each gel spot and mix for 15 min at 37°C and 800 rpm.

5.5. After 15 min, combine the supernatant with supernatant in the tube from step 5.2.

5.6. Use Speedvac to dry samples (the sample combined with the supernatant from step 5.2 and 5.5) about 1 hour.

5.7. After drying, add 7 µL 32% methanol, 0.5% ammonium phosphate and put samples into a sonication bath to sonicate for 10 min.

6. .Loading to PAC target for MALDI mass spectrometry analysis

6.1. Deposit 1 µL sample solution in matrix spot.

6.2. Allow three minutes incubation.

6.3. Add 7 µL washing buffer (10 mmol L^{-1} ammonium phosphate, 0.1% TFA) and remove the whole droplet after 3~5 seconds.

10.3. Buffers and solutions for proteomic analyses

DTT (1 mol L^{-1}) stock solution

Add 0.92 g Tris in a 15 mL conical screw cap tube and add 5 mL of Milli-Q water to bring the final volume to 6 mL. After completely dissolution, aliquot 75 µL of this solution to several PCR tubes and store at -80^{o}C.

Tris (1 mol L^{-1}) stock solution

Add 0.24 g Tris in a 2 mL microcentrifuge tube and add 1.7 mL of Milli-Q water to bring the final volume to 2 mL. After complete dissolution, store at 4^{o}C. This solution is only Tris base solution, the pH does not need to be adjusted.

Bromophenol blue stock solution

Composition: 1% bromophenol blue and 50 mmol L^{-1} Tris base

Add 100 mg of bromophenol blue and 60 mg of Tris base to a 15 mL centrifugation

tube and add Milli-Q water to bring the final volume to 10 mL. Vortex till it is completely dissolved and aliquot 1.2 mL of this solution to several microcentrifuge tubes and store at 4 ^{o}C.

Tris-HCl (1.5 mol L^{-1}), pH 8.8 stock solution (4× resolving gel buffer solution)

Add 181.71 g of Tris base, 600 mL of Milli-Q water to a glass beaker and dissolve the Tris base. Adjust the pH value of this solution to 8.8 using 1 mol L^{-1} HCl. Add Milli-Q water to bring the final volume to 1000 mL and check the pH value of the final solution. Filter this solution through a 0.20 μm membrane to an autoclaved glass bottle.

Lysis buffer

Composition: 7 mol L^{-1} urea, 2 mol L^{-1} thiourea, 30 mmol L^{-1} Tris and 4% (w/v) Triton X-100, pH 8.5.

Add 42 g urea, 15.2 g thiourea, 0.36 g Tris, 4 g Triton X-100 in 100 mL Milli-Q water. Adjust the pH to 8.5.

Rehydration solution

Only for dampening IEF sample application pieces in IPGphor Strip holder

Composition: 9 mol L^{-1} urea, 2 mol L^{-1} thiourea, 4% CHAPS and 0.2 mg/mL Tris

Add 10.81 g urea, 3.04 g thiourea and 0.8 g CHAPS, 37 μL 1 mol L^{-1} Tris (only Tris base solution, pH not adjusted) to a 20 mL glass beaker and add about 10 mL of Milli-Q water to bring the final volume to 20 mL. After complete dissolusion, aliquot 0.4 mL of this solution to several 2 mL microcentrifuge tubes and store at -20^{o}C.

Resolubilization solution (for resolubilization of protein pellets)

Composition: 9 mol L^{-1} urea, 2 mol L^{-1} thiourea, 4% CHAPS, 0.2 mg/mL Tris, 0.2% SDS and 0.002% bromophenol blue.

Add 32.43 g urea, 9.13 g thiourea and 2.4 g CHAPS, 111 μL 1 mol L^{-1} Tris (only Tris base solution, pH not adjusted), 1.2 mL of 10% SDS stock solution and 120 μL of 1% bromophenol blue stock solution to a 100 mL glass beaker and add about 30

mL of Milli-Q water to bring the final volume to 60 mL. Dissolve the solution completely. Aliquot 1.5 mL in microcentrifuge tubes and store at -20^{o}C.

SDS (10%) stock solution

Add 100 g of SDS powder in a 1 L plastic beaker, and add Milli-Q water to bring the final volume to 1 L. Add magnetic stirring bar for mixing. After the SDS have been completely dissolved, filter this solution through a 0.20 μm filter to two autoclaved 0.5 L glass bottles.

SDS equilibration buffer

Composition: 50 mmol L^{-1} Tris-HCl pH 8.8, 6 mol L^{-1} urea, 30% (v/w) glycerol and 2% (v/w) SDS.

Add 108.15 g of urea, 60 mL of 10% SDS stock solution, 103.5 mL (126.3 g) of glycerol (86% w/w), and add some Milli-Q water and 10 mL 1.5 mol L^{-1} Tris-HCl, pH 8.8 stock solution (4× resolving gel buffer solution) into a 500 mL glass bottle. Bring the final volume to 300 mL with Milli-Q water and dissolve this solution. Store in 13 mL aliquots in 15 mL of centrifugation tube at -20^{o}C.

Prepare it at least 3 hours before run the gels.

In one Falcon containing SDS equilibration buffer add 1% (w/v) (10 mg in 1 mL) of DTT. In another Falcon containing SDS equilibration buffer add 5% (w/v) (50 mg in 1 mL) of iodoacetamide. Gently shake to dissolve the DTT and iodoacetamide. At this step, avoid to make bubbles in the SDS equilibration buffer.

SDS electrophoresis buffer for agarose sealing solution (without SDS)

Composition: 24 mmol L^{-1} Tris-base and 0.2 mol L^{-1} glycine.

Add 2.9 g of Tris-base, 15.01 g of glycine, in a 1L glass bottle. Add Milli-Q water to bring the final volume to 1 L. Filtrate this solution through a 0.20 μm membrane to an autoclaved 1 L glass bottle. SDS should not been added to this solution. Store this solution at 4^{o}C.

Agarose sealing solution

Composition: 1% agarose, 0.002% bromophenol blue stock solution and 0.1% (w/v) SDS.

Add 0.5 g of agarose to a 100 mL glass bottle; add 50 mL of SDS electrophoresis buffer (24 mmol L^{-1} Tris-base and 0.2 mol L^{-1} glycine) using a graduated cylinder in this bottle. Add 100 µL 1% bromophenol blue stock solution and 500 µL of 10% SDS stock solution. Heat in a microwave on low power until the agarose is completely dissolved.

Tank electrophoresis buffer

Composition of 20 L tank electrophoresis buffer (for at least 6 gel cassettes): 24 mmol L^{-1} Tris-base, 0.2 mol L^{-1} glycine and 0.1% (w/v) SDS.

Add 58 g of Tris-base, 300 g of glycine, 200 mL of 10% SDS stock solution in the electrophoresis tank and add Milli-Q water to bring the final volume to 20 L. Use the circulating pump to dissolved the buffer components. After complete dissolution, put the two barrier combs back to their original position. This buffer can be used for about 3 runs of SDS-PAGE electrophoresis.

Fixing solution

Composition: 10% acetic acid and 30% ethanol.

Add 600 mL of ethanol (or 857 mL of 70% ethanol) to a 2 L glass bottle and add Milli-Q water to bring the volume to 1.8 L. Finally, add 200 mL acetic acid and mix the solution.

Colloidal Silver Comassie G-250 staining

Composition: 8.5% H_3PO_4, 10% $(NH_4)_2SO_4$, 0.1% Coomassie Blue G-250 and 20% (w/v) methanol.

Firstly, add 250 mL Milli-Q water to a glass bottle and add 250 mL of 85% H_3PO_4 and mix. Secondly, add 250 g of $(NH_4)_2SO_4$ to a 500 mL glass breaker and then add Milli-Q water to bring to a final volume of 500 mL. Add a magnetic stirring bar for complete mixing. Thirdly, add 2.5 g Coomassie Blue G-250 to a 500 mL glass beaker and then add Milli-Q water to bring to a final volume of 500 mL. Add a magnetic stirring bar for complete mixing. After the $(NH_4)_2SO_4$ and Coomassie

Blue G-250 is completely dissolved, mix then add 500 mL Milli-Q water to bring the volume to 2 L. Mix at high stir speed over night. After complete dissolution, add 400 mL of methanol to complete this solution. It is better to store this solution in a brown bottle.

Displacing solution for casting gradient gels

Composition: 0.375 mol L^{-1} Tris-HCl pH 8.8, 43% (w/w) glycerol and 0.001% bromophenol blue.

Add 100 mL (122 g) of glycerol (86% w/w) 50 mL Milli-Q water, 50 mL 1.5 mol L^{-1} Tris-HCl, pH 8.8 (4× resolving gel buffer solution) and 200 µL of 1% bromophenol blue stock solution to an appropriate and clean container.

APS (10%) for casting gels

For 12 gels: add 1 g ammonium persulfate (APS) to a 15 mL centrifugation tube. Then add Milli-Q water to bring the final volume to 10 mL and vortex for complete mixing.

TEMED (10%) for casting gels

For 12 gels: add 150 µL of TEMED and 1350 µL of Milli-Q water to a 2 mL microcentrifuge tube. Vortex for complete mixing.

SDS (0.1%)

Add 5 mL of 10% SDS stock solution to a 500 mL graduate cylinder, and add Milli-Q water to bring the final volume to 500 mL. After mixing, pour this solution to a bottle.

Gel storage solution

Composition: 0.375 mol L^{-1} Tris-HCl pH 8.8 and 0.1% SDS.

Add 20 mL of 10% SDS stock solution, 500 mL of 4× resolving gel buffer solution (1.5 mol L^{-1} Tris-HCl, pH 8.8) to a 2 L glass bottle. After then add Milli-Q water to bring the final volume to 2 L and store this solution at $4^{o}C$.

Solution for casting gels

Composition of solution for 12 gels (1200 mL): 480 mL acrylamide stock solution Rotiphorese Gel 30 (37,5:1) 30%, 300 mL Tris-HCl 1.5 mol L^{-1}, pH 8.8, 394 mL Milli-Q water, 12 mL 10% SDS, 12 mL 10% APS, 2 mL 10% TEMED. Add APS and TEMED only before cast the gel.

NH_4CO_3 (0.1 mol L^{-1})

Add 3.95 g NH_4HCO_3 to a 500 mL graduate cylinder, and add Milli-Q water to bring the final volume to 500 mL. Filter this solution through a 0.2 μm membrane to an autoclaved glass bottle. Store at 4°C.

NH_4CO_3 (0.1 mol L^{-1}) with DTT

Add 31 mg DTT into a 15 mL conical tube and add 10 mL 1 mol L^{-1} NH_4HCO_3 solution to bring the final volume to 10 mL.

NH_4CO_3 (0.1 mol L^{-1}) with iodoacetamide

Add 102 mg iodoacetamide into a 15 mL conical tube and add 10 mL 1 mol L^{-1} NH_4HCO_3 solution to bring the final volume to 10 mL.

Trypsin working solution (2 μg/mL)

One vial of 20 μg trypsin (sequencing grade modified trypsin, Promega) is combined with 100 μl trypsin resuspension buffer (Promega) and incubated 30 min at room temperature. Then add 900 μl 1 mol L^{-1} NH_4HCO_3 solution. After mixing, aliquot 50 μl into 0.5 mL microcentrifuge tubes and store at −80°C. Before using, thaw and add 450 μl Milli-Q to make 500 mL trypsin working solution.

Formic acid (5%)

Add 25 mL formic acid to 500 mL graduate cylinder, and add Milli-Q water to bring the final volume to 500 mL. Store at 4°C.

Wash solution for Zip Tip

Composition: 2% methanol, 0.5% formic acid

Add 2 mL methanol and 0.5 mL formic acid to a 100 mL graduate cylinder, and add Milli-Q water to bring the final volume to 100 mL. Store at 4°C.

Elution solution for Zip Tip

Composition: 65% methanol, 0.5% formic acid

Add 65 mL methanol and 0.5 mL formic acid to a 100 mL graduate cylinder, and add Milli-Q water to bring the final volume to a 100 mL. Store at 4°C.

PAC target washing buffer

Add 1 mL trifluoroacetic acid (TFA) to 1 L graduate cylinder, and add Milli-Q water to bring the final volume to 1 L to make 0.1% TFA solution. Add 23 mg $NH_4H_2PO_4$ and 20 mL 0.1% TFA solution to a glass bottle Store at 4°C.

Saturated matrix solution

Composition: 0.06% TFA, 40% acetonitrile and 10 mg/mL α-Cyano-4-hydroxycinnamic acid

Add 1 mL trifluoroacetic acid (TFA) to 1 L graduate cylinder, and add Milli-Q water to bring the final volume to 1 L to make a 0.1% TFA solution. Add 10 mg α-Cyano-4-hydroxycinnamic acid, 400 µl acetonitrile and 600 µl 0.1% TFA solution into a 1.5 mL microcentrifuge tube. Vortex for mixing. Store at 4°C.

10.4. List of reagents

Table 10.1 Chemicals

Chemical	Annotation	Manufacturer
Acetic acid	CH_3CO_2H	Carl Roth GmbH + Co. KG., Germany
Acetonitrile	CH_3CN	Carl Roth GmbH + Co. KG., Germany
Acrylamide and bisacrylamide stock solution	Rotiphorese® Gel 30 (37,5:1)	Carl Roth GmbH + Co. KG., Germany
Agarose	Biozym LE GP agarose	Biozym Scientific GmbH, Germany
Ammonium hydrogen carbonate	NH_4HCO_3	Merck KgaA, Germany
Ammonium persulfate	$(NH_4)_2S_2O_8$	Sigma-Aldrich GmbH, Germany
Ammonium sulfate	$(NH_4)_2SO_4$	Carl Roth GmbH + Co. KG., Germany
Bromophenol Blue	3′,3″,5′,5″Tetrabromophenolsulfonephthalein	Sigma-Aldrich GmbH, Germany
CHAPS	3-((3-Cholamidopropyl)-dimethylammonio)-1-propanesulfonate	Biomol GmbH, Germany
Coomassie Blue G250	Coomassie brilliant blue G-250	Merck KgaA, Germany
DTT	DL-Dithiothreitol	Sigma-Aldrich GmbH, Germany
Ethanol	Ethanol (96%)	Merck KGaA , Germany
Formic acid	HCOOH	J.T.Baker Chemical Company, USA
Glycerol	Glycerol (86%)	Carl Roth GmbH + Co. KG., Germany
Glycine	$C_2H_5NO_2$	Carl Roth GmbH + Co. KG., Germany
Iodoacetamide	ICH_2CONH_2	GE Healthcare, United Kingdom
Methanol	CH_3OH	Carl Roth GmbH + Co. KG., Germany
Phosphoric acid	H_3PO_4 (85%)	Carl Roth GmbH + Co. KG., Germany
Potassium phosphate dibasic	K_2HPO_4	Carl Roth GmbH + Co. KG., Germany
Potassium phosphate monobasic	KH_2PO_4	Carl Roth GmbH + Co. KG., Germany
SDS	Sodium dodecyl sulfate	Bio-Rad Laboratories GmbH, Germany
Silicon M100	Polydimethyl siloxane	Carl Roth GmbH + Co. KG.
TEMED	N,N,N′,N′-Tetramethylethylenediamine	Sigma-Aldrich GmbH, Germany
TFA	Trifluoroacetic acid	Merck KgaA, Germany
Thiourea	Thiocarbamide	Sigma-Aldrich GmbH, Germany
TMB	3,3´,5,5´tetramethylbenzidine	Sigma-Aldrich GmbH, Germany
Tris	Tris(hydroxymethyl) aminomethane	Carl Roth GmbH + Co. KG., Germany
Triton X-100	polyethylene glycol p-(1,1,3,3-tetramethylbutyl)-phenyl ether	Sigma-Aldrich GmbH, Germany
Urea	Carbamide	Sigma-Aldrich GmbH, Germany
α-Cyano-4-hydroxycinnamic acid		Sigma-Aldrich GmbH, Germany

Table 10.2. Commercial buffer and other materials

Chemical	Annotation	Manufacturer
IPG buffer pH 3-10 NL		GE Healthcare, United Kingdom
IPG strip pH 3-10 NL	Immobiline DryStrip pH 3-10 NL, 18 cm	GE Healthcare, United Kingdom
Trypsin	Sequencing grade modified	Promega Corporation, USA
Ziptips C18		Millipore Corporation, USA
Anti-HDEL (2E7)	Sc-53472	Santa Cruz Biotechnology, USA
Anti-mouse (secondary antibody)	HRP conjugated	Calbiochem, Germany
PVDF membrane	Polyvinylidene difluoride	Bio-Rad Laboratories GmbH, Germany
PAC target	Prespotted AnchorChip target	Bruker Daltonics GmbH, Germany
Glass beads	0.5 mm	Sartorius AG, Germany

10.5. List of abbreviations

Abbreviation of protein names are given in Appendix I and III.

Abbreviation	Full name
2D-GE	Two-dimensional gel electrophoresis
ATP	Adenosine triphosphate
EM	Electron microscopy
ER	Endoplasmatic reticulum
ERAD	Endoplasmatic reticulum associated degradation
GC	Gas chromatography
HBsAg	Hepatitis B surface antigen
HPLC	High performance liquid chromatography
IP	Insulin precursor
IPG	Immobiline DryStrip gel
MALDI-TOF MS	Matrix assisted laser desorption ionization time-of-flight mass spectrometry
MS	Mass spectrometry
NADH	Nicotinamide adenine dinucleotide
NADPH	Nicotinamide adenine dinucleotide phosphate
PPP	Pentose phosphate pathway
PTM(s)	Post-translational modification(s)
ROS	Reactive oxygen species
SDS-PAGE	Sodium dodecyl sulfate polyacrylamide gel electrophoresis
TEM	Transmission electron microscopy
TFA	Trifluoroacetic acid
TCA	Tricarboxylic acid
UPR	Unfolded protein response
VLP	Virus like particle

Curriculum Vitae

Personal information

Name:	Ana Letícia de Souza Vanz
Date of Birth:	19.05.1981
Place of Birth:	Erechim – RS, Brazil
Nationality:	Brazilian

Education

April 2009 to date	**PhD student**
	Biochemistry
	Institute of Technical Chemistry
	Leibniz Universtität Hannover, Germany
	Advisors: Prof. Dr. Thomas Scheper and Prof. Dr. Ursula Rinas
2006-2008	**MSc**
	Cellular and Molecular Biology
	Bioscience Institute of Pontifícia Universidade Católica do Rio Grande do Sul (PUC-RS), Porto Alegre, Brazil
	Advisors: Dr. Diógenes S. Santos and Dr. Luiz A. Basso
1999-2003	**BS - Pharmacy**
	Health Science Center of Pontifícia Universidade Católica do Rio Grande do Sul (PUC-RS), Porto Alegre, Brazil

Publications

Vanz AL, Lünsdorf H, Adnan A, Nimtz M, Gurramkonda C, Khanna N, Rinas U. **Physiological response of *Pichia pastoris* GS115 to methanol-induced high level production of the Hepatitis B surface antigen: catabolic adaptation, stress responses, and autophagic processes**. *Microb Cell Fact* 2012, 11(1):103

Vanz ALS; Renard G; Palma M; Chies JM; Dalmora SL; Basso LA; Santos DS. **Human granulocyte colony stimulating factor (hG-CSF): cloning, overexpression, purification and characterization**. *Microb Cell Fact,* 2008, 7: 13.

Oral presentation

Vanz AL, Nimtz M, Rinas U. Cellular response to secretory insulin precursor production in *P. pastoris.*

Place: 7th Conference on Recombinant Protein Production (Laupheim, Gernany 2013)

Posters

Vanz AL, Lünsdorf H, Roth G, Nöhren G, Rinas U. Autophagy in recombinant *P. pastoris*: adaptation response to nutrient conditions.

Place: 7th Conference on Recombinant Protein Production (Laupheim, Gernany 2013)

Vanz AL, Adnan A, Gurramkonda C, Nimtz M, , Khanna N, Rinas U. Proteomic evaluation of time-points during HBsAg expression in *Pichia pastoris.*

Place: 6th Conference on Recombinant Protein Production (Vienna, Austria, 2011)

Vanz AL, Adnan A, Gurramkonda C, Nimtz M, , Khanna N, Scheper T, Rinas U. Comprehensive analysis of *Pichia pastoris* proteome expressing recombinant proteins.

Place: 1st European Congress of Applied Biotechnology (Berlin 2011)